Development of a Novel Topical Controlled Release System for Otic Drug Delivery

by

Liza Anna Bruk

Bachelor of Science, University of Pittsburgh, 2015

Submitted to the Graduate Faculty of the

Swanson School of Engineering in partial fulfillment

of the requirements for the degree of

Doctor of Philosophy

University of Pittsburgh

2020

UNIVERSITY OF PITTSBURGH

SWANSON SCHOOL OF ENGINEERING

This dissertation was presented

by

Liza Anna Bruk

It was defended on

June 22, 2020

and approved by

Cuneyt M. Alper, MD, Professor, Department of Otolaryngology

Kacey G. Marra, PhD, Professor, Departments of Plastic Surgery and Bioengineering

Srivatsun Sadagopan, PhD, Assistant Professor, Departments of Neurobiology and Bioengineering

Dissertation Director: Morgan V. Fedorchak, PhD, Assistant Professor, Departments of Ophthalmology, Bioengineering, Chemical Engineering, and Clinical and Translational Sciences

Development of a Novel Topical Controlled Release System for Otic Drug Delivery

Liza Anna Bruk, PhD

University of Pittsburgh, 2020

Acute otitis media (OM) is the leading indication for pediatric antibiotic prescriptions, accounting for 25%. While the use of topical ear drops can minimize antibiotic dose and adverse systemic effects compared to oral antibiotics, their use has limitations due to low patient compliance, high dosing frequency, and difficulty of administration. Improper treatment can lead to chronic OM and may require surgical intervention. Previous studies have shown that gel-based otic delivery is possible with invasive intratympanic injection or chemical permeation enhancers which have demonstrated toxicity effects. Further, infection or trauma can cause tympanic membrane (TM) perforation, which can be chronic in up to 46% of cases. Even healing perforations may require months for complete closure, increasing susceptibility to infection, hearing loss, and other side effects. Current treatment standards include surgical grafting, which may result in similar detrimental side effects. Research has accordingly focused on alternative grafts and growth factor or stem cell therapy, which come with logistical and regulatory hurdles.

A novel method of delivering therapeutics to the TM and middle ear was developed using a topical, thermoresponsive gel depot containing antibiotics or stem cell conditioned media (CM)-loaded polymer microspheres. Results indicate that the noninvasive, sustained presentation can allow therapeutically relevant drug concentrations to penetrate the TM to the middle ear for up to 14 days from one topical administration. Auditory brainstem recordings indicate that complete coverage of the TM is achieved and administration can be scaled up if needed. Biocompatibility of all materials is indicated by cytotoxicity testing as well as increased wound healing in CM and

CM MS-treated *in vitro* scratch wound proliferation assays. Despite some variability in the models, *in vivo* data suggest the system may treat bacterial infection and tympanic membrane perforation, with future studies investigating further scaled up release and longitudinal safety testing. To our knowledge, this dissertation represents the first truly topical drug delivery system to the middle ear for OM with intact TM without the use of CPEs and topical delivery of stem cell secretome to the TM for chronic perforation healing.

Table of Contents

List of Tables

List of Figures

Preface

I have been very fortunate to spend the last nine years in the University of Pittsburgh Bioengineering department for undergraduate and graduate studies. Pittsburgh has become my home and I feel very lucky to have spent these years at such a world-class institution. This city and university are where I learned to be a scientist and an engineer and become my most authentic self.

First and foremost, I want to thank my advisor, Dr. Morgan Fedorchak. During my first year, I benefitted from the unique experience of being the first and only lab member, working side by side with Morgan to set up the lab and learning how to become a capable, independent researcher. She taught me how to apply engineering solutions to scientific problems, think independently, and tackle any problems science threw our way. I am extremely grateful for her allowing me to develop non-scientific skills through my extracurricular activities in leadership positions in the Pitt Graduate Biomedical Engineering Society, STEM outreach via teaching with Investing Now, and volunteer consulting with Fourth River Solutions. I look forward to further developing these skills in my career. I am grateful to have Morgan as a mentor, teacher, and friend.

I have been very proud to watch the lab grow and I look forward to seeing all the excellent science that continues to come out of the Ophthalmic Biomaterials Lab. I would like to thank all past and present members of the lab for their support, knowledge, and passion. In particular, thank you to Jayde Resnick, who is willing to learn any technique and come in to lab at any time, even to help me complete an animal study during a pandemic. Thank you especially to Jorge Jimenez; I could not have done this without his endless support in and out of the lab, talking through scientific problems, and generally making me a better scientist and person for knowing him. I also

thank the undergraduate students I was fortunate to mentor and who made me a better scientist through teaching, particularly Kate Dunkelberger and Lindsey Helsel.

I would like to acknowledge and thank my committee members as well. Thank you to Dr. Cuneyt Alper for his valuable clinical insight, to Dr. Kacey Marra for her insights in biomaterials and tissue engineering topics, and to Dr. Vatsun Sadagopan for his scientific support, knowledge, and generosity with his time and resources.

I am extremely grateful to all the friends I have been fortunate to make in Pittsburgh. Thank you to Jorge Jimenez, Chris Reyes, Yoojin Lee, and Danielle Minteer, who have always supported me and been there to talk about food, music, science, or all of the above. Thank you to those I have been fortunate to call classmates and friends since college, particularly Alex Moore, Sarah Stephenson, Devon Albert, Nicole Dejean, Matt Hankey, Gerald Ferrer, John Erickson, Harrison Lynch, and Gabe Frank, for their unwavering love and support through all these years. A special thank you to my oenophile friends Anne Faust, Yolandi van der Merwe, Erinn Grigsby, John Barrett, Erika Pliner, Stephanie Wiltman, and Jessi Mischel. I could not have done this without their encouragement, late-night conversations, and generally being the best group of nerds.

Last but certainly not least, I thank my family for their endless love, encouragement, and patience. Thank you to my mother who taught me to be a strong, creative, independent woman and engineer and to my father who has called me “professor” since I was young so he must have seen this coming and who can always make me laugh under any circumstances. Thank you to Olga, Darryl, and Sonia; I will miss living only a few miles apart. Finally, a very special thank you to my grandmother, who is no longer with us and who I wish could have been here to see me finish this PhD.

1.0 Introduction and Specific Aims

1.1 Controlled Drug Delivery

Controlled drug delivery as a field originated in the 1960s and evolved over the decades to become a field of great interest and commercial and clinical success in the 21st century [1,2]. Drug delivery systems are beneficial due to ability to control the route of administration and dosage based on therapeutic need and properties of the drug itself [2]. Most of the first drug delivery systems were oral or transdermal delivery systems, formulated for constant zero-order release kinetics [1–3]. However, zero-order kinetics did not necessarily translate to constant plasma drug concentration, particularly from oral delivery systems, due to drug metabolism and absorption, resulting in a large peak followed by a decrease, rather than a maintenance of drug levels between minimum effective concentration and maximum concentration to prevent toxicity. Further, a zero-order release is not ideal for all drug types or relevant for most effective therapy of all conditions [3]. Oral delivery systems are also limited by lack of site-specific targeting and poor blood circulation times [4].

Accordingly, research became more focused on more localized or targeted drug delivery systems optimized for the therapeutic needs of the specific drug and condition [1,5]. Ocular and transdermal drug delivery systems are often targeted for development of non-invasive systems; however, a number of implantable or injectable drug delivery systems have been developed, including several implantable devices developed for female contraceptive use [1,6]. Controlled drug delivery systems have also shown promise in the field of tissue engineering, with scaffolds and other delivery systems releasing growth factors and other signaling molecules [7,8].

1.1.1 Otic Biomaterials

In addition to aforementioned ocular and transdermal use, biomaterials have a rich history of use in the ear, perhaps most notably the use of cochlear implants. Recent research into improvement of cochlear implants has focused on coatings to improve electrode function by locally releasing dexamethasone to prevent fibrous encapsulation and neurotrophic factors to preserve neurons and encourage neuronal regeneration [8]. One recent study has also investigated the use of 3-D printed microneedle arrays (MNAs) for delivery of therapeutics through the round window membrane to the cochlea [9]. Drug-eluting stents have long been used for cardiovascular applications and can be adapted for otolaryngology, in particular for use in the Eustachian tube, stenosis of which can be a cause of chronic otitis media [8,10–12]. Recent research has increasingly focused on drug targeting and local use of biodegradable microparticles and nanoparticles for drug delivery and tissue engineering in otolaryngology [7,8].

1.1.2 Microspheres for Controlled Drug Delivery

Biodegradable polymer microspheres are an attractive method of providing controlled, localized drug release and have been investigated for a variety of applications. Drug release from microspheres occurs via biphasic or triphasic release with the primary phases being: 1) initial burst release, 2) lag phase, and 3) final phase [6,13,14]. Biphasic and triphasic release differ in that biphasic release does not include a lag phase [14]. Initial burst often occurs due to drug physically adhered to the surface of the microsphere or porosity of the matrix resulting in a fraction of the drug to diffuse out of the microspheres quickly [6]. The lag phase is primarily governed by no release or slow diffusion-based release in which drug diffuses slowly out of the polymer matrix

due to slow or no degradation/erosion. The final phase is governed by degradation/erosion of the polymer matrix resulting in greater and continuous drug release. An example of these phases can be seen in Figure 1.

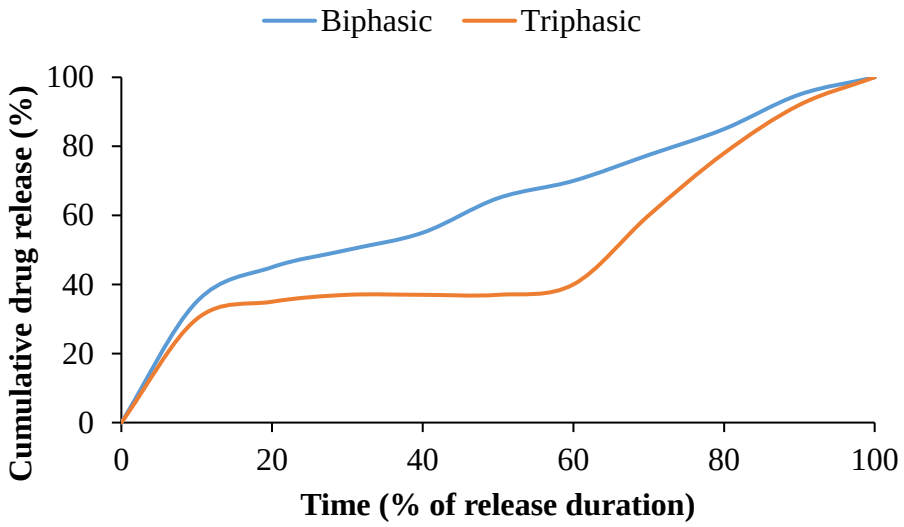

Figure 1: Biphasic vs. triphasic release profiles. Biphasic release is characterized by an initial burst followed by continuous release governed by polymer matrix degradation. Triphasic release is characterized by an initial burst, lag phase governed by little to no degradation resulting in no release or slow diffusion-based drug release, and a final continuous release phase governed by poymer degradation. These phases have different characteristics (percentage of cumulative drug release, percentage of release duration, etc) dependent on the properties of the individual controlled release system.

Microspheres can be tuned to provide a variety of release profiles by adjusting polymer molecular weight, copolymer ratios, matrix porosity, microsphere size, and drug concentration and dispersion in the polymer matrix [13–17]. Release profiles can also be tuned by adjusting parameters during microsphere fabrication. Microspheres are often fabricated using evaporation

based techniques, including oil-in-oil (O/O) or oil-in-water (O/W) single emulsions and water-in-oil-in-water (W/O/W) or solid-in-oil-in-water (S/O/W) double emulsion fabrication [17–20]. For commercial scaling purposes, other fabrication methods such as spray drying can be employed [20]. In particular, W/O/W fabrication is amenable to encapsulation of water-soluble drugs and will be described further for encapsulation of relevant therapeutics in this dissertation.

In this fabrication method, drug is dissolved in water and the aqueous drug solution is added to a solution of polymer dissolved in organic solvent (Figure 2). These solutions are stirred vigorously, usually via sonication or homogenization, to create the first water-in-oil emulsion. This emulsion is added to a solution of water and surfactant to stabilize the emulsion and stirred vigorously again to create the second W/O/W solution. The organic solvent is removed by evaporation while continuously stirring the emulsion and precipitated microspheres are washed to remove any excess reagents and dried to prevent hydrolysis during storage [20]. Fabrication parameters that can influence drug encapsulation and subsequent release profile include the choice of organic solvent and stirring rate of sonication/homogenization which affect drug encapsulation efficiency and size of resulting microspheres [13,20]. Therefore, if optimal release profile (magnitude, duration, etc) is not achieved for the target application, these parameters can be adjusted to tune the release profile, in addition to previously mentioned factors including choice of polymer and polymer properties.

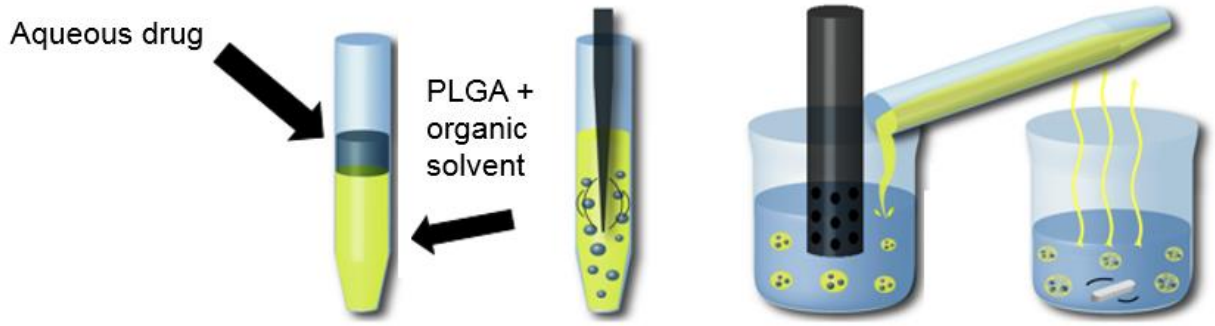

Figure 2: Double emulsion water-in-oil-in-water (W/O/W) microsphere fabrication method. Aqueous drug in water is added to poly(lactic-co-glycolic acid) dissolved in organic solvent and sonicated to create the first water-in-oil emulsion. This emulsion is transferred to a solution of water and surfactant and homogenized to created the second W/O/W emulsion. The organic solvent is allowed to evaporate before the microspheres are washed and freeze dried.

1.1.3 Poly(lactic-co-glycolic acid) in Biomedical Applications

A polymer frequently used in biomedical applications, particularly microsphere-based controlled release systems, is poly(lactic-co-glycolic acid) (PLGA) [6,14,15,20,21]. PLGA has a long track record of clinical use and approval by regulatory authorities including the United States Food and Drug Administration as it is biodegradable and its degradation products, lactic acid and glycolic acid, are biocompatible and easily cleared from the body [14,15,20,22,23]. Biodegradation is beneficial as it eliminates the need for a potentially invasive procedure to remove the delivery system [21]. Because of its widespread use, PLGA is widely commercially available in a variety of properties include molecular weights and copolymer ratios, increasing ease of use for further research into PLGA-based delivery systems [14,21]. Further, PLGA is extremely well

characterized and a number of mathematical models exist for determining release profiles of various therapeutics from PLGA-based delivery systems, including microsphere-based applications [13–15,20,24].

1.1.4 Responsive Polymer Gels for Controlled Drug Delivery

In recent years, a growing number of studies have also focused on gel-based drug delivery systems. "Smart" responsive polymers can be designed to respond to physiological and/or external triggers, including temperature, pH, glucose levels, ionic concentration, and ultra-violet irradiation [3,25–28]. These smart polymers or hydrogels are networks of polymers that can take up large amounts of water and be formed into particles, films, coatings, etc, and are therefore commonly used in a wide variety of biomedical applications [4,25,27,29]. Gels are similar but are consistent of a larger solid compared to liquid component [27]. One of the first uses for hydrogels in medicine was the advent of contact lenses in the 1960s, which are still in widespread use today [25,27]. Since then, a number of gel and hydrogel formulations have been developed for tissue engineering, diagnostics, drug delivery, and other applications [25,29].

Thermoresponsive hydrogels and gels in particular are useful for biomedical applications due to ability to be injected as a liquid and solidify *in situ* [30–32]. Thermoresponsive gels have either a lower critical solution temperature (LCST) or upper critical solution temperature (UCST), with LCST-driven gelation more relevant to *in situ* gelation for most biomedical applications. Below its LCST, a gel exists in a hydrophilic, water-swollen state and becomes hydrophobic above its LCST, expelling its water content and solidifying [25,28,33,34].

1.1.5 Poly(N-isopropylacrylamide) in Biomedical Applications

In addition to a variety of natural and synthetic polymers, poly(N-isopropylacrylamide) (pNIPAAm) is often used in biomedical applications as a thermoresponsive gel matrix [28,32]. Poly(N-isopropylacrylamide) is attractive for biomedical applications due to a lower critical solution temperature (LCST) of approximately 32-33°C, which falls between room temperature and human physiological temperature of 37°C [28,31,32]. Because pNIPAAm is reverse thermoresponsive, it can return to a swollen state when temperature is lowered below LCST. These properties are beneficial for injectable and topical administration for localized drug delivery, allowing the gel to be injected or applied as a liquid and solidifying *in situ* [6,29,30]. However, pNIPAAm hydrogels can have poor mechanical properties and relatively fast diffusion-based release [30,34–36]. Addition of copolymers or crosslinkers of varying hydrophobicity or hydrophilicity, can influence mechanical properties and LCST of the gel, including the addition of poly(ethylene glycol) (PEG) which is hydrophilic and can increase LCST as well as increase speed of rehydration upon reverse transition [26,32,34–36]. Gels made using pNIPAAm are usually fabricated using free radical polymerization and can result in some toxicity, however gel concentrations used in biomedical applications have generally shown to be nontoxic due to high water content [26,27,30,35,37].

While controlled drug delivery can be achieved by gel-based or microsphere-based drug delivery systems alone, microspheres have been incorporated into gel-based systems to add a level of further control to the drug release and gels have been incorporated into microsphere-based systems as a carrier/retention mechanism for increased ease of use for injectable and topical applications [6,15,27,36,38].

1.2 Acute Otitis Media

1.2.1 Incidence and Severity of Otitis Media

Acute otitis media (AOM), characterized by middle ear inflammation, acute onset, and duration of illness ranging from several days to two weeks, accounts for 20 million pediatrician visits annually and is the main indication for pediatric antibiotic prescription in the United States [39–42]. In fact, over 25% of antibiotic prescription is for the sole purpose of treating AOM [40,41]. Approximately 80% of children under three years old experience AOM at least once[40,41] and 30-40% of children experience at least six instances of AOM before the age of seven [36,37]. Recurrent AOM can develop into chronic otitis media, which often requires surgical intervention such as myringotomy and placement of tympanostomy tubes for ventilation and drainage [12,45,46]. Chronic otitis media has also been associated with sensorineural hearing loss, which may lead to speech and learning deficits [46–50]. In the US alone, 500,000 children undergo tympanostomy surgery annually at a cost of $5 billion [51]. Developing countries see over 10 times more incidence of OM than the US and European nations [12,47,52].

1.2.2 Current Clinical Standards and Associated Shortcomings

Oral antibiotics remain the standard of care, although such treatment is recognized as impractical due to the risks of systemic side effects and antibiotic resistance associated with persistent biofilm formation [10,41,42,53,54]. Further, oral antibiotics may not provide adequate drug concentration to the middle ear to clear these persistent biofilms [55,56].

Though less frequently prescribed for AOM, and only in cases of non-intact TM due to perforation or placement of ventilation tubes, topical ear drops are also problematic, with less than 10% of the applied drug reaching the middle ear [57]. For example, 0.2% ciprofloxacin is, if applied correctly to non-intact TM, delivered in quantities of 1mg/day [58]. The minimum inhibitory concentration (MIC) of ciprofloxacin to inhibit microorganisms commonly responsible for OM, including *Streptococcus pneumoniae* and *Haemophilus influenzae* [10], has been determined to be up to 1-2μg/mL [59,60]. With proper instillation, the standard topical antibiotic drop treatment [58] delivers up to 1000 times excess antibiotic to the middle ear and surrounding tissues, which can contribute to local and systemic side effects much like their oral counterparts [61]. Further limitations of standard topical ear drops include low patient compliance, particularly when self-medicating and for treatment durations greater than one week, associated with high dosing frequency and difficulty of administration [62–64]. An ideal controlled release system should be simple to use and deliver to the middle ear an antibiotic dose closer to the target MIC at a frequency that is manageable by patients and/or their caregivers.

1.2.3 Sustained and Controlled Drug Delivery for Otitis Media Treatment

Accordingly, research has focused on expanding and improving topical antibiotic treatment to address the aforementioned shortcomings. Studies by Otonomy, Inc. have shown success in releasing drugs from hydrogel vehicles placed either via intratympanic injection or during tympanostomy surgery [65–67]. While sustained release and efficacy in clearing infection and inflammation were observed from 2 weeks to 3 months, these systems require invasive procedures. Further, the gel cannot be retrieved from the middle ear if there are complications and long-term

toxicity effects due to degradation byproducts have not been investigated. Topical sustained release systems have also been investigated to improve AOM treatment in cases with intact TMs, including ciprofloxacin-loaded hydrogels augmented by combinations of chemical permeation enhancers (CPEs), which resulted in increased transtympanic permeation [57,68,69]. However, CPEs carry a risk of toxic side effects [70] and have been shown to be cytotoxic during the preclinical validation of this system, with only 20% keratinocyte viability after 3 days [68]. Further, recent studies suggest that outcomes may be improved when antibiotic treatment lasts 10 or more days [71], currently unachievable by these hydrogel-only systems. Achieving this duration of drug release typically requires a secondary controlled release vehicle such as hydrolytically degradable polymer microspheres [29]. Degradable microspheres offer the ability to sustain delivery of drug for an extended period of time from a single, localized dose, tunability for various drugs and dosing ranges, and consistent daily release of therapeutic concentrations [57].

1.3 Chronic Tympanic Membrane Perforation

1.3.1 Incidence and Severity of Tympanic Membrane Perforations

Perforation of the tympanic membrane (TM) is common due to infection or trauma, and particularly large or chronic perforations can be non-healing [72]. Approximately 6-46% of such injuries are non-healing, with the remainder requiring up to 8 weeks for complete closure [73,74]. Even complete healing of the TM can take weeks or months, during which time patients are more susceptible to infection and can experience tinnitus, vertigo, or loss of hearing during the healing phase. The estimated prevalence of chronic TM perforation is 5 out of every 1000 patients [75].

Developing nations and active military zones have been associated with even higher rates of traumatic TM injury, particularly due to pressure-induced rupture [76,77].

1.3.2 Current Clinical Standards and Associated Shortcomings

Clinical work to this point has been limited to smaller perforations, many of which heal spontaneously [78]. Non-healing TM perforation or rupture is thought to be due to decreased regenerative activity at the margin of the perforation [79]. Despite some discussion surrounding the correct treatment of curled or abnormal TM edges [80,81], the current standard is generally myringoplasty or tympanoplasty. These surgical techniques seek to close the compromised TM using a graft or synthetic material, which dramatically decreases the risk of infection. However, these interventions carry risk of temporary or permanent nerve damage, hearing loss, tinnitus, or dizziness, and outcomes tend to be more severe for larger perforations [82]. In the previously cited prevalence study, over 88% of subjects with chronic perforations were opposed to the idea of surgical grafting [75]. These data suggest a need for alternative treatment methods that can induce or accelerate healing in the context of a minimally or noninvasive, conservative treatment approach.

1.3.3 Grafting, Growth Factor, and Stem Cell Treatment

Accordingly, recent research has focused on expanding and improving treatment options to address the aforementioned shortcomings using standard tissue engineering strategies [23,83] . Naturally derived or synthetic alternatives to autologous grafts have been investigated, including paper patch [84,85], 3D printed polymer scaffolds [86], gel foam [80], collagen [87–89], silk [88–

91], atelocollagen [79], alloderm [92], and other natural material-derived patches [93–97]. In large perforations, patch administration does in fact shorten the healing time and reduce the need to repeat procedures but may cause increased otorrhea [80,84,85].

The administration of soluble factors, either alone or embedded in an appropriate scaffold material, has shown promise, particularly in small perforations. This includes ofloxacin [98,99], epidermal growth factor (EGF) [97,100,101], human umbilical cord serum [102], and fibroblast growth factor 2 (FGF-2) [79,103–105]. The use of FGF-2 in particular has been reported to modulate the rate of healing for small perforations (≤25% of total TM area) in clinical studies [106,107]. Some forms of FGF has also been approved by the FDA for applications such as side effects of bone marrow transplants [108].

One recent study demonstrated regeneration of a large perforation (60% of TM area) in Sprague Dawley rat model [109] after four weeks of non-healing. A hybrid polycaprolactone/collagen/alginate scaffold impregnated with mesenchymal stem cells (MSCs) was affixed to the remaining TM tissue using fibrin glue. MSCs are multipotent stem cells that can be isolated from adipose, bone marrow, or other tissues and are involved in most phases of wound healing [110]. All perforations treated with MSCs healed, compared to only 72% of controls. Similar results have been shown for embryonic stem cells [106,111] and with MSCs in separate mouse models [112–114]. These results tend to suggest a high regenerative capacity of MSCs, potentially greater than that of single growth factor (GF) administration. This may be due to a lack of biologically-relevant circumstances in simple soluble GF administration. For example, it has been shown that extracellular vesicles (EVs) serve as a significant reservoir for FGF-2 and that stimulatory effects on cell growth and proliferation are diminished in vesicle free media [115]. The binding of endogenous FGF-2 to cell-surface/extracellular proteoglycans (some of which are

membrane-bound on EVs) has also shown increased activity during angiogenesis [116]. This binding and secretion behavior is not captured in single GF administration, nor is the traditional gradient-like pattern of vesicle shedding characteristic of many wound healing applications [117]. These concerns can be addressed with controlled delivery of growth factors for tissue engineering applications [7].

1.4 Specific Aims and Hypotheses

1.4.1 Specific Aim 1: Development and Testing of a Topical Controlled Release System to Release Clinically Relevant Therapeutic Levels.

Sub-Aim 1a: Development and testing of a topical controlled release system to release clinically relevant antibiotic levels.

Hypothesis 1a: This aim tested the hypothesis that a thermoresponsive gel/microsphere system will encapsulate and release therapeutically relevant levels of antibiotics for treatment of acute otitis media, with *in vitro* safety and efficacy demonstrated by lack of cytotoxicity and ability to kill bacterial culture.

The objectives of this sub-aim were to:

- Optimize encapsulation and release of antibiotics, specifically ciprofloxacin and ceftriaxone, from MS in a linear manner over 14 days.
- Characterize morphology and material properties of microspheres and gel.
- Test preliminary safety and efficacy of microsphere formulations using *in vitro* cytotoxicity and bacteria killing assays.

Sub-Aim 1b: Development and testing of a topical controlled release system to encapsulate and release stem cell secretome.

Hypothesis 1b: This aim tested the hypothesis that a thermoresponsive gel/microsphere system will encapsulate and release free and extracellular vesicle-bound pro-regenerative factors from mesenchymal stem cell conditioned media, with *in vitro* safety and efficacy demonstrated by scratch wound healing and lack of cytotoxicity.

The objectives of this sub-aim were to:

- Optimize encapsulation and release of mesenchymal stem cell conditioned media for release of extracellular vesicles and soluble growth factors relevant to tympanic membrane regeneration over 21 days.
- Characterize morphology and material properties of microspheres.
- Test preliminary safety and efficacy of microsphere formulations using *in vitro* cytotoxicity and scratch wound proliferation assays.

1.4.2 Specific Aim 2: Assessment of Transtympanic Permeability, Safety, and Efficacy Using *Ex Vivo* and *In Vivo* Acute Otitis Media Models.

Hypothesis: This aim tested the hypotheses that sufficient levels of released drug can diffuse across the tympanic membrane in an *ex vivo* model of transtympanic permeability and that the new drug release system can be safe and effective *in vivo*, as demonstrated by testing for clearance of infection and lack of irritation due to drop placement. Results of the *ex vivo* studies helped guide development in Specific Aim 1a and serve as justification to proceed to *in vivo* studies.

The objectives of this aim were to:

- Quantify ciprofloxacin penetration through tympanic membranes in an *ex vivo* setup.
- Determine preliminary *in vivo* efficacy of ciprofloxacin and ceftriaxone-loaded microsphere/gel drop in chinchilla acute otitis media disease model.
- Determined preliminary safety profile of blank, ciprofloxacin, and ceftriaxone-loaded microsphere/gel drop in chinchilla acute otitis media disease model.

1.4.3 Specific Aim 3: Demonstration of Tympanic Membrane Healing *In Vivo*.

Hypothesis: This aim tested the hypothesis that mesenchymal stem cell conditioned media and conditioned media-loaded polymer microspheres/gel drop can increase wound healing of *in vivo* tympanic membrane perforation with a lack of irritation due to placement of materials. These studies help further inform development of the delivery system in Specific Aim 1b.

The objectives of this aim were to:

- Determine preliminary efficacy of MSC CM and CM-loaded microspheres in a guinea pig non-healing TM perforation model.
- Determine preliminary safety profile of MSC CM and CM-loaded microspheres in a guinea pig non-healing TM perforation model.

1.4.4 Impact of Dissertation and Specific Aims

There is a clear need for safe, simple, and effective drug delivery to the ear. The goal of the studies described herein was to develop and test an innovative method of sustained presentation

of antibiotics and stem cell secretome to and across the TM. Previous work by this group has shown that ocular permeability barriers can be overcome using a validated drug delivery system including a topical, thermoresponsive gel depot containing drug-loaded PLGA microspheres [118,119]. Although there are similarities in these topical routes of administration which indicate the potential for the system to be effective as an otic topical drug delivery system, the drug presentation to the ear anatomy is quite different from ocular presentation and lends to novelty of the system. Therefore, the sustained presentation afforded by the stable gel depot is proposed to allow a therapeutically relevant amount of drug to penetrate the TM without harmful additives. We hypothesized that development and optimization of a novel drug delivery system can noninvasively sustain localized release of antibiotics and stem cell secretome to the TM and middle ear, as demonstrated by *in vitro, ex vivo,* and *in vivo* testing.

Development of materials in Specific Aim 1 can establish a drug delivery platform for topical treatment of the TM and middle ear, specifically with optimization of MS for release of antibiotics, ciprofloxacin and ceftriaxone, as well as mesenchymal stem cell conditioned media. This also allowed for development of methods for tailoring of this drug delivery platform for different release profiles and durations for various treatment needs and expanding the platform for encapsulation of other therapeutics for delivery both to the ear and other applications. *In vitro* material safety and efficacy testing in Specific Aim 1 also served as indication of preclinical potential and justification to proceed with *in vivo* testing upon optimization of the materials.

In addition to *in vitro* efficacy testing in Specific Aim 1a, Specific Aim 2 investigated *ex vivo* permeability of antibiotic released from hydrolysable MS retained in gel carrier compared to permeability due to topical administration of standard antibiotic drops used clinically. As the goal of this dissertation work was to avoid chemical permeation enhancers for use with intact TMs,

these *ex vivo* permeability studies served as indication that sufficient antibiotic levels can permeate into the middle ear compared to the standard topical drops and based on antibiotics' minimum inhibitory concentration for clearance of the most prevalent bacteria present in OM. In conjunction with *in vitro* efficacy data, these studies served as justification to proceed to testing in an animal model of OM, which provided insight into *in vivo* safety and efficacy, as well as future directions for further optimization of materials for improved efficacy.

Specific Aim 3 expanded upon *in vitro* efficacy results in Specific Aim 1b to determine effects on wound healing and development of a preliminary safety profile due to administration of CM-loaded MS/gel treatment compared to treatment with topical CM drops. This will build upon and add to prior studies indicating positive effects on wound healing due to growth factor and/or stem cell therapy, allowing for further development of stem cell secretome-based therapies. This study also allowed for development and future directions for optimization of a guinea pig model of chronic TM perforation, as well as providing insight on best practices for administration and removal of the drug delivery system to improve upon potential for eventual clinical translation.

The drug delivery platform is unique in that it would require only a single drop for the duration of treatment and will provide clinically relevant levels of therapeutic to the target area in a controlled and safe manner. Gel-based drug delivery to the middle and inner ear has previously been shown to be possible with intratympanic injection or facilitated by chemical permeation enhancers [57,65,67,120]. Intratympanic injections involves an invasive procedure and CPEs come with risk of side effects due to the harsh nature of the chemical additives [70]. In contrast, a topical controlled release system that works via continuous drug presentation at the TM may offer an alternative treatment option. Furthermore, the isolation and therapeutic use of MSC secretome is an emerging field that therefore endows all new methods and discoveries with a level of

innovation. The application of such secreted material in the ear, particularly for TM regeneration, is (to our knowledge) unexplored, given that it is such a specialized field. However, the ear offers easy access and has shown potential compatibility with MSC-based regenerative strategies [109], making it an ideal system for advancing the knowledge and translational potential of secretome-based therapeutics. This proposed system may be the first fully acellular yet cell-mimetic tissue engineering approach to treatment of TM perforation.

Patient compliance may be dramatically improved, as only a single, clinician-administered drop will be needed for treatment. Side effects may be mitigated due to localization to the middle ear and minimization of applied drug. Removal of the non-degradable gel upon completion of treatment duration may further reduce long-term adverse side effects due to lingering material or degradation products, though specific removal techniques must further be investigated.

Furthermore, our system uses well-characterized biodegradable polymer matrices, proven safe and capable of higher initial loading, endowing our system with sustained drug release in a longer and more consistent manner than current investigational methods [121]. The proposed treatment modality has shown success in topical ocular delivery [118,119,122], and thus, delivery to the ear is a natural and important extension of this unique technology. Further optimization of the CM-loaded MS formulation would allow for development of a precise regenerative material that may be more suitable to the distinctive environment surrounding the TM than cell therapy, particularly the potential for increased FGF activity through inclusion of EVs in the encapsulated secretome. Finally, our methods result in biomaterials that behave more like stem cells than artificial vesicles or single growth factors with capability of releasing regenerative factors and EVs in a gradient-like pattern. Therefore, we have developed a drug delivery platform for otic drug delivery that can be adapted for a variety of therapeutics, treatment durations, and conditions.

2.0 Development and Testing of a Topical Controlled Release System to Release Clinically Relevant Antibiotic Levels

2.1 Introduction

2.1.1 Ciprofloxacin Use for Otitis Media Treatment

Ciprofloxacin is an ideal candidate for encapsulation and has been extensively utilized in the aforementioned gel-based studies due to local toxicity effects of other standard topical antibiotics including tobramycin, neomycin, and gentamycin [53,123], effects which have not been observed due to ciprofloxacin treatment [124]. It is current standard prescribed oral and topical antibiotic due to a long track record of safety and efficacy as well as FDA approval. Further, ciprofloxacin is a fluoroquinolone that affects most of the microorganisms responsible for OM, and although it is a rarely occurring pathogen in AOM, ciprofloxacin is in fact the only antibiotic that treats *Pseudomonas*-based OM [53,124]. Minimum inhibitory concentrations (MIC) to clear 50-90% of *Haemophilus influenzae* and *Streptococcus pneumonaie* isolates are, respectively, 0.03 and 0.5-2μg/mL [59,60]. Because of these factors, several previous studies of sustained or controlled release systems have also investigated ciprofloxacin delivery for treatment of otitis media [57,67–69,120].

2.1.2 Ceftriaxone Use for Otitis Media Treatment

Several of the bacterial strains most common in OM, including *H. influenzae* and *S. pneumoniae* readily form biofilms, which may inhibit the effectiveness of antibiotic therapy [10,54]. Although less commonly used than other treatments, the current treatment when there is suspicion of resistance or low patient compliance is a three-day course of intramuscular ceftriaxone treatment, which has shown to be as effective as a two-week treatment course of amoxicillin and has proven effective in treatment of penicillin-resistant infections and persistent *Streptococcus*-based infections [125–129]. Ceftriaxone is administered via intramuscular injection rather than orally due to poor permeability and instability in the gastrointestinal environment. To address this issue, one recent study investigated oral delivery of ceftriaxone via a nanoemulsion-based drug delivery system in conjunction with permeation enhancers [130]. Ceftriaxone is an effective treatment for clearance of both gram-positive and gram-negative bacteria, with MIC required to clear 90% (MIC_{90}) of various bacteria ranging 0.03-2µg/mL, specifically MIC_{90} of 0.03µg/mL for *H. influenzae* and MIC_{50} and MIC_{90} of 0.06µg/mL and 2µg/mL for *S. pneumonaie* [59,60,131].

Therefore, to maximize efficacy of treatment, ciprofloxacin and ceftriaxone were chosen for encapsulation in the drug delivery system described herein. Further, to our knowledge, ceftriaxone has not been encapsulated in a topical drug delivery system previously.

2.2 Materials and Methods

All materials were obtained from Sigma-Aldrich (St Louis, MO) unless otherwise noted.

2.2.1 Ciprofloxacin-loaded Microsphere Formulation

Ciprofloxacin-loaded microspheres (MS) were prepared using a water-in-oil-in-water (W/O/W) double emulsion procedure adapted from previous work [38,121,132]. To prepare the MS, 200mg poly(lactic-co-glycolic) acid (PLGA) (MW 24-38 kDa; viscosity 0.32-0.44dL/g) were dissolved in 4mL dichloromethane to which 250µL of 100mg/mL ciprofloxacin in 1M acetic acid was added. The dissolved drug and polymer mixture were then sonicated for 10 seconds at 30% amplitude (EpiShear Probe Sonicator, Active Motif, Carlsbad, CA) followed by homogenization in 60mL of 2% poly(vinyl alcohol) (PVA) (Polysciences, Warrington, PA) for 1 minute at 7000rpm (Silverson L5M-A, East Longmeadow, MA). The resulting liquid-phase emulsion was added to 80mL of 1% PVA and stirred at 600rpm for 3 hours, resulting in precipitation of solid MS. Drug-loaded and blank MS, fabricated by substituting deionized (DI) water for aqueous drug, were then washed 4 times by centrifugation, resuspended in DI water, flash frozen in liquid nitrogen, and lyophilized for 48-72 hours (Benchtop Pro, SP Scientific, Warminster, PA).

2.2.2 Ceftriaxone-loaded Microsphere Formulation

Ceftriaxone-loaded MS were prepared using similar steps as above via an oil-in-water (O/W) single emulsion procedure in which 200µL of a 30mg/mL solution of ceftriaxone in dimethyl sulfoxide (DMSO) was added to dissolved polymer and followed by homogenization and

subsequent precipitation, lyophilization, and washing steps as described above, with an appropriate amount of NaCl added to PVA to balance the osmolality of the ceftriaxone solution. Blank MS were fabricated using the same methods, with DMSO alone substituted for ceftriaxone dissolved in DMSO.

2.2.3 Antibiotic-loaded Microsphere Morphology Characterizations

Size, shape, porosity, and drug loading and release were characterized for each set of MS prepared. Scanning electron microscopy (SEM) was used to examine shape and morphology of all MS formulations (JEOL JSM 6335F, Peabody, MA). MS diameter was quantified by volume impedance measurements with mean and standard deviation determined for n=15,000 MS per sample (Multisizer, Beckman Coulter, Brea, CA). Density of MS was determined via a measurement device custom-made using a 1mL syringe (Figure 3). A known mass, approximately 15-30mg, of MS was added and MS packed by pushing down on the plunger, allowing for volume to be determined and density calculated from the known mass and volume.

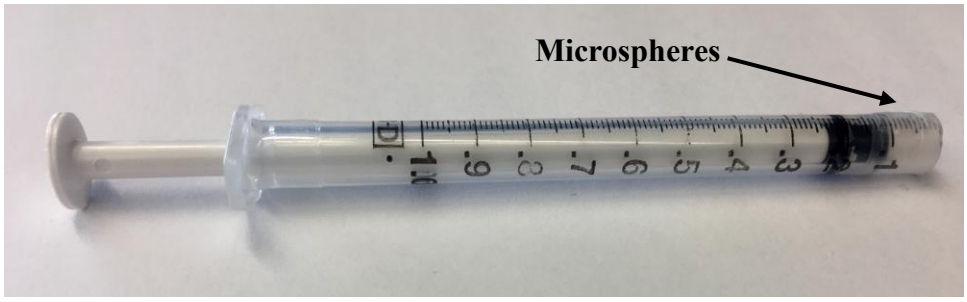

Figure 3: Custom syringe mechanism to measure density of microsphere formulations.

2.2.4 *In Vitro* Drug Release from Antibiotic-loaded MS

In vitro drug release kinetics were determined using 10mg of MS suspended in 500mL phosphate buffered saline (PBS) and continuously rotated at 37ºC. The supernatant was removed via centrifugation every 24 hours and replaced with fresh PBS. For each formulation, total drug loading was taken to be cumulative drug release when all MS were fully degraded, and therefore drug release was exhausted, after 14 days.

Ciprofloxacin concentration in the supernatant was quantified via UV/Vis absorbance measures taken at 246nm (SoftMax Pro 5, Molecular Devices, Sunnyvale, CA), with background signal from blank MS subtracted from each measurement and regressed against the standard curve, validated for 1-10µg/ml. High performance liquid chromatography (HPLC; 1220 Infinity LC, Agilent Technologies, Santa Clara, CA) using the following settings was used to confirm: Kromasil C18 column (4.6mm x 150mm, 3.5µm particles), 10µL injection volume, 80:20 acetonitrile:0.1% trifluoracetic acid mobile phase, 1mL/min flow rate, detection at 275nm. This method has been reported previously [57] and validated for the range 100ng/mL-10mg/mL.

Ceftriaxone concentrations were quantified using the following settings adapted from previously reported studies [133]: reverse phase Zorbax Eclipse Plus C18 Column (4.6mm × 150 mm, 5µm particles), 20µL injection volume, 70:5:25 HPLC water:acetic acid:acetonitrile mobile phase, flow rate 1mL/min, detection at 254nm.

2.2.5 Cytotoxicity Assays

Cytotoxicity of the MS was analyzed by both Vybrant MTT (3-(4,5-dimethylthiazol-2yl)-2,5-diphenyltetrazolium bromide) Cell Proliferation Assay Kit and LIVE/DEAD

Viability/Cytotoxicity Kit (Thermo Fisher Scientific, Waltham, MA). Studies were carried out using human primary epidermal keratinocytes (ATCC, Manassas, VA), the primary cell type found in TM tissue [125]. To perform the assay, ~3,000 cells/well were plated in 96 well plates and incubated in 200µL Dermal Cell Basal Medium with Keratinocyte Growth Kit (ATCC) for 24h at 37°C with 5% CO_2 to achieve a monolayer. Cells with medium only were used as the positive control for viability in both assays and cells incubated with 70% methanol for 5-10mins prior to each assay were used as a negative control, per kit instructions. All test groups included 100µL medium and 100µL test material: PBS, 1µg/mL ciprofloxacin (CIP), 5µg/mL ceftriaxone (CFX), 1mg blank MS, 1mg CIP MS, 1mg CFX MS, blank MS releasate, CIP MS releasate, CFX MS releasate. Releasates were collected via the same methods as described above, with only 24h releasates used for this study as highest release for both antibiotics are seen after 24h: 0.79 ± 0.13µg ciprofloxacin and 1.58 ± 0.04µg ceftriaxone. Once a monolayer of cells was achieved, treatment groups were applied and incubated for an additional 24h. Microspheres were also applied (1mg MS in 200µL basal medium) to wells with no cells to account for any background signal. MTT assay was performed by additional incubation for 4h with 10µL MTT stock solution, followed by incubation for 10mins with 50µL DMSO. Absorbance in each well was then determined via spectrophotometer at 540nm. Percent viability was determined by normalizing to 100% viability in the positive control group.

For the LIVE/DEAD assay, the same test groups were used as above. The assay was performed via addition of 100µL LIVE/DEAD working solution (2µm calcein AM/4µm ethidium homodimer-1) to each well and incubating for 45 minutes at 25°C prior to measuring absorbance at 530nm and 645nm to detect live and dead cells, respectively. Percent viability was determined

by normalizing to 100% viability in the positive control group. The mean and standard deviation absorbance values for both assays were determined for n=3 samples in each test group.

Gel cytotoxicity has been previously investigated and reported by Fedorchak et al [38].

2.2.6 *In Vitro* Bacteria Killing

Non-typeable *Haemophilus influenzae* (strain 86-028NP) bacteria were cultured at a concentration of approximately 10^6 CFU/mL. To these bacterial cultures, treatment groups of blank MS, ciprofloxacin-loaded MS, ceftriaxone-loaded MS, 1µg/mL ciprofloxacin, 5µg/mL ceftriaxone, or no treatment were applied. All MS groups were added in a concentration of 10mg MS/mL bacterial culture medium to approximate intended treatment dose of 10mg MS, containing 2.56 ± 0.14µg ciprofloxacin or 2.71 ± 0.03µg ceftriaxone. Concentrations of free antibiotic for positive controls were chosen based on literature values for minimum inhibitory concentrations of ciprofloxacin and ceftriaxone to *H. influenzae* and other relevant bacteria [59,60] and were confirmed by this group. After incubation for 24-48 hours at 37°C, viable bacteria were counted by serially diluting the cultures followed by plating on agar plates and incubating at 37°C for 24-48 hours.

2.2.7 Thermoresponsive Gel Formulation and Scale Up

The gel was prepared via free radical polymerization of 500mg N-isopropylacrylamide (NIPAAm) (Fisher Scientific, Waltham, MA) and 500µL poly(ethylene glycol) (PEG; MW ~200kDa), in the presence of 9.44mL DI water, 50µL of 100mg/mL ammonium persulfate (APS), and 20 µL tetramethylethylenediamine (TEMED). The gel precursor was refrigerated for 24h and

then washed in DI water at ~40ºC. This formulation is a 10x scale up of a previously reported gel fabrication method [37,38,135].

2.2.8 Thermoresponsive Gel Characterization

The gel formulation underwent testing for degradation rate, swelling ratio, and lower critical solution temperature (LCST) as previously reported [38,135]. LCST was determined via UV/Vis absorbance measurements at 415nm over a temperature range of 25-40°C, increased by 1°C increments and allowing 15 minutes between readings for temperature equilibration.

Degradation rate was determined by comparing solid fraction of liquid gel at baseline and every 7 days for 28 days in the gel phase, with the gel stored in PBS at 37°C. Solid fraction was quantified by the following formula, where Wi refers to mass of gel on day i = 7, 14, 21, 28:

$$Solid\ fraction = \frac{Wi - \text{ave}(Wd)}{Wi} \qquad \textbf{Equation 2-1}$$

Swelling ratio was determined by placing 100µL of gel in 37°C for 72h or until the liquid was fully evaporated. Dry mass was compared to swollen mass prior to evaporation for n=3 samples. Swelling ratio (SR) was determined by the following formula, where Ws refers to mass of swollen gel in water and Wd refers to dry gel:

$$SR = \frac{Ws - Wd}{Wd} \qquad \textbf{Equation 2-2}$$

To qualitatively analyze retention of gel in the ear canal, a transparent plastic human ear model was used. A 300µg/mL solution of fluorescein isothiocyanate (FITC) in DI water was prepared and 50µL of the solution was added and mixed with 200µL of gel. Using a 1mL syringe with capillary tubing attached to the tip, 100µL of fluorescently dyed gel was applied to the ear canal on the tympanic membrane. The model was placed in a 100mL beaker with the ear canal facing up and left in a 37°C incubator for 30 minutes for the gel to solidify. After 30 minutes, the ear model was removed from the beaker and placed in the incubator with the ear canal perpendicular to the bottom of the incubator. The ear model was evaluated by visual inspection and photography after 2, 3, and 24 hours.

2.2.9 Auditory Brainstem Responses

Animal studies conformed to the NIH Guide for Care and Use of Laboratory Animals and all procedures were approved by the University of Pittsburgh IACUC. Two groups of n=3 guinea pigs were used to test the effect of the administration of the gel system on conductive hearing sensitivity using the auditory brainstem response (ABR) with free-field sound presentation. Each animal underwent ABR testing under the following conditions: both ears unplugged, left ear plugged with foam and dental silicone, left ear plugged and gel applied to the right ear, gel in right ear after removing plug from left ear, both ears unplugged after removal of gel. To plug the left ear, a piece of foam was inserted into the ear canal, covered with vinyl polysiloxane impression material (Examix NDS, GC America, Alsip, IL), and allowed to set for 5 mins. Gel was instilled in volumes of 25 or 100 µL to the right ear using a 200µL pipette and allowed to set for 5 mins. Gelation and presence of gel in the ear canal were confirmed via visual inspection.

ABR experiments were performed under 1-2% isoflurane anesthesia, with ABR acquired via three subcutaneous electrodes (27-gauge needle electrodes, Rochester Electro-medical) placed at standard locations (signal – vertex of skull, reference – below pinna overlying mastoid, ground – below the other pinna). Click stimuli (100μs long) with alternating polarity repeating every 100ms (10 per second) were presented ~1000 times each at 14 sound levels (5dB-75dB in 5dB steps), with the loudest sound level presented first (total duration ~27min). ABR signals were collected at 30kHz sampling rate and bandpass filtered (200-2000Hz). A rejection criterion of peak-to-peak response greater than 50μV was used to discard trials that included potential artifacts. The distributions of baseline fluctuations at each sound level was obtained from a 2.5-ms segment of the ABR recording just prior to the onset of each click. Wave 1 of the ABR at the loudest stimulus level was defined as the first positive peak after stimulus onset. At the other sound levels, wave 1 was defined as the first positive peak occurring at a time equal to or later than wave 1 at the loudest level. The peak-to-peak amplitude (wave 1 trough to wave 2 peak) was taken as the ABR amplitude on each trial. The hearing threshold of the tested ear was taken to be the lowest sound level at which the mean ABR amplitude exceeded 4 standard deviations of the distribution of baseline fluctuations.

2.2.10 Statistical Analysis

Data for *in vitro* release assays, MS density, gel degradation, and cytotoxicity testing are represented as average ± standard deviation for at least n=3 samples. Volume impedance measurements of MS diameter are represented as average ± standard deviation for n=15,000 particles per sample. Gel degradation data were compared using Student's t-test at each time point. Auditory brainstem response threshold shifts from baseline were analyzed using Kruskal-Wallis

test with Dunn's post-hoc testing within each group and Mann Whitney U test for comparison between applied gel volumes. All statistical analyses were performed using GraphPad Prism software (San Diego, CA).

2.3 Results

2.3.1 Ciprofloxacin-loaded MS Release Profile

Ciprofloxacin release was quantified via HPLC using the standard curve shown in Figure 4. Release can also be quantified via spectrophotometry using the standard curve shown in Figure 5. Release of ciprofloxacin follows an approximately linear pattern over 14 days, resulting in approximately 2.56 ± 0.14µg released from 10mg MS (Figure 6).

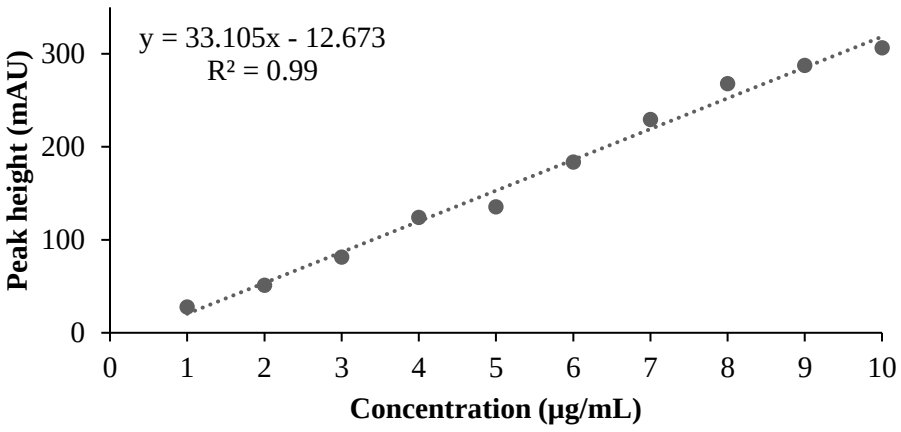

Figure 4: Ciprofloxacin standard curve determined using high performance liquid chromatography.

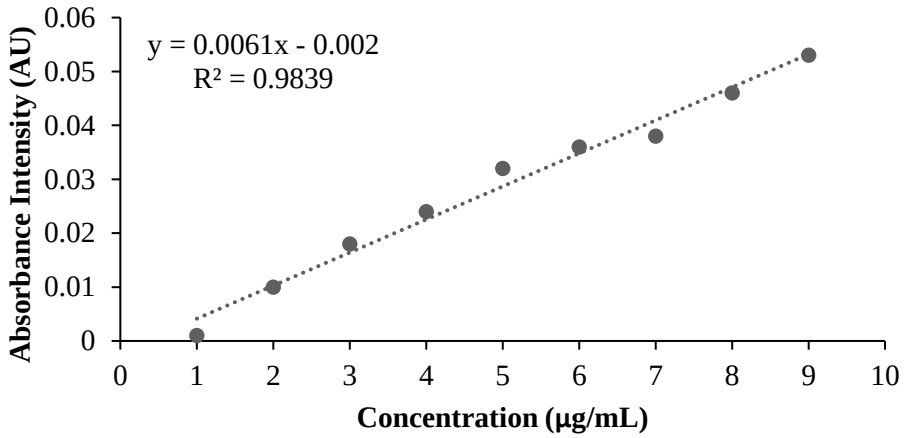

Figure 5: Ciprofloxacin standard curve determined using UV/Vis spectrophotometry.

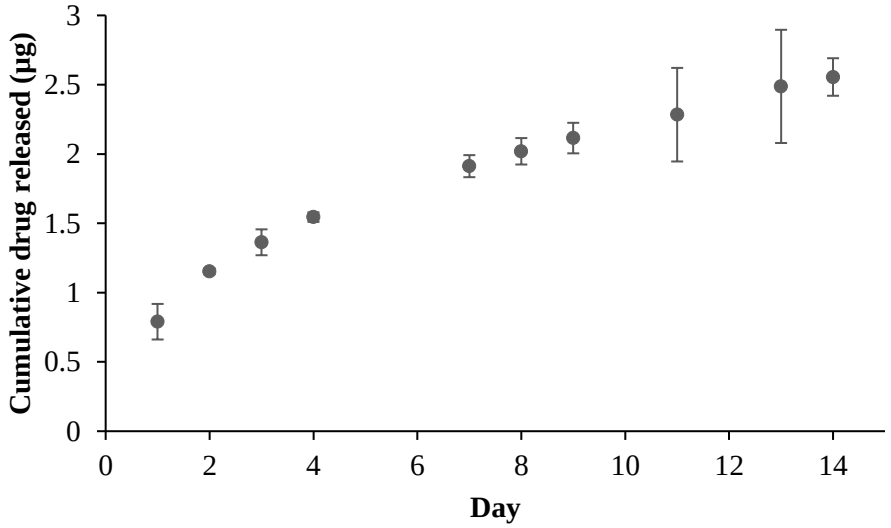

Figure 6: *In vitro* antibiotic release from 10mg ciprofloxacin-loaded microspheres over 14 days. Error bars represent the mean ± standard deviation for n=3 samples.

2.3.2 Ceftriaxone-loaded MS Release Profile

Release was quantified via HPLC using the standard curve shown in Figure 7. Ceftriaxone-loaded MS demonstrate 58% burst release on Day 1 followed by linear release over 14 days, resulting in approximately 2.71 ± 0.03µg released from 10mg MS (Figure 8).

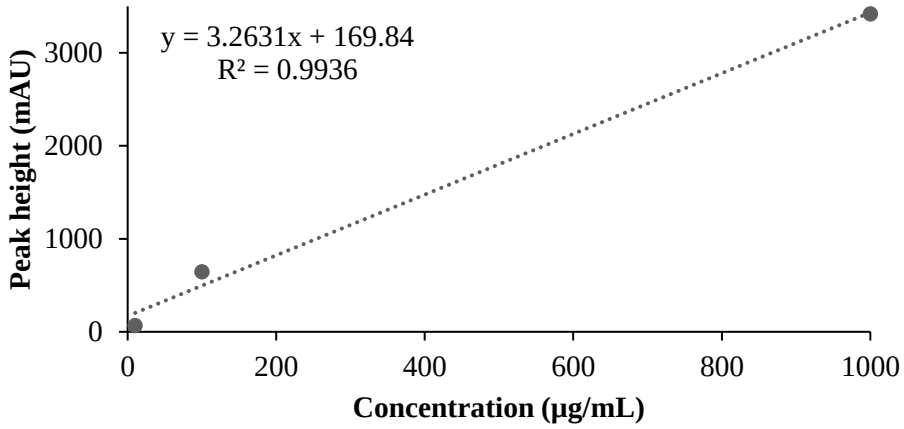

Figure 7: Ceftriaxone standard curve determined using high performance liquid chromatography.

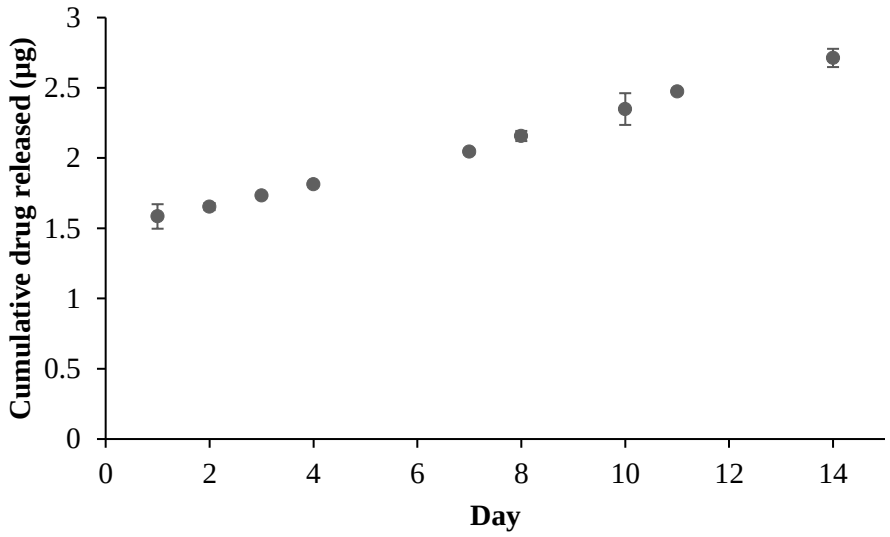

Figure 8: *In vitro* antibiotic release from 10mg ceftriaxone-loaded microspheres over 14 days. Error bars represent the mean ± standard deviation for n=3 samples.

2.3.3 Antibiotic-loaded MS Morphology

Scanning electron microscopy images (Figure 9) confirm spherical morphology of MS. Volume impedance measurements of microsphere diameter (Table 1) confirm visual analysis of microsphere size with SEM and are consistent with previously observed diameter ranges for similar microsphere formulations developed by this group [114,115]. Ceftriaxone MS diameter was adjusted to larger diameter by decreasing homogenization speed during fabrication to reduce initial burst release and slow degradation rate to extend treatment duration [25].

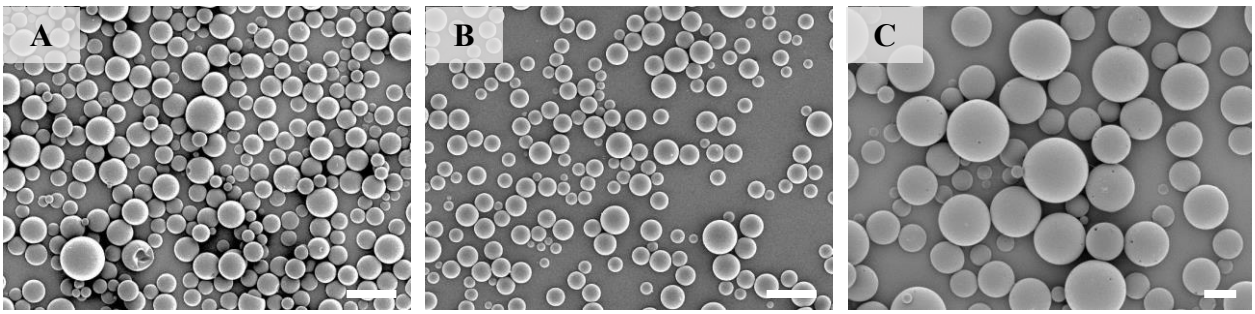

Figure 9: Scanning electron microscopy images of A) blank, B) ciprofloxacin-loaded, and C) ceftriaxone-loaded microspheres. Scale bar = 10μm.

Table 1: Average diameters and densities of blank, ciprofloxacin, and ceftriaxone microsphere formulations.

Microsphere type	Diameter (μm)	Density (mg/mL)
Blank	7.85 ± 5.37	776.9 ± 21.6
Ciprofloxacin	6.88 ± 3.36	752.5 ± 22.6
Ceftriaxone	16.69 ± 5.65	650.7 ± 25.1

2.3.4 Cytotoxicity Due to Antibiotic-loaded MS and Releasates

Both MTT and LIVE/DEAD viability assays suggest acceptable levels of cytotoxicity [136–138] following 24h of treatment with aqueous drug, blank and drug-loaded microspheres, and microsphere releasates (Figure 10). Aqueous ciprofloxacin and ceftriaxone resulted in, respectively, 90.4 ± 5.9% and 128.1 ± 8.0% cell viability in the MTT assay and 101.3 ± 0.1% and 94.2 ± 0.2% viability in the LIVE/DEAD assay. Blank, ciprofloxacin-loaded, and ceftriaxone-

loaded MS resulted in, respectively, 66 ± 10.7%, 67.4 ± 7.1%, and 90. 9± 6.0% viability in the MTT assay and 103.6 ± 2.2%, 90.3 ± 4.8%, and 99.3 ± 3.1% viability in the LIVE/DEAD assay. Releasates from blank, ciprofloxacin-loaded, and ceftriaxone-loaded MS resulted in, respectively, 68.8 ± 10.2, 121.8 ± 4.0%, and 86.8 ± 3.8% viability in MTT assay and 97.1 ± 0.8%, 96.5 ± 0.2%, and 57.6 ± 0.4% viability in the LIVE/DEAD assay. Positive controls of medium and PBS resulted in 100 ± 8.2% and 112.8 ± 4.5% viability in the MTT assay and 100 ± 1.2% and 98.8 ± 0.5% viability in the LIVE/DEAD assay. Negative control of 70% methanol resulted in 6.2 ± 0.2% and 7.7 ± 0.01% viability in the MTT and LIVE/DEAD assays, respectively.

The MTT assay is a commonly used method to test medical device-related cytotoxicity; discrepancies between cell viability percentages due to use of different cytotoxicity assays have previously been noted, with the MTT assay more sensitive to detection of cytotoxicity [139,140]. These results support this observation and suggest the microspheres and releasates will be biocompatible *in vivo*. Lack of cytotoxic response due to application of gel has been previously tested and reported [38].

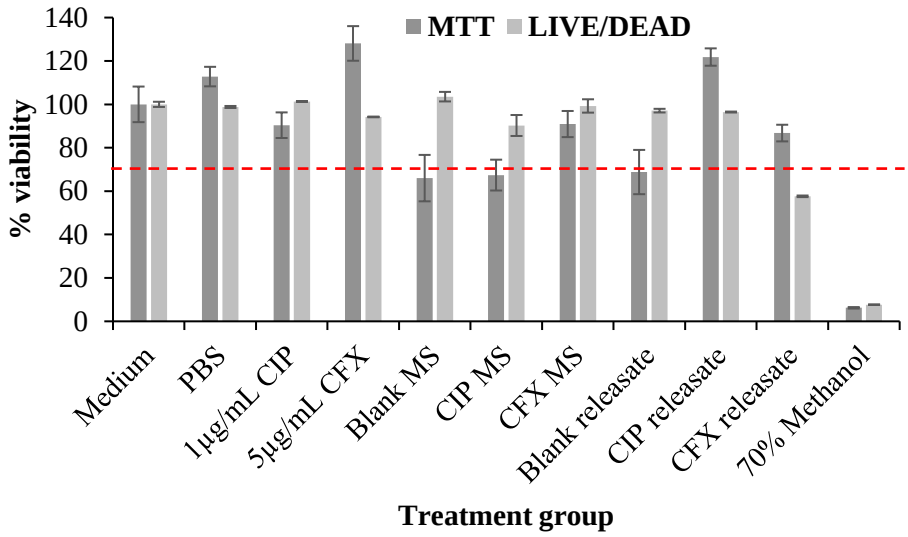

Figure 10: Cytotoxicity due to antibiotics, microspheres, and releasates. Cell viability assays show acceptable levels of cytotoxicity due to application of blank and drug-loaded microspheres and microsphere releasates to human dermal keratinocytes for 24h. Error bars represent mean ± standard deviation for n=3 samples except Medium, PBS, Blank MS, and Blank releasate groups which have n=6 samples. Red dashed line indicates 70% viability, the minimum recommended for medical devices.

2.3.5 *In Vitro* Bacteria Killing

All *H. influenzae* bacteria were cleared after treatment for 24h and 48h with ciprofloxacin-loaded MS, ceftriaxone-loaded MS, free ciprofloxacin, and free ceftriaxone, with significantly reduced bacterial count compared to treatment with blank (no drug loaded) MS and no treatment control (Figure 11). No significant difference between MS groups and releasate groups indicates antibiotic released from MS is as effective at clearing bacterial infection as free antibiotic.

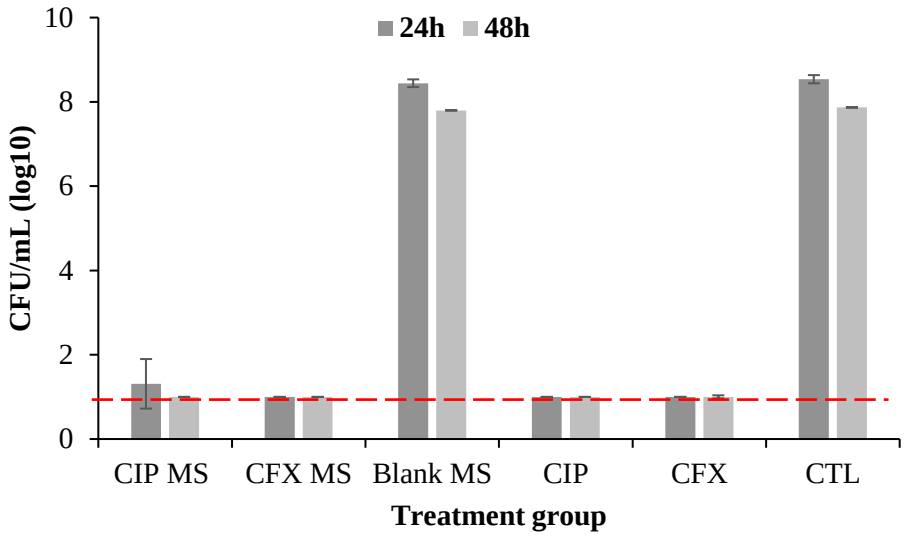

Figure 11: *In vitro* clearance of bacteria treated with antibiotics and microspheres (MS). Clearance of *H. influenzae* after 24-48h due to treatment with ciprofloxacin (CIP) MS, ceftriaxone (CFX) MS, blank MS, 1µg/mL CIP, 5µg/mL CFX, or no treatment control (CTL). MS were applied in concentration of 10mg/mL bacterial culture. Errors bars represent the mean ± standard deviation for n=8 samples for CIP MS and CFX MS groups and n=4 samples for all other groups. Red dotted line indicates complete bacterial clearance.

2.3.6 Thermoresponsive Gel Characteristics

Swelling ratio, which indicates increase in gel weight due to water absorption, was calculated to be 5.13 ± 0.52 for n=5 gel samples and is comparable to previous smaller batch results [38,135] and other groups investigating pNIPAAm based gels [34]. LCST (Figure 12) was determined via spectrophotometric absorbance measurements as ~35.5°C, which is also comparable to previous results and indicates gel can shed its excess water content and transition to solid form at physiological temperatures [38]. No significant change in solid fraction over 28 days (Figure 13) indicates no degradation as expected for non-biodegradable pNIPAAm [28].

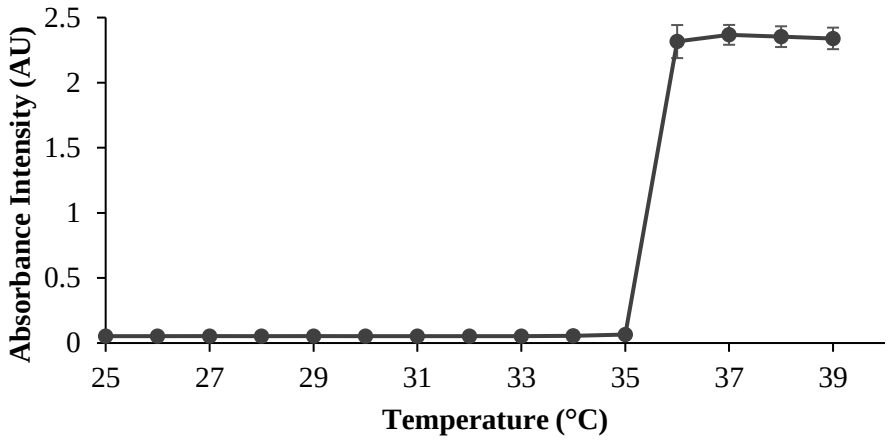

Figure 12: Lower critical solution temperature (LCST) of thermoresponsive pNIPAAm gel. LCST was determined via UV/Vis absorbance measurement at 415nm. Error bars represent mean ± standard deviation for n=3 samples.

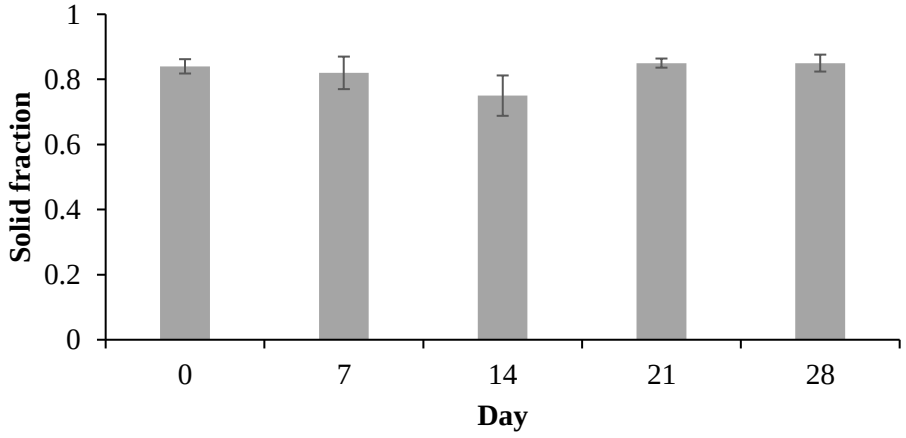

Figure 13: Degradation testing of pNIPAAm gel over 28 days. Lack of degradation was determined by observing no change in solid fraction at 37°C over 28 days. Error bars represent the mean ± standard deviation for n=3 samples. Student's t-test ($p<0.05$) was used to determine significance between each time point.

Thermoresponsive gel was easily applied to the TM of an adult human ear model and retention was confirmed after 3 hours inversion at 37°C (Figure 14). The gel was left in the ear model for up to 24h, however the gel dried due to low-moisture conditions in the incubator, which should not occur *in vivo* due to humidity in the external auditory canal [141]. These results suggest that the gel drop can be instilled to the TM and retained *in situ* for the duration of treatment.

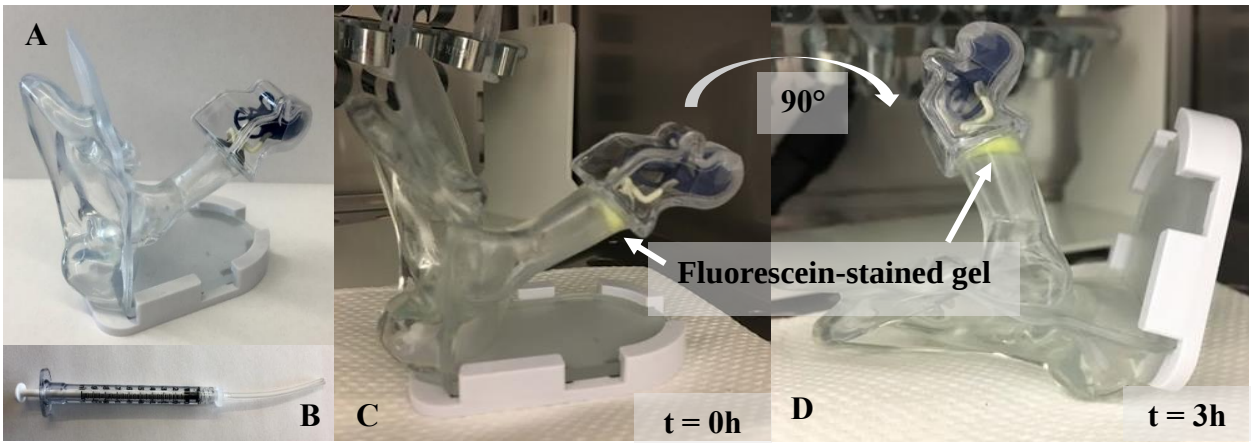

Figure 14: Model of drug delivery system retention. Administration of 100µL gel/MS suspension (gel stained with fluorescein for visualization) to TM in synthetic human ear model (A) using a modified syringe applicator (B). Retention was confirmed after 3 hours inversion (C,D).

2.3.7 Auditory Brainstem Responses

Auditory brainstem responses (Figure 15) in two groups of guinea pigs indicate application of gel to the ear canal results in a similar threshold shift as application of an earplug. All parameters were the same for both groups except volume of gel applied. The testing scenario of 100µL contained n=2 animals, compared to n=3 animals in all other testing scenarios, due to difficulty of

vinyl polysiloxane earplug removal causing perforation of the tympanic membrane in the left ear, confounding the gel-only ABR results for that animal. Subsequent groups consisted of a piece of foam applied to the ear prior to vinyl polysiloxane to prevent TM perforation upon removal. In both groups, there was no significant difference in threshold shift between one ear plugged with ear plug and one ear with 25µL or 100µL gel instilled. In both of these testing scenarios, the other ear was left unplugged. There was no significant difference in hearing threshold shift due to different gel volumes applied. Threshold shift of sound pressure level due to one ear containing either an earplug or gel was significantly different compared to both ears unplugged.

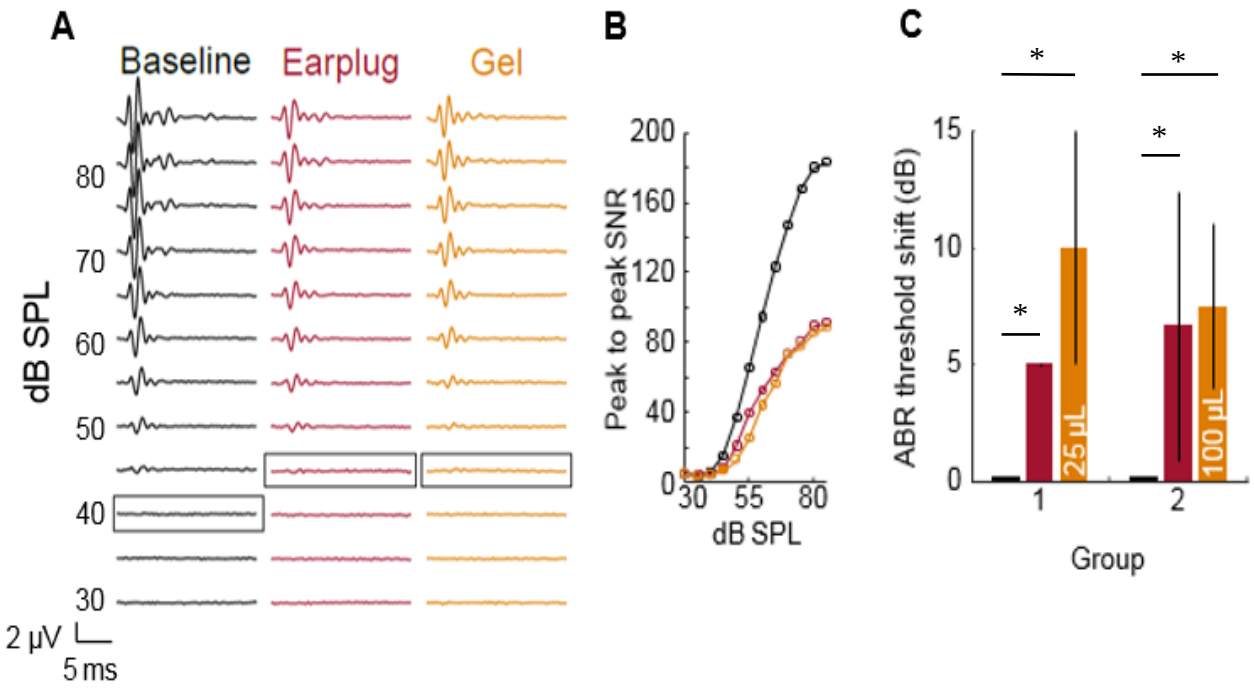

Figure 15: Threshold shifts recorded via auditory brainstem response (ABR) in guinea pigs. Each group was tested with both ears unplugged as baseline, left ear plugged with earplug, and right ear with gel applied. Group 1 received a 25µL gel drop and Group 2 received a 100µL drop. Representative ABR traces (A) and peak to peak signal to noise ratio (SNR) (B) are shown along with threhold shift relative to baseline for each group (C). Threshold shift in sound pressure level (SPL) are indicated with a box (A). Threshold shifts are represented as mean ± standard deviation for n=3 animals per group (n=2 for 100µL gel drop testing scenario). Threshold shifts within each group were analyzed for significance (*$p<0.05$) with Kruskal-Wallis test and Dunn's post-hoc testing. Significant differences were observed due to application of earplug and gel compared to baseline but no significance was observed between earplug and gel application. Significant differences in threshold shift due to applied gel volume were analyzed via Mann Whitney U test and no significance was determined.

2.4 Discussion

As the leading indication for antibiotics prescribed to pediatric patients in the United States, acute otitis media is responsible for over 20 million physician visits annually for the 80% of children who experience AOM [39–41]. In addition to the high incidence of physician visits, recurrent AOM can develop into chronic AOM which may require expensive and invasive surgical intervention and/or result in detrimental long-term effects on hearing, speech, and learning [12,45–50]. Current standards of treatment remain oral antibiotics, which come with risk of systemic side effects and rise of antibiotic resistance [10,41,53,54], and topical antibiotic drops, which come with issues of patient noncompliance due to frequency of dosing regimen and difficulty of administration and risk of local and systemic side effects due to high drug concentration required to overcome permeability barriers in the TM [57,61–64]. For these reasons, drug delivery systems involving thermoresponsive hydrogels with or without degradable microspheres have been investigated in previous research studies [57,65,67–69,120]. The drug delivery system developed by our group aims to improve on these previous studies by incorporating hydrolysable antibiotic-loaded polymeric MS to further control drug release into a thermoresponsive, nondegradable gel carrier that can be applied topically to the TM without need for potentially harmful chemical permeation enhancers.

In vitro release data indicate MS can release sufficient drug to treat the most common bacterial strains present in acute otitis media. Minimum inhibitory concentration to clear 90% (MIC_{90}) of *H. influenzae* is 0.03µg/mL and 1-2µg/mL for *S. pneumonaie* [59,60,131]. Bacteria killing studies confirmed that release from antibiotic-loaded MS can kill all *H. influenzae* bacteria in an *in vitro* solution over 24-48 hours. A standard dose duration for AOM antibiotic prescriptions is 7-14 days [58,71,128], therefore microsphere release was tailored to last the full treatment

duration. High initial antibiotic concentration followed by continuous presentation has been shown to be effective against non-responsive bacteria and biofilms, therefore this release pattern is desirable [125–127,129,142].

To increase clinical translation potential, materials with a proven track record of safety were used in this study. Ciprofloxacin and ceftriaxone are currently frequently used clinically and PLGA-based materials have a strong track record of approval by the United States Food and Drug Administration [15,20,23]. *In vitro* cell viability results shown in Figure 10 confirm these findings with two different cytotoxicity assays [139,140], with minimum acceptable cell viability [136–138] achieved due to treatment with antibiotics, blank and antibiotic-loaded microspheres, and microsphere releasates. MS were applied directly to the cells in a concentration of 1mg MS/200µL media, resulting in approximately 70% cell viability after 24h. This is a high concentration of MS applied to cells, representing a worst-case scenario for cytotoxicity; however, this concentration still yields an acceptable level of *in vitro* cell toxicity with less toxicity expected *in vivo* and clinically due to less concentrated presentation and shielding by the gel carrier.

Cell viability due to thermoresponsive gel has been previously investigated by this group, with acceptable cell viability achieved after washing steps [38]. For use in this study, gel production was scaled up tenfold and desired characteristics were maintained, indicating potential for larger scale production for clinical use. The gel is used as a carrier to improve retention of drug-loaded MS *in situ* and prior ocular studies by this group indicate similar efficacy *in vivo* with and without gel, but gel allows for non-invasive, simpler administration and retention [38,121]. Gel is nondegradable to improve its efficiency as a carrier for retention and to reduce potential for toxicity due to degradation products.

Auditory brainstem recording studies shown in Figure 15 demonstrated no significant difference in hearing threshold shift due to the two different gel volumes applied (25µL and 100µL), indicating instilled gel/MS volume can be scaled up if needed to increase drug concentrations presented to the TM. Threshold shift of sound pressure level relative to noise floor due to one ear containing either an earplug or gel was significantly different compared to both ears unplugged. This suggests that mass effect from gel/MS treatment would have a temporary conductive effect on hearing for the treatment duration. However, there is an inherent temporary conductive hearing loss in cases of otitis media due to bulging of the inflamed tympanic membrane [52,143,144], therefore minimal attenuation of hearing during treatment duration is not expected to greatly affect patient quality of life and treatment can help prevent permanent sensorineural hearing loss, a side effect of chronic otitis media [47–50]. Further studies are needed to evaluate long term ototoxicity of the biomaterials, with an expanded look at the topical safety of ceftriaxone in particular, using longitudinal ABR testing to determine effect on hearing sensitivity during treatment and at a time point after treatment duration has been completed [65,69,145,146].

3.0 Assessment of Transtympanic Permeability, Safety, and Efficacy using *Ex Vivo* and *In Vivo* Acute Otitis Media Models

3.1 Introduction

Animal models are necessary for preclinical determination of safety profiles and treatment efficacy, as well as to inform further development and improvement of treatment mechanisms, including drug delivery systems [147–149]. For topically applied drug delivery systems, *ex vivo* permeability experiments, inform development of the system prior to proceeding to *in vivo* studies. In addition to intratympanic [145] and transtympanic [44,68] delivery systems, permeability experiments are standard for other topical delivery systems, including transdermal and transcorneal [44,68,149].

The tympanic membrane, primarily composed of keratinocytes [134], has similar permeability barriers to the skin with the hydrophobic outermost layer, the stratum corneum, acting as the primary barrier to permeability of topically applied treatments [44,70,148,149]. To bypass this barrier, topical treatments have incorporated chemical permeation enhancers (CPEs) [70,148,149] or employed the use of microneedle arrays (MNAs) [150], among other mechanisms. Molecules generally permeate the stratum corneum by following a tortuous intracellular path, with CPEs facilitating transport by disrupting the stratum corneum layer [70,149]. MNAs facilitate transdermal permeation by physically bypassing the outer layers of the skin [150]. Very little studies have been done on MNA use for the ear, with only inner ear studied [9,151] and no studies for use on the TM.

For *ex vivo* testing of transdermal permeation, primate or porcine skin most closely model human skin; however, rodent models including guinea pigs are often employed to approximate permeability with species-specific permeability highly dependent on the molecule tested [148]. For investigation of transtympanic permeability of ciprofloxacin in particular, chinchilla and guinea pig models have both been employed [44,68].

While there are inherent interspecies differences in TM morphology [144], guinea pigs were used in *ex vivo* transtympanic permeability studies and chinchillas were used for *in vivo* otitis media studies. Both are standard accepted animal models for otic studies with similar TM thickness of 10µm in guinea pigs [152] and 15µm in chinchillas [144], compared to 35-150µm thickness in humans, dependent on location on the TM [46,144,152]. Guinea pigs were chosen for *ex vivo* studies due to species availability at the primary research site, the University of Pittsburgh, with *in vivo* chinchilla studies performed at the Medical College of Wisconsin using a well-established disease model for otitis media [153–155]. Further, guinea pigs are a standard model for middle and inner ear pharmacokinetics due to a large middle ear and easy access to the cochlea, while chinchillas are ideal for otitis media studies due to similar sensitivity to pathogens and disease progression at humans [120], in addition to ease of transbullar injection to inoculate middle ear with bacteria without disturbing the TM which was imperative to this study's focus on intact TMs. *Haemophilus influenzae* was chosen as one of the leading pathogens causing AOM, accounting for approximately half of middle ear fluid isolates in children [39,153–155].

3.2 Materials and Methods

3.2.1 *Ex Vivo* Transtympanic Permeability

Dunkin-Hartley guinea pigs (GPs) of both sexes were purchased from Charles River. All animal studies were performed with approval from and in accordance with the University of Pittsburgh Institutional Animal Care and Use Committee (IACUC) standards. Forty-four GPs were used for this study and randomized into three groups: 21 in the negative control group (100µL gel with 10mg blank MS), 21 in the test group (100µL with 10mg ciprofloxacin-loaded MS), and 2 in the positive control group (0.2% weight/volume ciprofloxacin). Animals were humanely sacrificed via anesthesia with 3-5% isoflurane followed by an overdose of intracardiac sodium pentobarbital.

Ear canals and tympanic membranes were harvested according to guidance by an otolaryngology lab technician. The TMs were visually inspected using a dissecting microscope to confirm lack of perforation. The ear canals were suspended in 10mL PBS in 50mL beakers with the TM parallel to the bottom of the beaker and only the TM surface in contact with the PBS. Due to potential for *ex vivo* tissue degradation, it was necessary to use 3 freshly harvested ears daily for the 14-day study duration [147].

For the negative control and test groups, 100µL gel mixed with 10mg of MS (blank and ciprofloxacin-loaded, respectively) was applied to the TM. Microspheres were aged for days 1-14 (in triplicate) by suspending in PBS and rotating in a 37°C incubator. Each day, 3 aliquots of MS were centrifuged, supernatant removed, and MS resuspended in gel. MS were suspended in gel by pipetting gel onto pre-weighed MS and mixing with pipette tip or needle. Drug concentration is assumed to be equal with each daily topical administration from a standard 0.2% ciprofloxacin drop [58], therefore only one time point with 3 ears was observed for the positive control group.

These drops were instilled in the same volume as in humans (250µL) [58], however due to physiological differences in ear canal volume between guinea pigs and humans [156–159], resulting drug concentration in receiving chamber was scaled down accordingly for comparison.

To determine drug concentration in the PBS receiving chamber, 1mL was removed and frozen daily and all 10mL in the beaker replaced with fresh PBS. All samples were centrifuged at 3500rpm for 5 minutes, then 500µL of supernatant from each was removed and centrifuged in 10kDa filters (Amicon Ultra, Merck Millipore, Cork, Ireland) at 8200rpm for 10 minutes. Drug concentration was determined both by spectrophotometry and HPLC analysis as previously described.

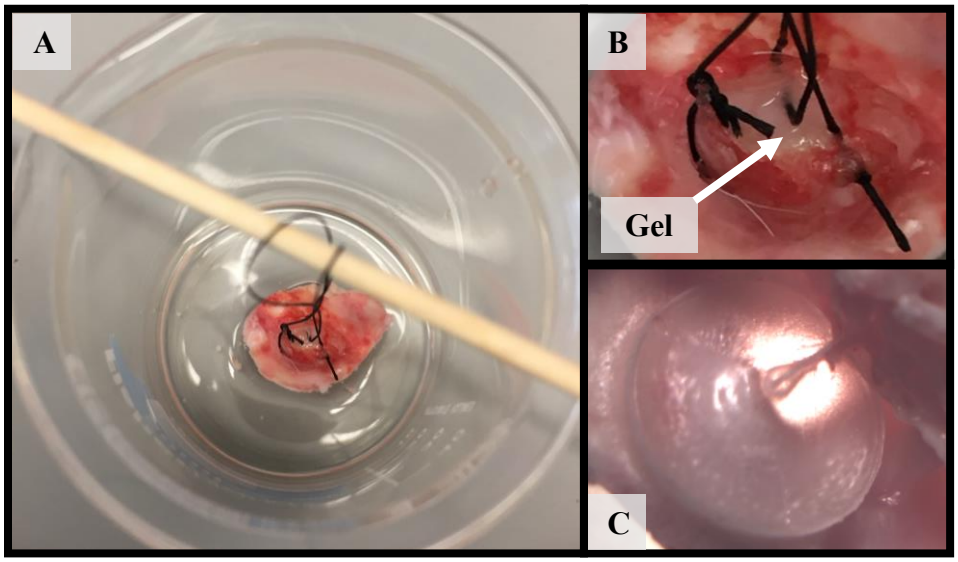

Figure 16: *Ex vivo* experimental setup: A) top view, B) application of MS/gel drop, C) reverse view of intact tympanic membrane.

3.2.2 *In Vivo* Acute Otitis Media Disease Model

Chinchillas of both sexes were purchased from Moulton Chinchilla Ranch (Rochester, Minnesota) and all studies were performed with approval from and in accordance with the Medical College of Wisconsin IACUC standards. All studies were performed humanely under anesthesia and bupivacaine was administered prophylactically to prevent any potential pain associated with bacterial infection and subsequent treatment.

The animals were randomized into four groups: no treatment control, treatment with blank MS/gel, treatment with ciprofloxacin MS/gel, treatment with ceftriaxone MS/gel. For MS/gel groups, MS were mixed with gel as previously described, by pipetting gel onto the MS and mixing with pipette tip or needle. One cohort of animals were inoculated with 1.94 $x10^5$ CFU/ear non-typeable *Haemophilus influenzae* (strain 86-028NP) via transbullar injection and received treatment after 24h, with the contralateral ear as internal control. For subsequent studies, all animals were inoculated and treated in both ears 72h after inoculation. Previous studies by other groups have also treated animals 72h after inoculation [68,69]. After infection was allowed to develop, tympanic membranes were imaged with MedRx otoscope (Largo, FL) and gel/MS was instilled to treatment groups using a 1mL syringe with 18G needle. At time points including days 1, 3, 7, and 14 post-treatment, n=3 animals (for the first cohort) or n=2 animals (for the subsequent two cohorts) per group were sacrificed and TMs imaged.

After sacrifice, the bullae were dissected, visually inspected, and imaged. The middle ear effusion and biofilm mass were collected when present. The middle ear lavage was performed using 1ml sterile PBS. The effusion/biofilm and lavage were combined to enumerate total viable bacteria by plating and presented as CFU/ear. This study was performed with two different gel/MS

instillation conditions: 1) 10mg MS/100µL gel; 100µL instilled per ear and 2) 15mg MS/100µL gel; 200µL instilled per ear.

3.2.3 Histopathology

Following sacrifice of the chinchilla cohorts treated 72h post-infection, the bullae were excised and fixed in 10% formalin. TMs were then carefully excised, dehydrated overnight in 70% ethanol, embedded in paraffin, sectioned in 5µm thick sections, and stained with hematoxylin and eosin (H&E). Paraffin histology was performed by the Tissue Culture & Histology Module within the University of Pittsburgh Department of Ophthalmology. Stained sections were imaged and evaluated using light microscopy (Leica Microsystems DM2500) with digital microscope camera (Leica Microsystems DFC295) by a blinded technician, with group/cohort masked prior to evaluation.

3.2.4 Statistical Analysis

Ex vivo transtympanic concentrations are represented as average ± standard deviation for n=3 samples per time point. Bacterial counts from *in vivo* efficacy studies were analyzed using Kruskal-Wallis test with Dunn's post-hoc testing to compare each time point within treatment groups. Statistical analyses were performed using GraphPad Prism software (San Diego, CA).

3.3 Results

3.3.1 *Ex Vivo* Transtympanic Permeability

Ex vivo studies indicate antibiotic can permeate across the tympanic membrane to the middle ear space without the use of potentially harmful chemical permeation enhancers (Figure 17). The standard topical 0.2% ciprofloxacin drops were applied in the same volume as they are typically applied in humans – 2 drops twice daily [58]. Due to size difference between guinea pig [156] and human [157–159] ears, concentration of ciprofloxacin in the receiving chamber due to treatment with these drops was scaled down by a factor of 3 to closer approximate physiological conditions. Dose of gel/MS drop can also be increased in humans as human ear canal volume is approximately 0.5-1.5mL [157–159] while 100µL gel with 10mg MS were applied in these studies.

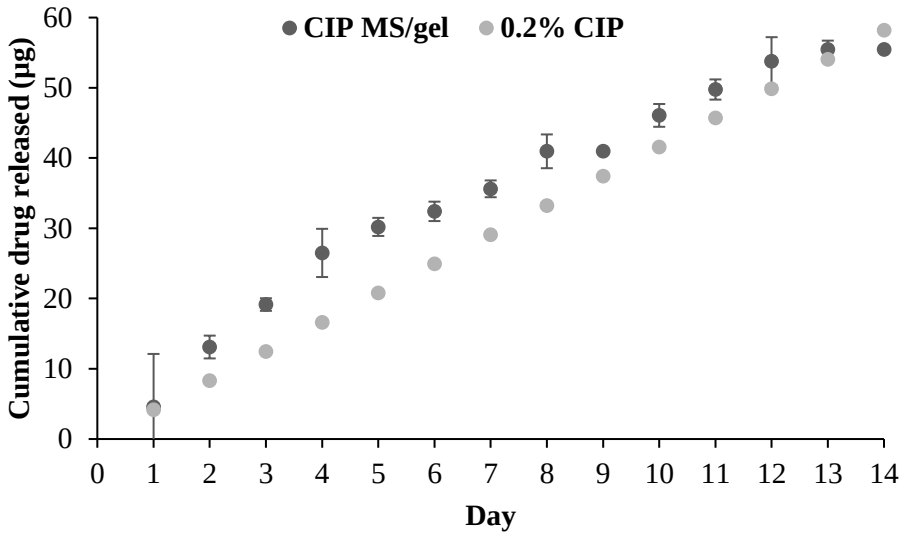

Figure 17: *Ex vivo* permeability of ciprofloxacin. *Ex vivo* permeability results showing transtympanic ciprofloxacin (CIP) release from gel-MS system and standard twice-daily topical drops (0.2% CIP), scaled to guinea pig ear canal volume compared to human ear canal volume. Error bars represent the mean ± standard deviation for n=3 ears per time point.

3.3.2 *In Vivo* Bacterial Counts

Most groups receiving no treatment (CTL) and treatment with blank MS/gel resulted in persistent bacterial infection throughout the study, confirming negative controls have no effect on bacterial clearance as expected for the disease model. For the cohort treated with 10mg/100µL gel 24h after inoculation with *H. influenzae* (Figure 18), CIP MS/gel treatment resulted in significantly decreased bacterial count at Days 7 and 14 post-treatment, with complete clearance observed at Day 14. CFX MS/gel treatment resulted in significantly decreased infection after 7 days of treatment, with a recurrence of infection by Day 14. No significant decrease in bacteria was observed in the cohort treated with 10mg MS/100µL gel 72h after bacterial inoculation (Figure

19). While infection persisted in all groups, the no treatment control group saw a significant decrease in bacterial infection by Day 14 post-treatment. For the subsequent cohort, treatment was increased to 30mg MS/200µL gel accordingly. In this final cohort (Figure 20), significant decrease in bacterial infection was observed by Day 7 post-treatment in blank MS/gel group and between Day 3 and 7 in CIP MS/gel group; however, there was no significant difference between Day 1 and 7 in the CIP MS/gel group, indicating persistence of bacterial infection over treatment duration.

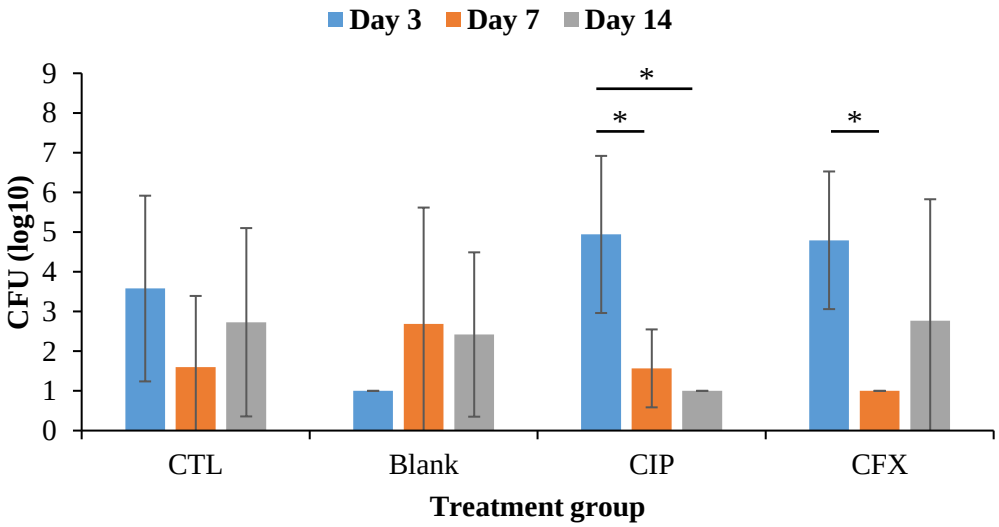

Figure 18: Colony forming units (CFU) of *H. influenzae* in chinchilla middle ear after treatment 24h post-inoculation with 10mg MS/100µL gel containing ciprofloxacin (CIP), ceftriaxone (CFX), blank, or no treatment control (CTL). Bacterial counts were deterimined upon sacrifice at days 3, 7, and 14 post-treatment. Significance (*$p<0.05$) was determined using Kruskal-Wallis and Dunn's post hoc testing. Significantly decreased bacterial counts were observed on Day 7 and Day 14 compared to Day 1 in the CIP MS/gel group and Day 7 compared to Day 1 in the CFX MS/gel group. Error bars represent mean ± standard deviation for n=9 samples in CTL group and n=3 samples for other groups.

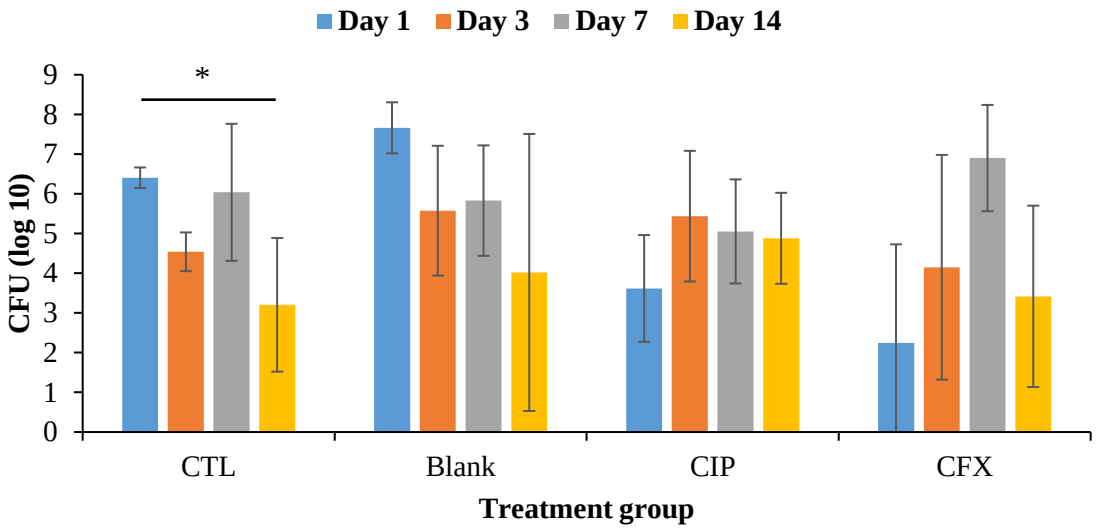

Figure 19: Colony forming units (CFU) of H. influenzae in chinchilla middle ear after treatment 72h post-inoculation with 10mg MS/100µL gel containing ciprofloxacin (CIP), ceftriaxone (CFX), blank, or no treatment control (CTL). Bacterial counts were deterimined upon sacrifice at days 1, 3, 7, and 14 post-treatment. Significance (*$p<0.05$) was determined using Kruskal-Wallis and Dunn's post hoc testing and was only observed for Day 14 compared to Day 1 in the CTL group. Error bars represent mean ± standard deviation for n=4 samples.

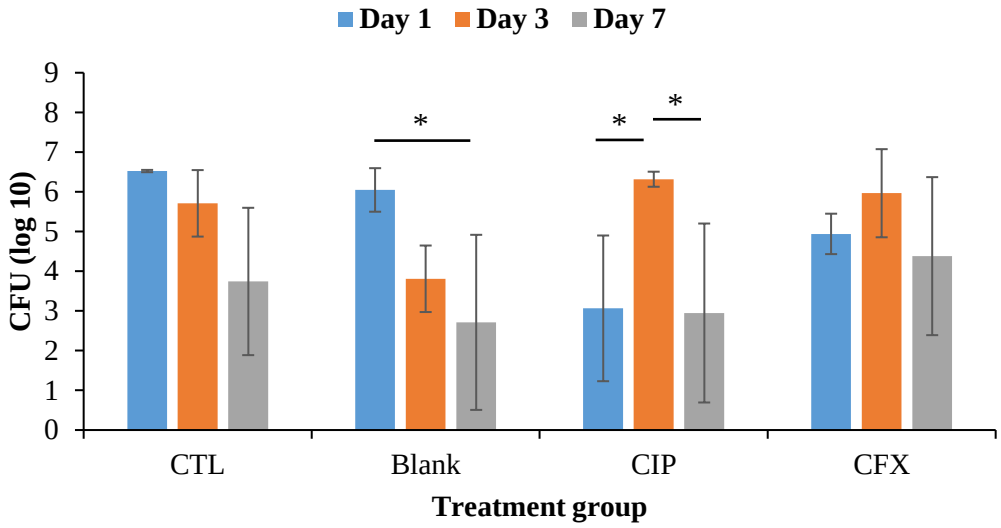

Figure 20: Colony forming units (CFU) of *H. influenzae* in chinchilla middle ear after treatment 72h post-inoculation with 30mg MS/200µL gel containing ciprofloxacin (CIP), ceftriaxone (CFX), blank, or no treatment control (CTL). Bacterial counts were deterimined upon sacrifice at days 1, 3, and 7 post-treatment. Significance (*p<0.05) was determined using Kruskal-Wallis and Dunn's post hoc testing. Bacterial counts were significantly decreased on Day 7 compared to Day 1 in the Blank MS/gel group. In the CIP MS/gel group, bacterial counts significantly increased from Day 1 to Day 3 and decreased from Day 3 to Day 7. Error bars represent mean ± standard deviation for n=4 samples.

3.3.3 Histopathology

H&E stained sections of excised TMs (Figure 21) indicate generally benign tissue response to treatment with MS/gel, with similar anatomy to previously reported otitis media chinchilla studies [57,68,69,144]. Significant edema is present in the interstitial layer of the control, untreated tissue (Figure 21C), as expected for inflammation inherent to OM. Enlargement in the interstitial layer is also present but less prominent in the gel/MS treated groups (Figure 21D-F), with all tissue diameters at consistent thickness below 20µm as is expected for normal tissue [57]. Further

analysis is warranted for material-specific tissue response in future studies. Retention of gel/MS drop during treatment was also confirmed during tissue dissection post-sacrifice (Figure 22).

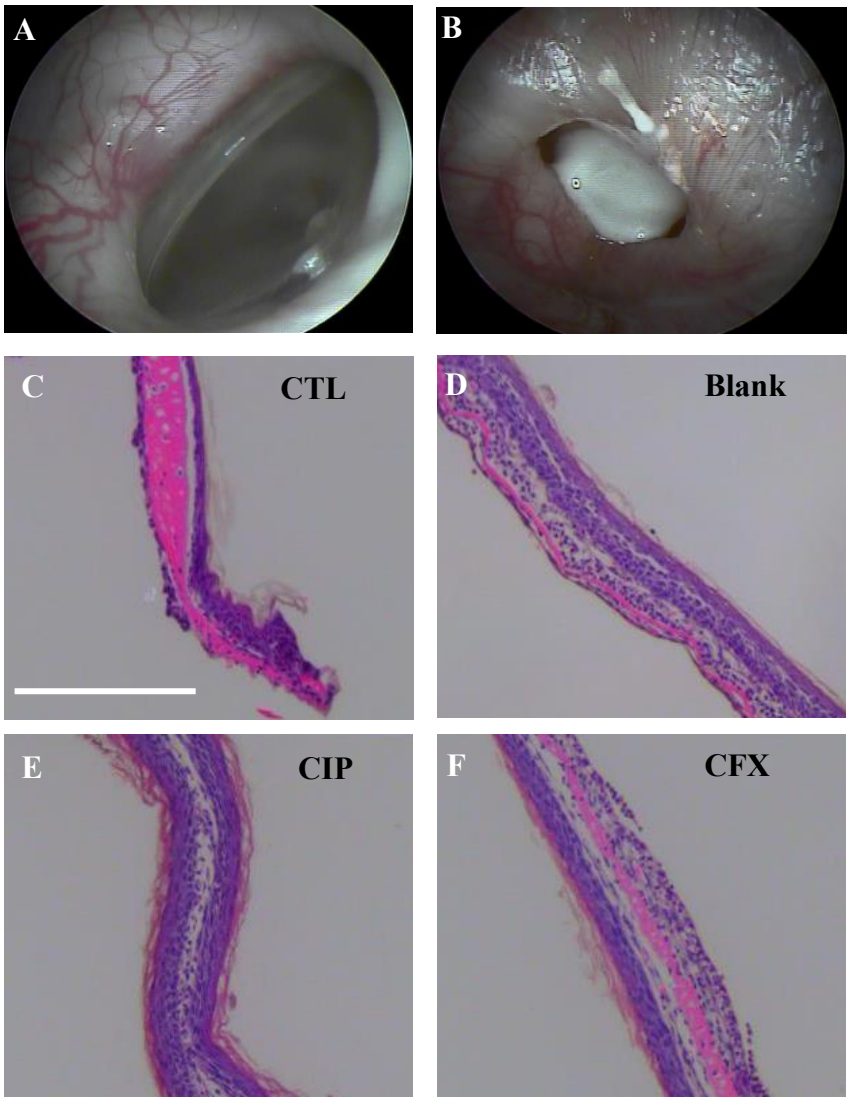

Figure 21: *In vivo* gel/microsphere (MS) placement and histopathology. Representative images of chinchilla tympanic membrane A) before and B) after gel/MS instillation. Representative hematoxylin and eosin (H&E)-stained sections of excised TMs representing non-treated control (CTL) and TMs treated with blank MS/gel, CIP MS/gel, and CFX MS/gel (C-F) imaged using light microscopy. Scale bar = 20µm.

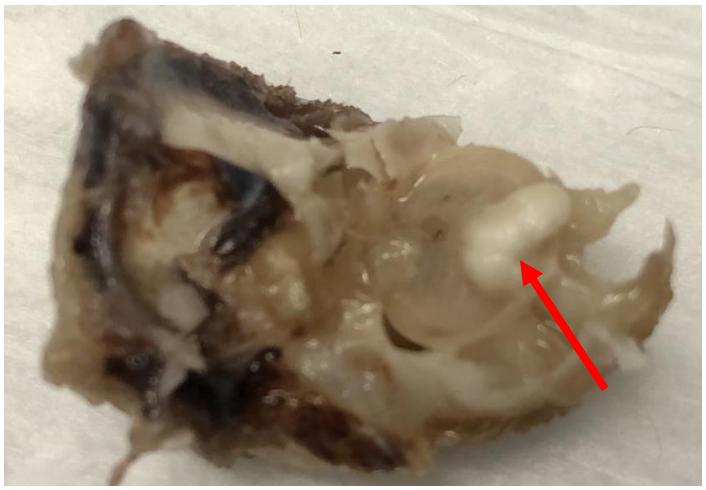

Figure 22: Gel/microsphere drop, indicated by red arrow, viewed through reverse side of chinchilla tympanic membrane during tissue dissection post-sacrifice during in vivo otitis media disease model study.

3.4 Discussion

To supplement *in vitro* release data which suggested sufficient drug release to treat acute otitis media, an *ex vivo* study of transtympanic permeability also indicates that antibiotic released from MS/gel system can permeate across the TM without the use of chemical permeation enhancers. Because this study used healthy (not infected) tissue *ex vivo*, permeability is expected to be comparable in infected ears *in vivo* and clinically due to inflammation inherent to AOM [46,160]. Transtympanic permeability of ceftriaxone due to treatment with ceftriaxone-loaded MS/gel was not tested. Due to similarity in drug release kinetics and molecular weight (MW = 554.48 and 331.35g/mol for ceftriaxone and ciprofloxacin, respectively), ceftriaxone release from MS is expected to permeate the TM as well. While these studies are not able to account for the myriad of complexities in diseased human tissues, including inflammation and increased thickness

of TM and inner mucosal layer, our results suggest that sustained, localized delivery from our drug delivery system is possible. Future studies can investigate permeability further with the use of Franz cell diffusion chambers [145,161].

In vivo efficacy studies in a chinchilla model of otitis media resulted in significantly decreased infection due to treatment 24h after inoculation (Figure 18) with CIP MS/gel, indicating ability of the drug delivery system to treat infection *in vivo* when treatment occurs at early time points after bacterial infection. We hypothesize that recurrence of infection by Day 14 after treatment with CFX MS/gel was due to the release kinetics of CFX from MS, where the burst release and subsequent linear release were effective in clearing bacteria but lower antibiotic concentrations at later time points allowed for remaining bacteria to redevelop infection. Most of the negative control groups had no effect on bacterial clearance, as expected for this disease model; however, acute otitis media in humans often clears up on its own [42], as observed by significantly decreased, but not fully cleared, bacterial infection in one no treatment group (Figure 19) and one blank MS/gel treatment group (Figure 20). In cohorts treated 72h after bacterial inoculation, visual observation confirmed presence of biofilm in the middle ear, potentially contributing to inability of antibiotics to clear infection [10,54–56].

Due to this observation, the subsequent cohort was treated with increased concentration of MS in gel and increased overall volume of materials applied to 30mg MS/200µL. However, bacterial infection and biofilm formation were persistent even with this increased treatment. While concentration of MS in gel was maximized, overall volume of treatment and/or loading of drug in microspheres can be increased further to maximize permeation of antibiotic across TM, as confirmed by results in *ex vivo* transtympanic permeation (Figure 17) and ABR (Figure 15) studies. Further, high variability was observed in both control and treatment groups, as indicated by large

standard deviations and recurrence of bacterial infection at later time points after decrease at earlier time points. The *in vivo* results also suggest that variability in the disease model may be decreased by separating animals into groups with or without biofilm formation for treatment with CFX or CIP, respectively. Additionally, there are some limitations to these *in vivo* studies as clinical course in humans cannot be extrapolated in animals due to highly variable disease development and progression in animals, with potential for the disease to not develop, to be self-limited, or to become systemic.

While the gel/MS drop can be removed easily from the eye [38] at the end of treatment duration, further investigation is necessary to determine the most effective removal system in a human ear model. Chinchilla ears are physiologically similar to human ears therefore they are a standard model for otic studies [69,120,162], however there are inherent species-specific differences in the physiology including external ear canals that are more tortuous than human external ear canals, so removal of the gel was not investigated in the chinchilla *in vivo* studies described herein.

4.0 Development and Testing of a Topical Controlled Release System to Encapsulate and Release Stem Cell Secretome

4.1 Introduction

To address the problem of wound healing of large or chronic TM perforations, growth factor and stem cell-based treatments have been investigated, particularly the use of FGF-2 and mesenchymal stem cells [79,103–107,109,112–114]. Due to the in-air suspension of TM tissue, injection of stem cells or scaffold materials prone to evaporative drying would likely not sustain cell viability long enough for healing to occur [163]. This may partially explain the lack of studies of MSC transplantation for TM healing [106,111,114] and the need for complex, bioprinted scaffolds for cell therapy [109]. Cell therapy also presents logistical and regulatory hurdles including scale-up and distribution [164,165]. Modified phospholipid vesicles are one alternative [166] but still lack potentially significant, cell-mimetic qualities such as gradient-based release and co-factor secretion.

Interestingly, it has been shown that the regenerative features of MSCs can be mediated by secreted paracrine factors independent of cell contact. These factors can be found in cell culture media conditioned by proliferating MSCs, and several groups have indeed demonstrated that the secretome or conditioned media (CM) from bone marrow MSC cultures possess many of the same properties as MSCs themselves *in vivo* [165,167,168]. These results seem to implicate a very significant regenerative role for the paracrine/soluble factors released by MSCs, without the need for true cell therapy.

Processing of MSC secretome has previously been optimized for encapsulation within hydrolytically-degradable polymer microspheres as a substitute for MSCs in tissue engineered vascular grafts. These microspheres offer the ability to sustain a gradient-like delivery of encapsulated material for an extended period of time from a single, localized dose [57,121,169]. Diffusion of proteins after near-zero order release rates from bulk-degrading matrices has been shown to result in gradient-like release patterns *in vivo* [170–172], which is a pattern characteristic of many wound healing applications [117]. Another important feature of these methods is the ability to encapsulate most or all secreted soluble factors and shed vesicles in the microspheres.

4.2 Materials and Methods

All materials were obtained from Sigma-Aldrich (St Louis, MO) unless otherwise noted.

4.2.1 Mesenchymal Stem Cell Conditioned Media Preparation

Adipose derived mesenchymal stem cells (MSCs) (RoosterBio Inc.) were cultured in T175 flasks in RoosterNourish MSC media. Source donors were adults under 45 years old to avoid potential deficits in MSC from more elderly patients [173–175]. Batches from two different source donors were used and subsequently will be referred to as Batch 1 and Batch 2. When flasks reached ~70% confluency, 20 mL of fresh media was added and cells were allowed to culture for 48 hours. The media was removed and centrifuged at 1200g for 5 minutes to remove any cell debris, flash frozen, and stored at -20°C. Remaining cells were subcultured and the process repeated until passage 3. Conditioned media (CM) was then filtered in 10kDa filter tubes (Amicon Ultra,

MilliporeSigma, Burlingame, MA), frozen, lyophilized, and reconstituted in 450µL DI water. Growth factor concentration in two different batches of conditioned media was quantified using both MicroBCA Protein Assay and Invitrogen Human FGF ELISA kits (Thermo Fisher Scientific, Waltham, MA). Contribution from extracellular vesicles was quantified by incubating CM with Pierce RIPA lysis buffer (Thermo Fisher Scientific, Rockford, IL) in a 1:7 ratio for 10 mins at 37°C.

4.2.2 Double and Single Emulsion CM-loaded MS Formulations

CM-loaded microspheres were prepared using a W/O/W double emulsion procedure: 200mg PLGA (MW 24-38 kDa; viscosity 0.32-0.44dL/g or MW 38-54kDa; viscosity 0.56-0.6dL/g) were dissolved in 4mL dichloromethane to which 200µL of reconstituted CM in 4.5mL DI water was added [38,121,132]. This reconstituted CM is a 1:10 dilution of the CM processed as described above. MS fabricated with 24-38kDa MW PLGA will be henceforth referred to as MS 503 and MS fabricated with 38-54kDa MW PLGA will be referred to as MS 504. The dissolved drug and polymer mixture were sonicated for 10 seconds at 30% amplitude (EpiShear Probe Sonicator, Active Motif, Carlsbad, CA) followed by homogenization in 60mL of 2% PVA (Polysciences, Warrington, PA) for 1 minute at 7000rpm (Silverson L5M-A, East Longmeadow, MA). The resulting emulsion was added to 80mL of 1% PVA and stirred at 600rpm for 3 hours. Blank MS were fabricated using the same methods, with DI water alone substituted for CM reconstituted in DI water. MS were washed 4 times by centrifugation, resuspended in deionized (DI) water, flash frozen in liquid nitrogen, and lyophilized for 48-72 hours (Benchtop Pro, SP Scientific, Warminster, PA).

Salt-balanced formulations were fabricated using the above methods and with an appropriate amount of NaCl added to PVA to balance the osmolality of the ceftriaxone solution. A double emulsion formulation was also fabricated using 4mL ethyl acetate (EtAc) as organic solvent instead of dichloromethane [176].

Single emulsion oil-in-oil formulation was fabricated for MS 503 using 200µL CM reconstituted in DMSO added to 200mg PLGA dissolved in 4mL dichloromethane. This mixture was homogenized at 7000rpm and subsequent steps for precipitation, lyophilization, and washing as described above. Blank MS were fabricated using the same methods, with DMSO alone substituted for ceftriaxone dissolved in DMSO.

4.2.3 CM-loaded MS Morphology Characterizations

Size, shape, porosity, and drug loading and release were characterized for each set of MS prepared. Scanning electron microscopy (SEM) was used to examine shape and morphology of all MS formulations (JEOL JSM 6335F, Peabody, MA). MS diameter was quantified by volume impedance measurements with mean and standard deviation determined for n=10,000 MS per sample (Multisizer, Beckman Coulter, Brea, CA). Density of MS was determined via a measurement device custom-made using a 1mL syringe (Figure 3). A known mass, approximately 20-40mg, of MS was added and MS packed by pushing down on the plunger, allowing for volume to be determined and density calculated from the known mass and volume.

4.2.4 *In Vitro* Release from CM-loaded MS

In vitro release kinetics were determined using 10mg of MS suspended in 500mL phosphate buffered saline (PBS) and continuously rotated at 37ºC. The supernatant was removed via centrifugation every 24 hours and replaced with fresh PBS. For each formulation, total loading was taken to be cumulative drug release when all MS were fully degraded and release was exhausted.

Total protein in the CM MS supernatant was quantified using a MicroBCA Protein Assay kit (Thermo Fisher Scientific, Rockford, IL). In brief, a working reagent was prepared according to kit instructions and 150µL of working reagent was added to each well of a 96-well plate containing 150µL of sample. After 2h incubation at 37°C, UV/Vis absorbance measures were determined at 562nm (SoftMax Pro 5, Molecular Devices, Sunnyvale, CA), with background signal from blank MS subtracted from each measurement and regressed against the standard curve. A standard curve was determined using bovine serum albumin (BSA) for the range 0.5-40µg/mL. FGF-2 concentration was quantified using a Human FGF ELISA kit (Invitrogen, Carlsbad, CA). Contribution from extracellular vesicles in releasates were lysed using the same lysis buffer procedure described above prior to analysis via MicroBCA and ELISA kits.

4.2.5 Cytotoxicity Assays

Cell viability in the presence of conditioned media and CM-loaded microspheres was analyzed by MTT assay alone, using the same methods as described above. Studies were carried out using, ~3,000 human primary dermal keratinocyte cells/well plated in 96 well plates and incubated in 200µL Dermal Cell Basal Medium with Keratinocyte Growth Kit (ATCC) for 24h at

37°C with 5% CO_2 to achieve a monolayer. Cells with medium only were used as the positive control for viability in both assays and cells incubated with 70% methanol for 5-10mins prior to each assay were used as a negative control, per kit instructions. Test groups included 100µL basal medium and 100µL test material: PBS, conditioned medium, 1mg blank MS, 1mg CM MS, blank MS releasate, CM MS releasate. Releasates were collected via the same methods as described above, with Day 2 releasates used for this study to most accurately represent 24h of release within the linear region of total protein release. Once a monolayer of cells was achieved, treatment groups were applied and incubated for an additional 24h. Background signal from MS was also accounted for by applying 1mg MS in 200µL basal medium to wells with no cells. MTT assay was performed by additional incubation for 4h with 10µL MTT stock solution, followed by incubation for 10mins with 50µL DMSO, and absorbance determined in each well via spectrophotometry at 540nm. Percent viability was determined by normalizing to 100% viability in the positive control group.

4.2.6 Scratch Wound Proliferation Assays

Scratch wound assay methods were adapted from Walter et al 2010 [177]. Human primary epidermal keratinocytes were incubated in Dermal Cell Basal Medium with Keratinocyte Growth Kit at 37°C with 5% CO_2 until flasks reach 70-80% confluency, then transferred to 24-well plate at a density of ~65,000 cells/well. Cells were incubated for 24-48h in 1mL basal medium until a confluent monolayer was achieved. A vertical scratch was accomplished using a 1000µL pipette tip and wells were rinsed 1-2 times with medium to remove any dislodged cells. Scratch wounds were then immediately treated, in quadruplicate, with a) 1mL basal medium, b) 1mL MSC conditioned media, c) blank MS 503 releasates, d) blank MS 504 releasates, e) CM MS 503 releasates, or f) CM MS 504 releasates.

MSC CM and MS releasates were prepared with 30mg MS suspended in 1mL basal medium and rotated at 37°C for 24h prior to centrifugation and filtration at 8200rpm for 30mins in 10kDa ultra centrifugal filters (Amicon, MilliporeSigma, Cork, Ireland). MS mass for release was scaled up from 10mg/500µL PBS to account for protein concentration lost to non-specific adsorption in filtration step (Figure 23).

Images were collected at time points of 0, 6, 12, 24, and 48h after treatment with inverted microscope at 10x magnification (Leica Microsystems DMi1, Buffalo Grove, IL) and digital camera (Canon Powershot G7X Mark II, Tokyo, Japan). Images were analyzed using ImageJ software with MRI Wound Healing Tool to determine scratch wound area at each time point, with data presented as wound healing percentage compared to t=0h scratch wound area.

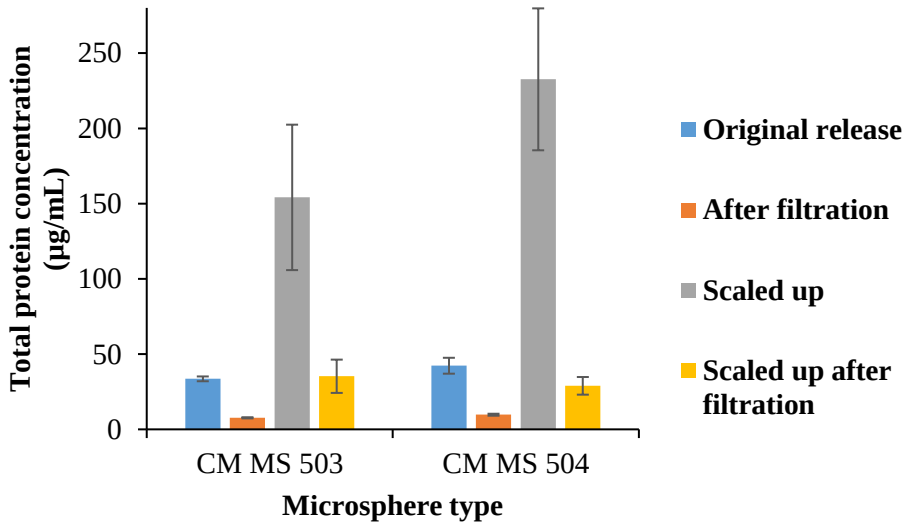

Figure 23: Conditioned media-loaded microphere (MS) releasate scaling for scratch wound proliferation assays. Releasates were scaled up to account for protein concentration lost to non-specific adsorption during filtration step to remove MS from relesates. Error bars represent the mean ± standard deviation for n=3 samples.

4.2.7 Statistical Analysis

Data for *in vitro* release assays, MS density, and cytotoxicity testing are represented as average ± standard deviation for at least n=3 samples. Volume impedance measurements of MS diameter are represented as average ± standard deviation for n=10,000 particles per sample. Student's t-test was used to analyze increases in total protein and FGF-2 concentrations due to lysis of extracellular vesicles. Wound healing percentages in scratch assay studies were analyzed using Student's t-test comparing scratch wounds treated with unconditioned to conditioned medium and blank to CM-loaded MS releasates at each time point. All statistical analyses were performed using GraphPad Prism software (San Diego, CA).

4.3 Results

4.3.1 CM-loaded MS Release Profiles

Concentrations in MS releasates were quantified using a bovine serum albumin standard curve (Figure 24). Standard double emulsion formulations exhibited 38% burst release followed by 11 days of approximately linear release and 66% burst release followed by 21 days of approximately linear release for CM MS 503 and CM MS 504 respectively (Figure 24). Single emulsion was also used to fabricate CM MS 503, resulting in greatest overall release magnitude over 15 days and highest burst release of 86% (Figure 25). Release assays were carried out for 11, 21, and 15 days, respectively, when all MS were degraded and therefore no longer releasing encapsulated therapeutics.

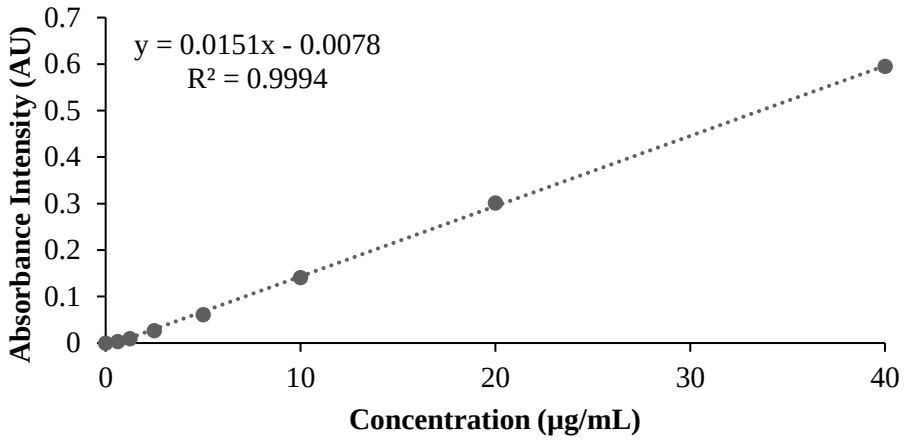

Figure 24: Bovine serum albumin standard curve determined via spectrophotometeric microBCA assay.

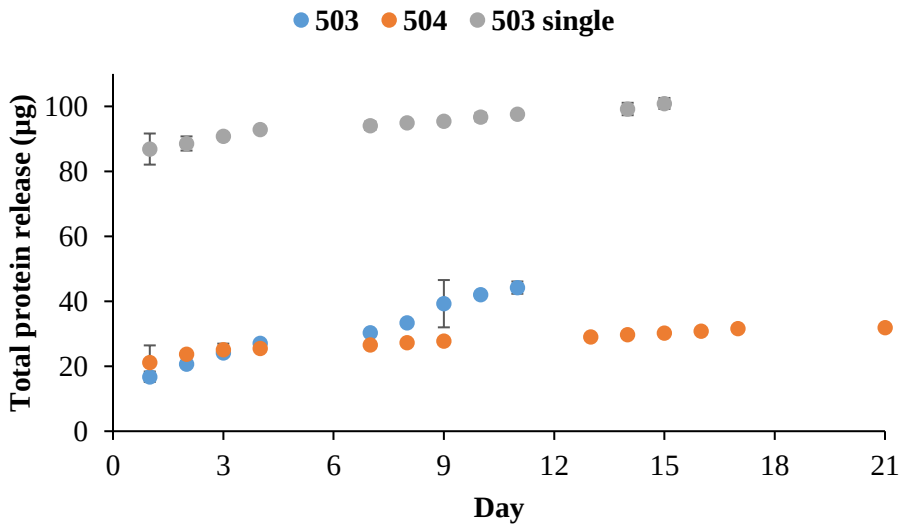

Figure 25: *In vitro* total protein release from 10mg of double and single emulsion CM-loaded microsphere (MS) formulations. Release assay was carried out until all MS were degraded, resulting in 11, 21, and 15 days of release from CM MS 503, CM MS 504, and CM MS 503 single emulsion, respectively. Error bars represent the mean ± standard deviation for n=3 samples.

Salt-balanced MS resulted in 21 days of release for both polymers but higher burst release of 79% and 68% for salt-balanced CM MS 503 and CM MS 504, respectively (Figure 26). MS fabricated with ethyl acetate as organic solvent resulted in high burst release as well – 70% and 78% for CM MS 503 EtAc and CM MS 504 EtAc, respectively – but MS degraded after 8 days (Figure 27).

Standard double emulsion CM MS 503 and CM MS 504 were used for subsequent studies. While most formulations tested provided similar overall release magnitudes of 20-40µg, these formulations were able to most closely achieve the desired 21-day release profile while minimizing burst release, therefore providing the most continuous release of MSC CM. While CM MS 503 did not achieve the 21-day release duration, it had the lowest burst release and therefore the most continuous release and also demonstrated greater overall magnitude of release than CM MS 504.

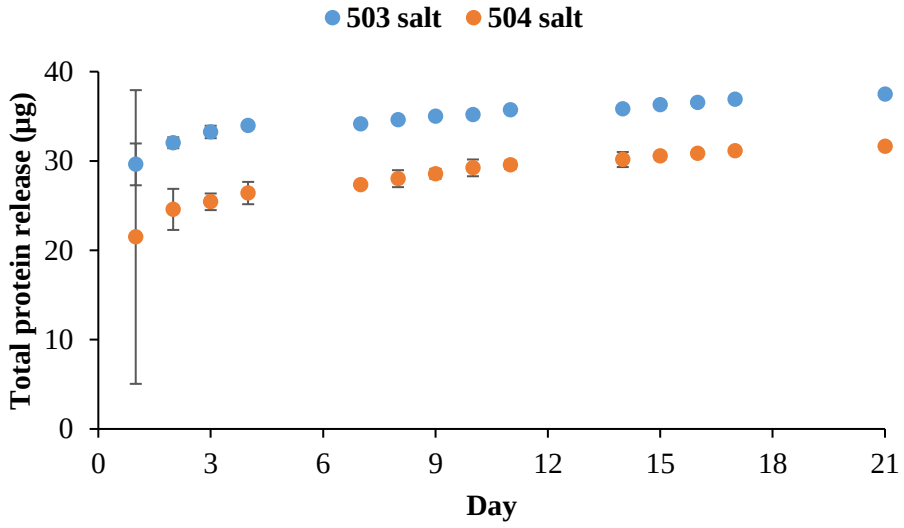

Figure 26: *In vitro* total protein release from 10mg of salt-balanced double emulsion CM-loaded microsphere formulations. Error bars represent the mean ± standard deviation for n=3 samples.

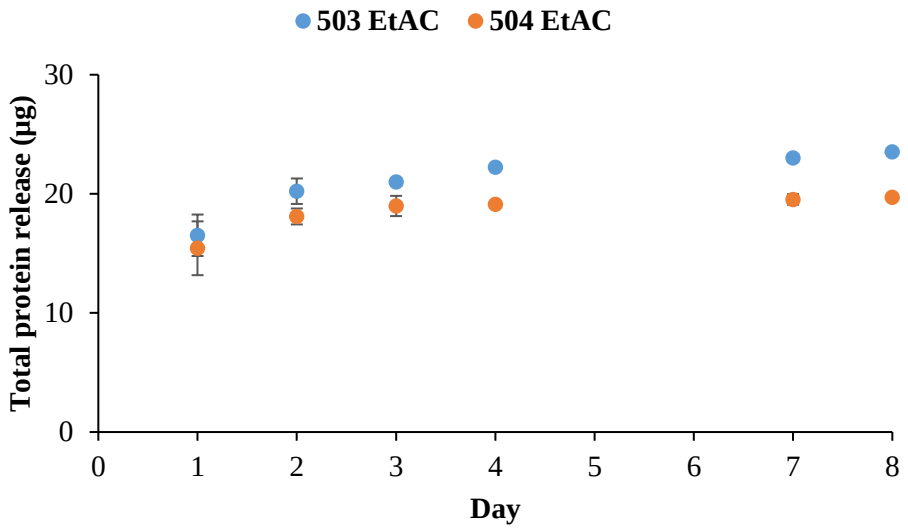

Figure 27: *In vitro* total protein release from 10mg of double emulsion CM-loaded microsphere formulations with ethyl acetate as organic solvent. Error bars represent the mean ± standard deviation for n=3 samples.

Concentration of FGF-2 was determined using the standard curve shown in Figure 28. FGF-2 ELISA results indicated a burst of ~65.5% or 135.3 ± 51.3pg on Day 1 followed by 15 days of release, yielding a cumulative 206.5 ± 14.3pg of FGF-2 released from 10mg of CM MS 504 (Figure 29). FGF-2 day 1 burst release is consistent with total protein day 1 burst release of 66% shown in (Figure 25). While CM MS 504 can release for 21 days before they fully degrade, FGF-2 release was only seen for the first 15 days.

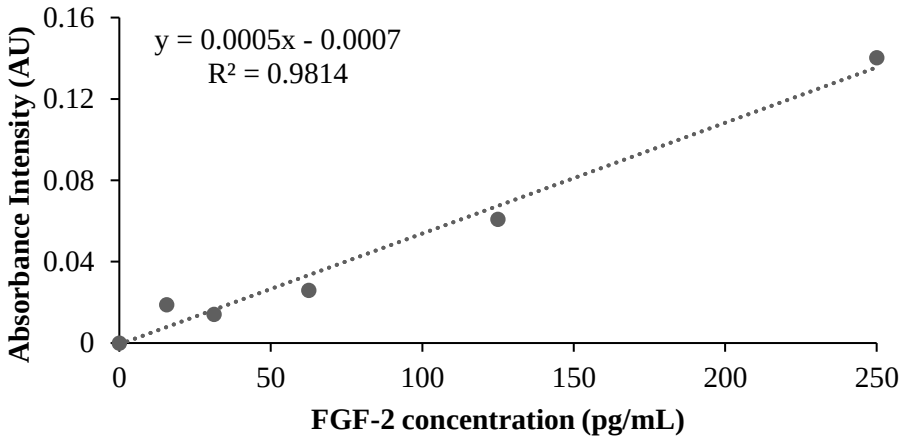

Figure 28: FGF-2 standard curve determined via spectrophotometric FGF-2 ELISA.

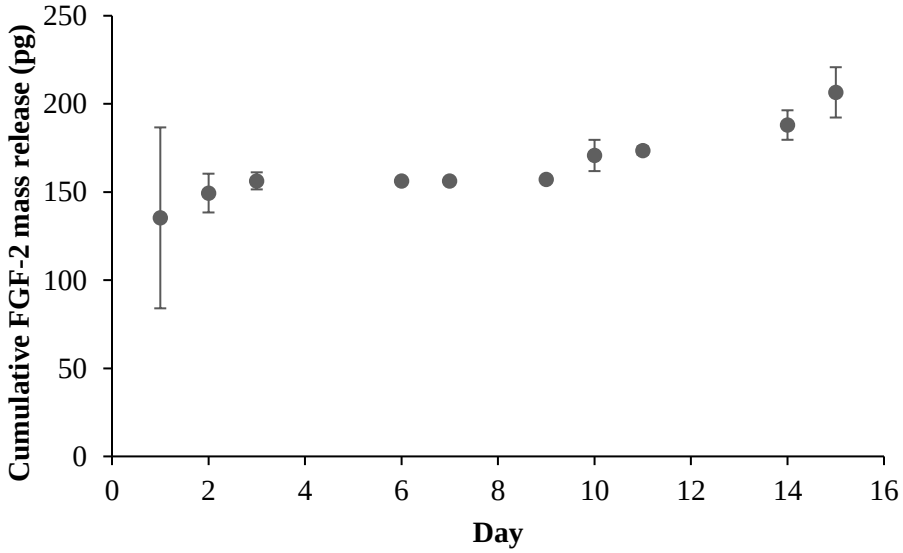

Figure 29: Cumulative *in vitro* FGF-2 release from 10mg of double emulsion CM MS 504. FGF-2 release was observed for 15 days, although it takes Error bars represent the mean ± standard deviation for n=3 samples.

4.3.2 Contribution from Extracellular Vesicles

Overall magnitude of total protein concentration in raw and lysed CM from Batch 1 was of the same magnitude between passages 1-7. For each passage, lysis resulted in approximately fourfold increase in total protein concentration due to EV contribution (Figure 30). Passages 1 and 2 of Batch 1 were compared to passages 1 and 2 of Batch 2 (Figure 21). While lysis of EVs in Batch 2 CM resulted in approximately fourfold increase in total protein concentration as well, overall magnitude of total protein in both raw and lysed samples are 7-8 times higher in Batch 2 than Batch 1. MS were therefore fabricated using conditioned media from Batch 2 to maximize encapsulated protein concentration. Batches are from two different source donors.

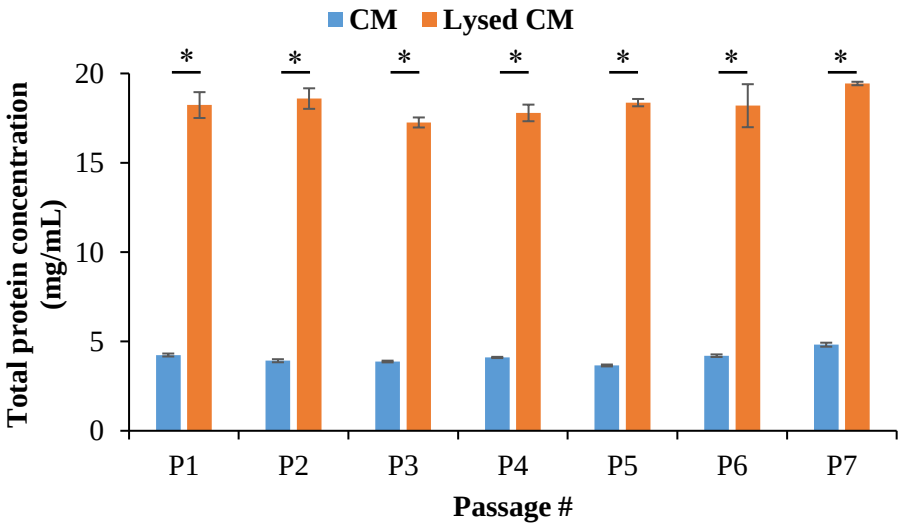

Figure 30: Total protein concentration in raw and lysed conditioned media from passages 1-7 of CM Batch 1. Lysis results in fourfold increase in total protein concentration, indicating significant contribution from extracellular vesicles. Passage number did not have an effect on magnitude of total protein concentration. Significance (*$p<0.05$) was determined via Student's t-test. Error bars represent the mean ± standard deviation for n=3 samples.

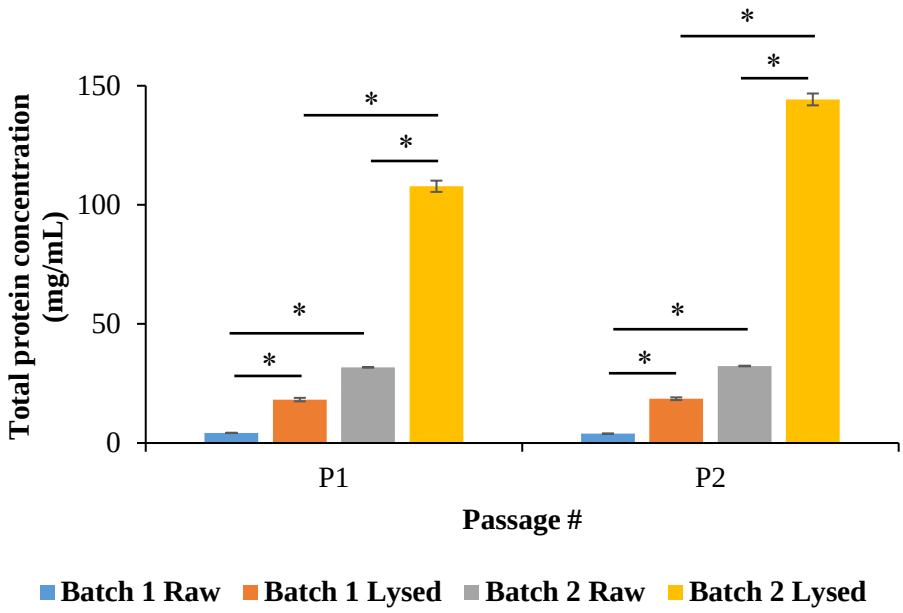

Figure 31: Total protein concentration in raw and lysed conditioned media from passages 1 and 2 of CM Batch 1 compared to CM Batch 2. Batches 1 and 2 are from two different source donors. Lysis resulted in fourfold increase (*$p<0.05$) in total protein concentration due to extracellular vesicle contribution in both batches, however overall total protein magnitude in both raw and lysed samples are 7-8 times greater (*$p<0.05$) in Batch 2 compared to Batch 1. Significance was determined using Student's t-tests. Error bars represent the mean ± standard deviation for n=3 samples.

FGF-2 concentration in Batch 1 CM was compared to FGF concentration in CM MS 503 fabricated using Batch 1 CM. While lysis of CM resulted in 2.4-fold increase in FGF concentration, contribution to FGF-2 concentration was increased by 89-fold due to lysis of EVs in Day 1 CM MS releasates (Figure 32), possibly indicating preferential encapsulation of EVs compared to free growth factors. In Day 1 releasates from MS fabricated using Batch 2 CM, 27% and 12.6% of cumulative total protein release from CM MS 503 and CM MS 504, respectively, is contained in extracellular vesicles (Figure 33).

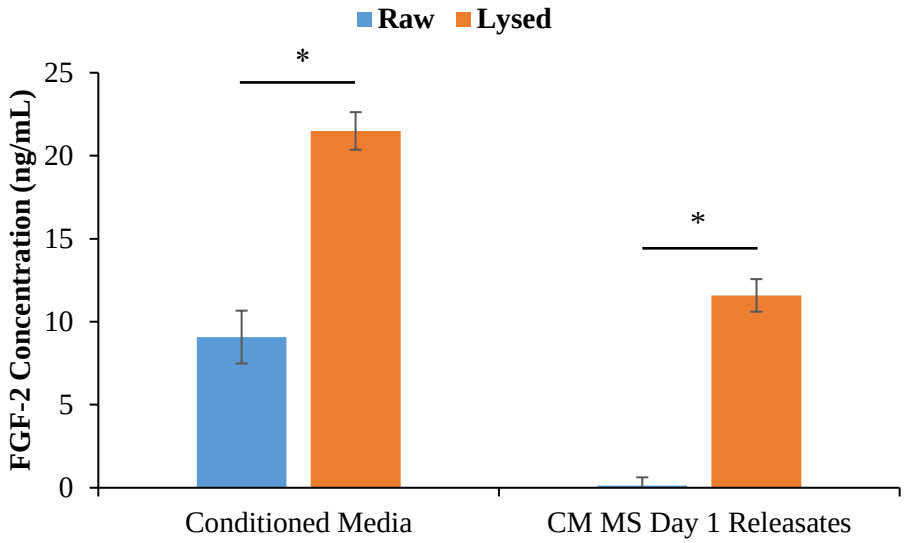

Figure 32: FGF-2 concentration in raw and lysed Batch 1 conditioned media compared to Batch 1 CM-loaded MS releasates on Day 1. Batches are from different source donors. Lysis resulted in 2.4-fold and 89-fold increase in FGF-2 concentration in conditioned media and CM MS releasates, respectively, suggesting preferential encapsulation of extracellular vesicles over free FGF-2. These are both significant (*$p<0.05$) increases as determined by Student's t-test. Error bars represent the mean ± standard deviation for n=3 samples.

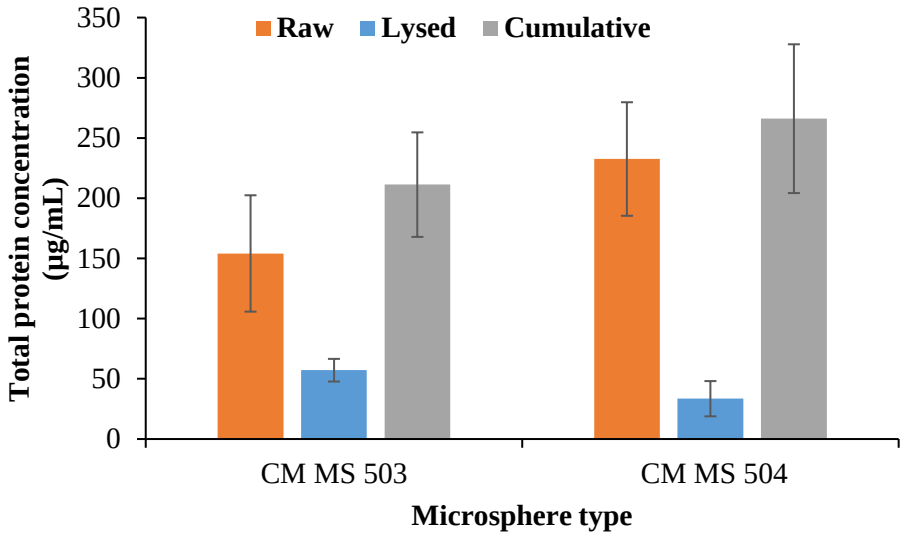

Figure 33: Extracellular vesicle (EV) contribution to total protein concentration in Batch 2 CM-loaded microspheres. Batches are from different source donors. EVs contributed to 27% and 12.6% of cumulative total protein release in CM MS 503 and CM MS 504 releasates, suggesting preferential EV encapsulation in MS fabricated using lower molecular weight PLGA. Error bars represent the mean ± standard deviation for n=3 samples.

4.3.3 CM-loaded MS Morphology

Scanning electron microscopy images (Figure 34) confirm spherical morphology of all microsphere types. SEM images also allow for visualization of any porosity in the MS, with porosity observed in several conditioned media-loaded and salt-balanced formulations. Visual estimates of diameter were confirmed with volume impedance measurements shown in Table 2. Lower densities were observed in more porous conditioned-media loaded MS than non-porous blank MS.

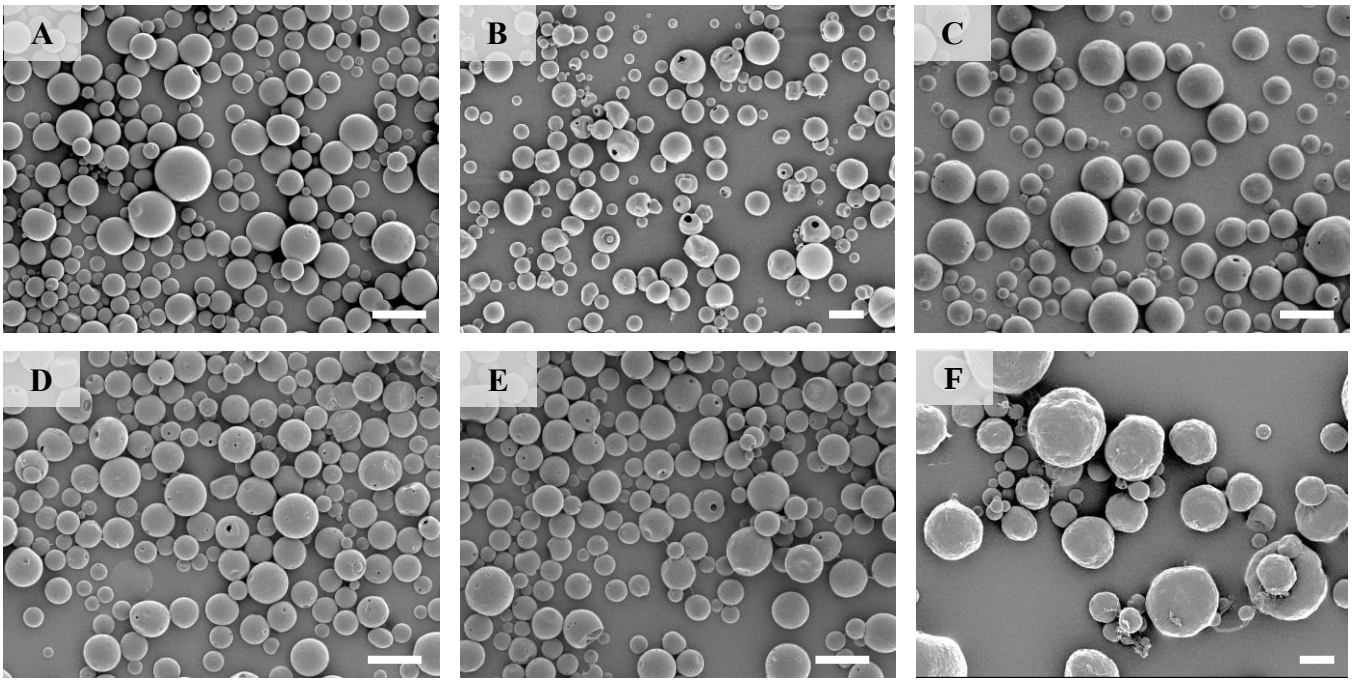

Figure 34: Scanning electron microscopy images of A) CM MS 503, B) CM MS 504, C) CM MS 503 single emultion, D) CM MS 503 salt-balances, E) CM MS 504 salt-balanced, and F) CM MS 504 with ethyl acetate organic solvent. Scale bars = 10µm.

Table 2: Average diameters and densities of blank and conditioned media-loaded microsphere formulations.

Microsphere type	Diameter (µm)	Density (mg/mL)
Blank 503	7.85 ± 5.37	776.9 ± 21.6
Blank 504	6.59 ± 2.20	623.6 ± 54.6
Conditioned media 503	5.31 ± 1.81	393.3 ± 63.0
Conditioned media 504	20.42 ± 3.78	419.2 ± 57.8

4.3.4 Cytotoxicity Due to CM-loaded MS and Releasates

Acceptable levels of cytotoxicity following 24h of treatment with conditioned media, blank and conditioned media-loaded MS, and MS releasates (Figure 35) are all suggested by the MTT viability assay.

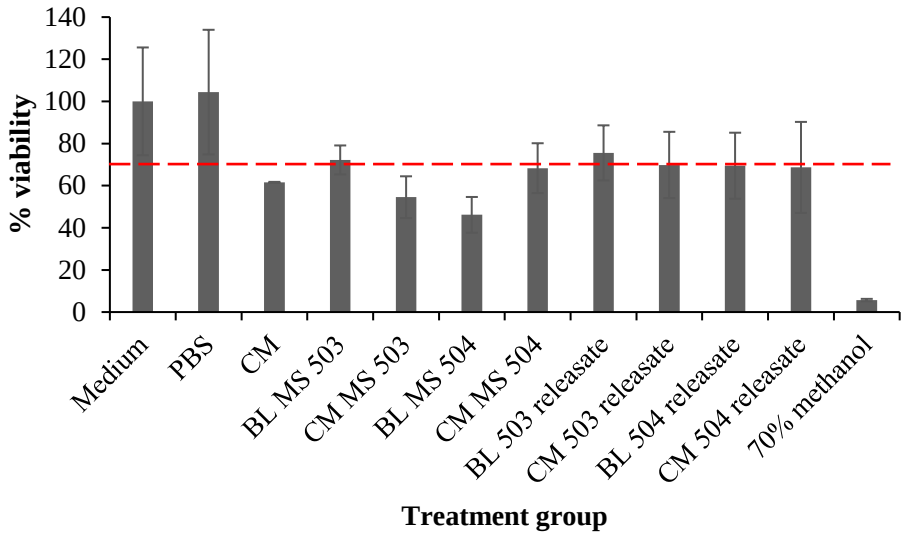

Figure 35: Cytotoxicity of conditioned media, microspheres, and releasates. MTT cell viability assay suggests approximately acceptable levels of cytotoxicity due to 24h application of blank and conditioned media-loaded microspheres and releasates to human dermal keratinocytes. Error bars represent mean ± standard deviation for n=3 samples for releasate groups and n=6 samples for all other groups. Red dashed line indicates minimum recommended viability for skin-contacting medical devices.

4.3.5 Scratch Wound Proliferation

No significant differences between groups were observed at t=6h. Significantly increased ($p<0.05$) wound healing was observed at t=12h for treatment with conditioned media compared to basal media and treatment with CM MS 503 releasates compared to blank MS 503 releasates. Treatment with CM MS 503 releasates also resulted in significantly increased ($p<0.05$) wound healing compared to blank MS 503 releasates at t=24h. All scratch wounds were completely healed by t=48h. Similar healing rates and lack of cell death further indicate conditioned media and releasates from both blank and CM-loaded MS are noncytotoxic. Representative images of scratch wound healing per group over time can be seen in Figure 37.

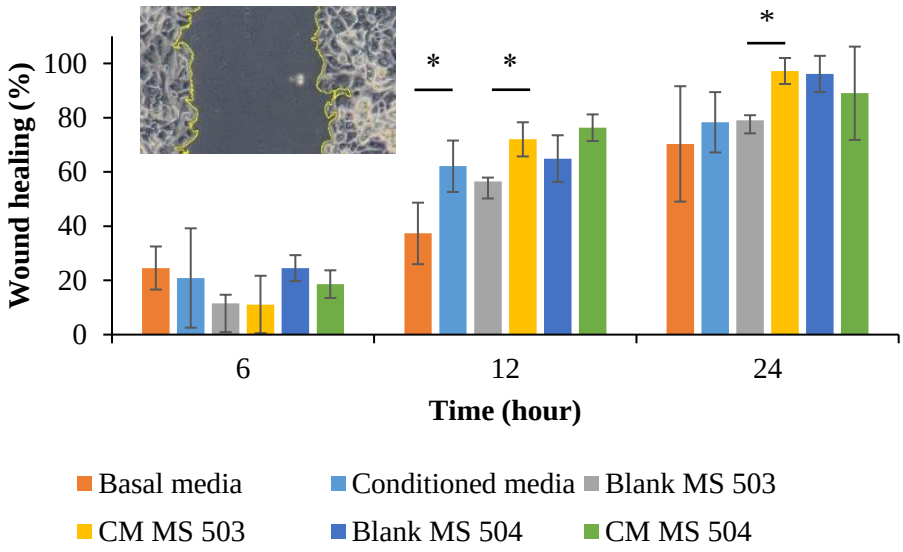

Figure 36: Scratch wound healing over time. Wound healing percentages at t=6, 12, and 24h after scratch, determined by comparing scratch wound area at each time point using ImageJ software. Errors bars represent mean ± standard deviation for n=4 samples for basal media and n=3 samples for all other groups. Significance (*$p<0.05$) was determined by Student's t-test. Significant wound healing was observed due to conditioned media compared to basal media at t=12h and CM MS 503 releasates compared to blank MS 503 releasates at t=12h and 24h. Similar healing rates and lack of cell death indicate conditioned media and MS releasates are noncytotoxic. Inset: representative image of wound margins in ImageJ.

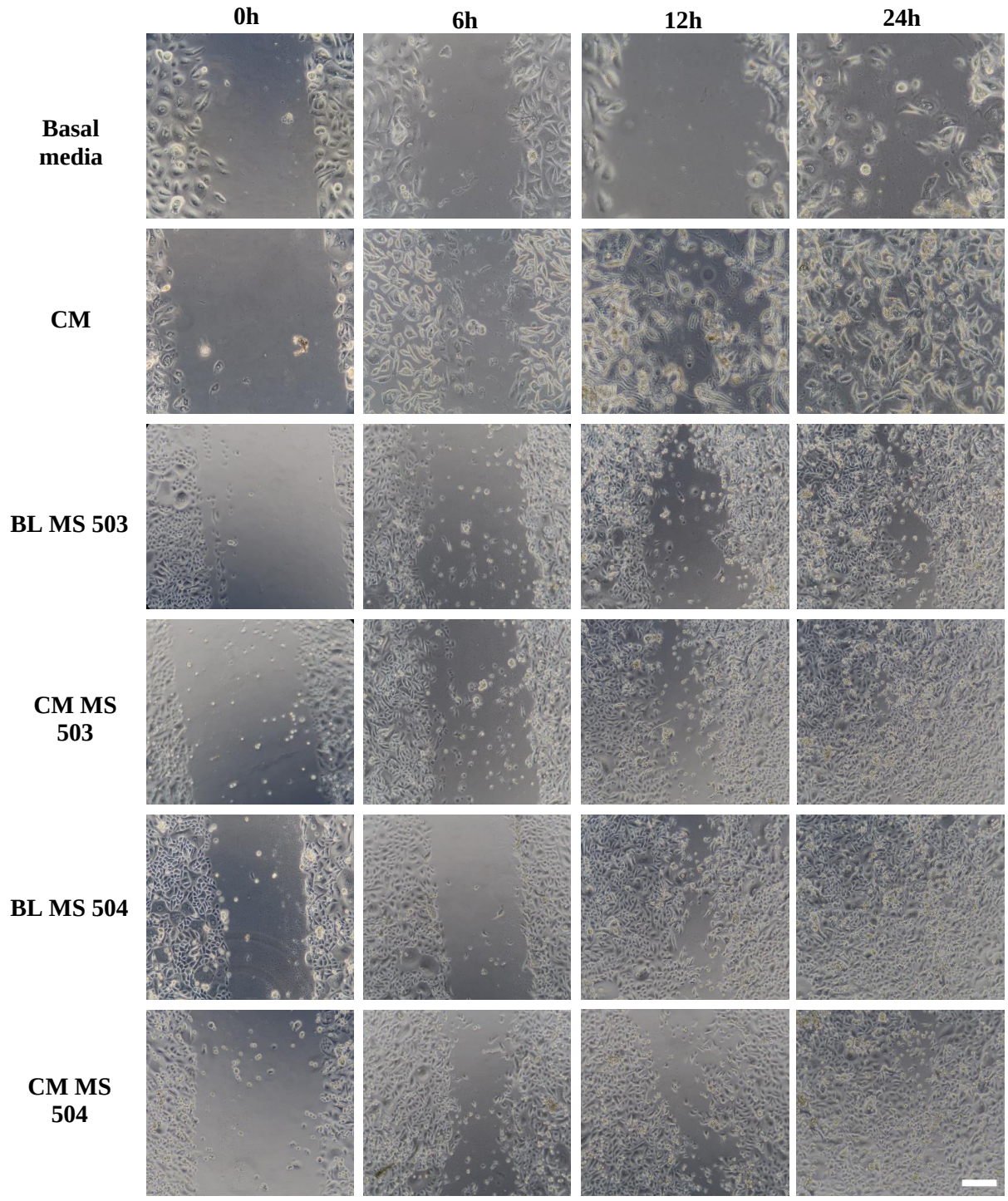

Figure 37: Representative digital images of scratch wounds in human primary dermal keratinocytes cultures in 24-well plates at t=0, 6, 12, and 24h. Scratch wounds were incubated with dermal basal media, mesenchymal stem cell conditioned media (CM), and releasates from blank and CM-loaded microspheres. Scale bar = 100μm.

4.4 Discussion

TM perforation can occur due to infection or trauma, including pressure-induced rupture common in active military zones [76,77], with particularly large or chronic perforations resulting in persistent, non-healing injury [72]. Those perforations that do heal spontaneously can require up to 8 weeks for complete healing [73,74]. Patients can experience further infection, tinnitus, vertigo, or loss of hearing during this time, resulting in temporary or permanent negative effect on quality of life. Current clinical grafting standards come with the risk of similar side effects and patients are often wary of surgical interventions [75,82]. To ameliorate these potentially detrimental side effects, recent research has focused on synthetic and naturally-derived grafting alternatives [79,80,84–97], including scaffolds delivering growth factors or topical application of growth factors relevant to wound healing [79,97–105]. Several of these studies include embryonic [106,111] or mesenchymal stem cell therapy [109,112,113], however there are limitations associated with cell viability, logistics, and regulation [164,165]. To address these limitations, our group developed a PLGA microsphere-based controlled delivery system to encapsulate and deliver MSC secretome to chronic/large-scale tympanic membrane perforations.

A variety of release profiles were achieved due to different fabrication methods, including different molecular weight polymers, different organic solvents, double versus single emulsion fabrication, and use of salt balance. This variety indicates that the delivery platform can be fairly easily modified to produce different release profiles based on therapeutic need for particular conditions, including protein delivery for tissue engineering applications [7,13,19,176]. However, the target release profile maximized the magnitude of release while also maximizing release duration and minimizing burst release to provide mostly continuous release for the full treatment duration.

Higher molecular weight PLGA (MS 504) was used to increase microsphere diameter and slow degradation rate to extend treatment duration to 21 days while lower molecular weight PLGA (MS 503) was used for shorter treatment duration of 11 days while increasing overall magnitude of release [13]. Observed MS diameters and densities are consistent with previously observed ranges for similar microsphere formulations developed by this group [121,132]. Organic solvent was adjusted as an effort to improve protein stability and encapsulation [176], however MS fabricated using ethyl acetate degraded much faster than those fabricated with DCM, which may be due to solvent extraction rate and provides an avenue to investigate further for future release profile tuning [17,178]. Salt balance increased MS porosity, in turn increasing initial burst release [13,15,17]. Due to maximization of release duration while minimizing initial burst release, standard double emulsion was found to be optimal to produce the desired continuous release profile.

Contribution on Day 1 from EVs to total protein release (Figure 33) made up 27% and 12.6% for CM MS 503 and CM MS 504, respectively, which may be due to higher molecular weight polymer resulting in tighter polymer matrix [14,20], in turn resulting in less EVs loaded compared to free protein or EVs trapped in polymer matrix until later time points due to size distribution of up to 150nm-1μm dependent on type of EV [179]. Encapsulation and subsequent release of EVs from MS can more accurately approximate natural physiological wound healing and tissue regeneration, including gradient-like presentation of vesicles and growth factors [117,179]. This allows for a biomimetic stem cell-like treatment modality while avoiding associated processing, viability, and regulatory issues [164,165].

Encapsulation and release of FGF-2 is of particular interest for wound healing of tympanic membrane perforations. CM MS were able to burst release 135.3 ± 51.3pg with a cumulative 206.5

± 14.3pg of FGF-2 released from 10mg of CM MS 504 (Figure 29). While lysis experiments were not performed on all 15 days of FGF-2 release, it can be extrapolated from Figure 31 that a significant portion of FGF-2 is bound in extracellular vesicles, with up to 89-fold increase in FGF-2 due to lysis of EVs on Day 1 resulting in approximately 12ng release. Previous studies have demonstrated a range of FGF-2 concentration to be effective for cell proliferation purposes, including an *in vitro* study suggesting 14pg/mm^2 in 3D printed fibrin substrates increased cell density on the substrates and lengthened time of cell survival [180]. Another study found that 1μg of bFGF encapsulated in microspheres and embedded in collagen scaffolds improved cell seeding of intestinal smooth muscle cells [181]. For TM perforation healing in particular, studies have shown that daily doses of approximately 80ng bFGF improved wound healing time and decreased otorrhea [73,182]. These cited values are mostly greater than the release seen in our MS formulation. However, further investigation is needed into vesicle shedding on each day of MS release and amount of FGF bound in and released from these vesicles.

Conditioned media alone, conditioned media-loaded MS, blank MS, and MS releasates exhibit approximately acceptable levels of cytotoxicity [136–138] following 24h of treatment applied to human dermal keratinocytes. These results suggest the microspheres and releasates will be biocompatible *in vivo*.

Scratch wound proliferation assays further suggest safety of conditioned media and conditioned media-loaded microspheres. No detrimental effect is observed due to treatment with conditioned media, both blank MS formulations, or both conditioned media-loaded MS formulations. Significantly increased proliferation at t=12h due to culturing scratch wound in mesenchymal stem cell conditioned media compared to basal media confirms previous results reported by Walter et al 2010 [177]. Significantly increased wound healing percentages due to

treatment with CM MS 503 releasates compared to blank MS 503 releasates suggest ability of MS to facilitate wound healing *in vitro*.

5.0 Demonstration of Tympanic Membrane Healing Over Time *In Vivo*

5.1 Introduction

The use of controlled release has been investigated and shown promise for tissue engineering and regenerative medicine, including the release of growth factors and other signaling molecules to promote tissue formation and wound healing [7]. Animal models are required for determination of preclinical treatment efficacy and safety, as well as to inform further optimization of treatment systems [147–149]. Guinea pigs were chosen for TMP studies as they are a standard model for otic studies and have easy access to the TM and middle ear [120]. Mouse, rat, and chinchilla models have also been used for investigation of TM regeneration, with a variety of methods used to create a chronic perforation, including thermal injury, repeat myringotomy, and application of inhibitors such as steroids, mitomycin C, and growth factor receptor inhibitors [72,88,92,94,109,112,113,183–185].

For treatment of TM perforations in the guinea pig model described herein, CM MS 504 were used due to their extended 21-day release profile, which can be seen in Figure 25.

5.2 Materials and Methods

5.2.1 *In Vivo* Tympanic Membrane Perforation Model

Animal studies were performed in accordance with the NIH Guide for Care and Use of Laboratory Animals and approval by the University of Pittsburgh Institutional Animal Care and Use Committee (IACUC). Eighteen male Dunkin-Hartley guinea pigs (GPs) were purchased from Charles River at 8 weeks and ~500g. All experimentation was performed under 1-2% isoflurane anesthesia.

Perforation was achieved under anesthesia using an 18G needle. Outer diameter of an 18G needle is 0.05in or 1.27mm, which results in a surface area of 1.27mm^2 based on the standard surface area equation for a circle, $A = \pi r^2$. Guinea pig TM diameter of approximately 2.5mm yields surface area of 4.91mm^2, therefore an 18G needle should result in perforation of approximately 25% of TM surface area.

TMs were imaged using video otoendoscopy (Karl Storz vetcam XL with xenon nova 175 light source, Edgewater, MD) before and after perforation. Mitomycin C (Alfa Aesar, Thermo Fisher Scientific, Ward Hill, MA) was applied at a concentration of 0.5mg/mL via gelfoam sponge for 5mins after perforation [183,185]. Perforation was followed by twice-daily treatment with 1% hydrocortisone (Zymox, PKB Animal Health, Westmont, IL) and 0.2% ciprofloxacin (Sigma Aldrich, St. Louis, MO) for 7 days and subsequently 3 undisturbed weeks allowing perforation to develop as confirmed by otoendoscopy [184]. For each otoscopic analysis, any ear wax or dried blood in the ear canal were cleared using a cotton tipped applicator and/or lavage with sterile water as needed.

Four weeks after perforation, animals were randomized into one of three treatment groups, with n=6 animals per group: no treatment, treatment with daily MSC CM topical drops, treatment with CM MS 504/gel. MSC CM was processed as described previously via filtration for 20mins at 4000rpm in 3kDa filter tubes (Amicon Ultra, MilliporeSigma, Burlingame, MA) and resulting filtrate diluted with DI H2O to approximate release from CM MS. Approximately 100µL of these drops were applied at the same time every day for 21 days. For the MS/gel treatment group, 200mg MS were mixed with 2mL gel and each animal received 100µL of the mixture administered via 1mL syringe and 18G x 1" needle. CM MS 504 were fabricated as described in Section 4.2.2. After sacrifice via intracardiac sodium pentobarbital under isoflurane anesthesia, TMs were excised, visually inspected, and photographed. Timeline of imaging and treatment is seen in Figure 38.

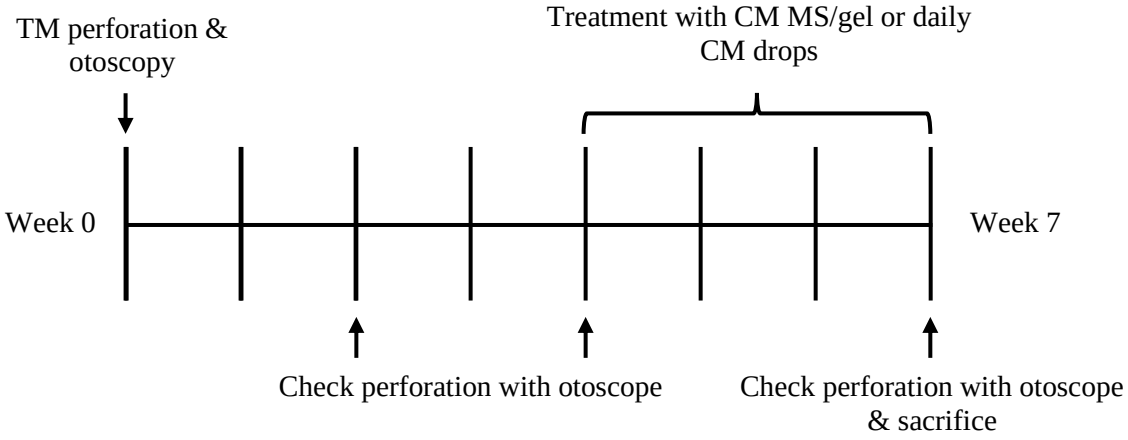

Figure 38: Timeline of *in vivo* tympanic membrane perforation and treatment.

5.2.2 Histopathology

Following sacrifice, TMs were excised and after visual inspection, fixed for 24h in 10% formalin. TMs were then dehydrated overnight in 70% ethanol, embedded in paraffin, sectioned in 5μm thick sections, and stained with hematoxylin and eosin (H&E). Paraffin histology was performed by the Histology Module within the McGowan Institute for Regenerative Medicine at the University of Pittsburgh, with stained sections imaged and evaluated using light microscopy (Leica Microsystems DM2500) and digital microscope camera (Leica Microsystems DFC295) by a blinded technician.

5.3 Results

5.3.1 Wound Healing of Tympanic Membrane Perforations

After sacrifice, both left and right TMs were removed from each animal and visually inspected as well as photographed to determine presence of perforation or any abnormal physiology. All left ears, which had no manipulations or treatment, were pristine as expected. Right ears were classified into three categories: 1) absent TMP, normal physiology; 2) absent TMP, abnormal physiology, 3) visible TMP. Representative images can be seen in Figure 39.

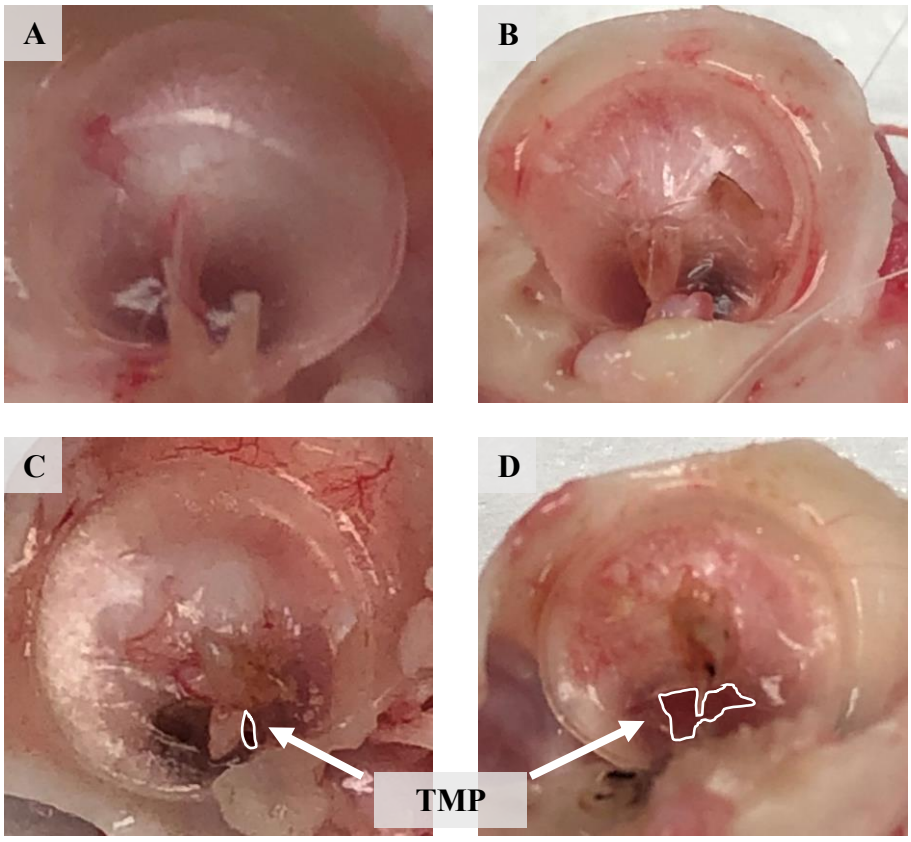

Figure 39: Representative images of tympanic membranes (TMs) post-sacrifice. A) Pristine TM from contralateral ear with no manipulations or treatment; B) No perforation but abnormal physiology characterized by sagging TM and presence of dried blood; C) small TM perforation (TMP); D) larger TMP. Wound margins are outlined in white for each TMP.

In the no treatment group, 2 of 5 ears had small visible TMPs with the remaining 3 having absent TMP but abnormal physiology, including sagging rather than tight TM and presence of blood or other fluid. In the group treated with daily CM drops, 2 of 5 ears also had visible TMPs, however 2 had absent TMPs with normal physiology and 1 had absent TMP with abnormal physiology, suggesting increased wound healing due to application of conditioned media. In both these groups, n=5 animals were analyzed as one animal from each group was removed from the

study early. One animal was in the no treatment group due to an adverse reaction to anesthesia and one was removed from the CM drops group due to infection unrelated to treatment.

In the group treated with CM MS/gel, gel was found inside the bulla, indicating either that it was placed through the TMP during instillation or sunk through the perforation into the bulla during the treatment duration. Presence of gel physically blocking the TMP from healing may have had an adverse effect on wound healing, with 3 of 6 of animals having visible TMP and abnormal physiology including gel protruding through the TMP and fluid and cerumen build up. Presence of gel on reverse side of TM and healed TM visualized after removal of gel can be seen in Figure 40. However, 1 animal had absent TMP with normal physiology and 2 animals had absent TMP but with some abnormal physiology including fluid and cerumen build up. For this group, all 6 animals were analyzed.

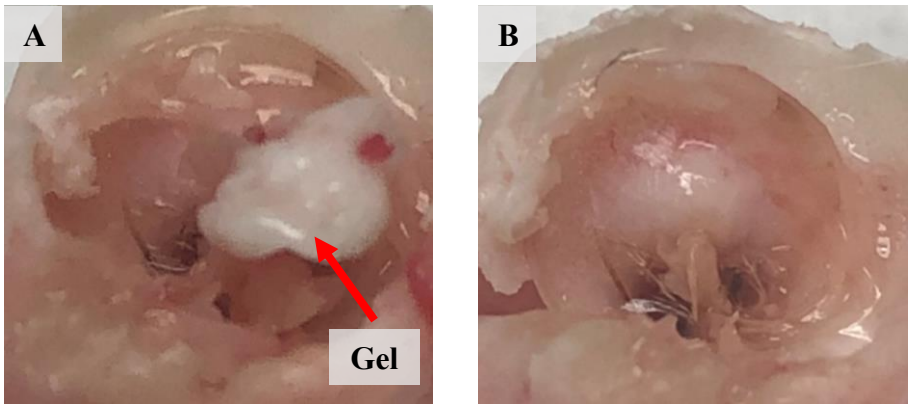

Figure 40: Conditioned media-loaded microspheres/gel after sacrifice and dissection: A) on reverse side of TM, inside bulla, and B) same TM but with gel removed showing lack of TMP but abnormal physiology.

Table 3: Results of tympanic membrane perforation (TMP) in vivo study. Results are displayed as number of ears for each observed TM condition post-sacrifice for each treatment group. For no treatment and daily CM drops, n=5 animals were analyzed while all n=6 were analyzed for CM MS/gel group due to 2 animals removed from the study due to adverse reaction to anesthesia and infection unrelated to treatment.

	Absent TMP, normal physiology	Absent TMP, abnormal physiology	Visible TMP
No treatment	0	3	2
Daily CM drops	2	1	2
CM MS/gel	1	2	3

5.3.2 Histopathology

While the tissue samples for pristine TM and TM with perforation absent and normal physiology (Figure 41A-B) where somewhat damaged during dissection and staining, H&E staining indicates normal physiology and lack of edema or immune response, comparable to previous examinations of healthy guinea pig TMs. TM with absent perforation but abnormal physiology (Figure 41C) displays increased edema. TM with visible perforation (Figure 41D) displays increased edema as well as enlargement compared to other samples, indicating damage and possibly infection due to perforation.

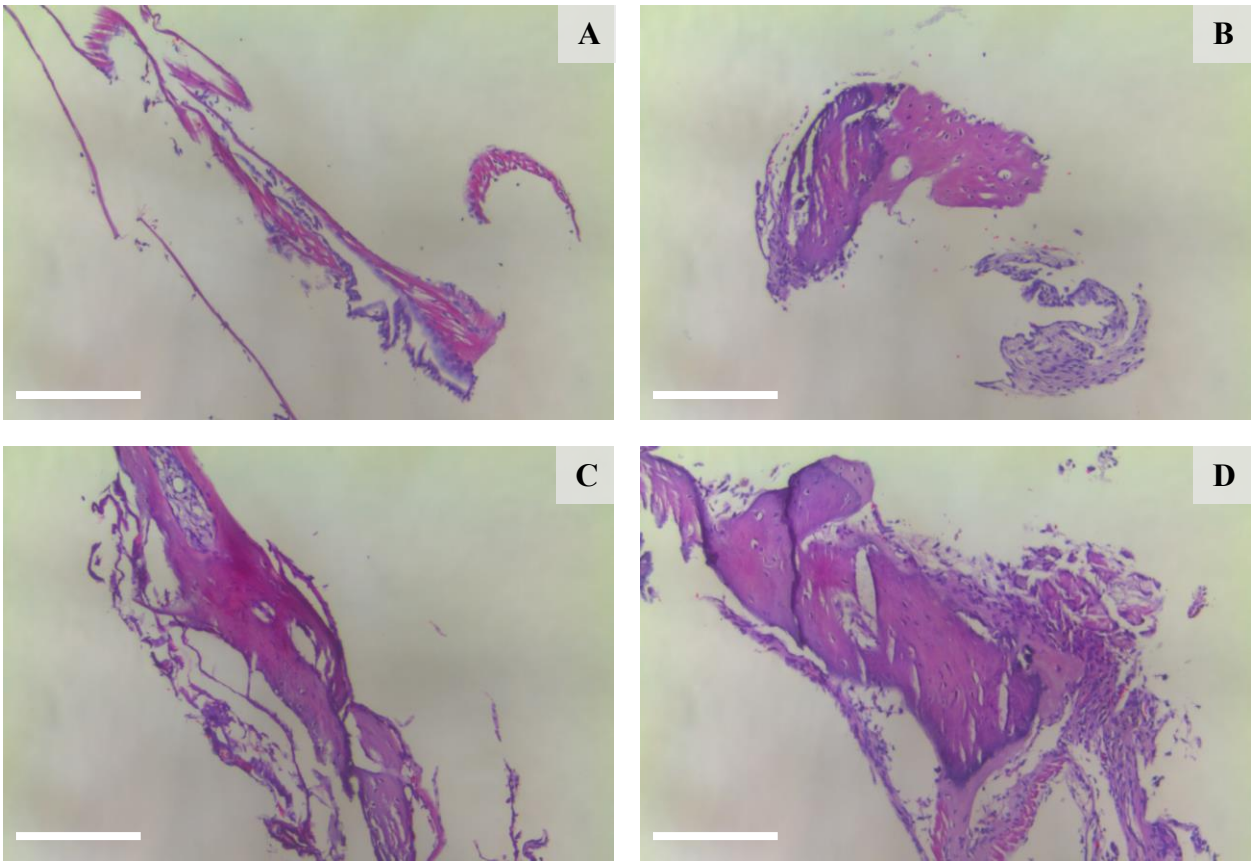

Figure 41: Representative images of hemotoxylin and eosin (H&E) stained guinea pig tympanic membranes (TMs). Images represent A) pristine TM; B) absent TMP, normal physiology; C) absent TMP, abnormal physiology; and D) visible TMP. Scale bars = 200nm.

5.4 Discussion

The group that received no treatment resulted in 40% persistent TMP, which agrees with previously cited statistics of 6-46% of TMPs being non-healing without treatment [73,74]. The remaining 60% displayed abnormal physiology including build-up of fluid, dried blood, and cerumen, indicating incomplete healing despite lack of visible TMP. While the group treated with

daily CM MS drops also resulted in 40% non-healing, only 20% had abnormal physiology and the remaining 40% had no visible TMP and normal physiology. These results suggest a positive effect on wound healing due to application of conditioned media drops, which is expected due to previous studies on growth factor and stem cell treatment exhibiting positive effects on wound healing [73,74,102,103,106,112,114].

CM MS 504 were chosen for CM MS/gel group study due to their extended 21-day release profile (Figure 16). Either during placement or during the treatment duration, all MS/gel systems migrated through the TMP into the bulla. In several cases, the gel/MS system was protruding through the TMP and physically preventing the wound from healing. This may have also contributed to increased fluid and cerumen build up, as abnormal physiology was observed in all TMs with TMPs and 33.3% of ears showed no visible TMP but persistent abnormalities. However, despite gel/MS migration into the bullae, 16.7% of ears had complete wound healing.

There were a number of limitations to the guinea pig TMP model described herein that can be addressed in future studies. Perforation was achieved using an 18G needle in this study, which occasionally resulted in injury to the external ear canal, causing blood and subsequently dried blood to confound imaging. Further, this technique may have caused a tear than a distinct TMP. To ensure precise placement of the needle, a myringotomy needle attachment can be used in conjunction with the otoscope. Further, irrigation and suction attachments can be used to better clear ear canal of any ear wax, blood, or moisture that can confound visualization and imaging. Myringotomy can also be performed repeatedly over several weeks to ensure TMP becomes chronic. Other techniques include injury using thermal cautery and folding of wound edges after myringotomy; however, there is some dispute as to the reliability of these methods [184].

Mitomycin C is an antibiotic that prevents cell proliferation and can delay healing but does not result in chronic TMP by itself. However, there is evidence that application of higher concentrations of mitomycin C for longer periods of time up to 7 days can delay healing but there are concerns of ototoxicity associated with high concentrations of mitomycin C [184,185]. The study described herein used a relatively high concentration of 0.5mg/mL applied via gelfoam sponge for 5mins after perforation. To delay healing duration and closer approximate chronic TMP *in vivo* while minimizing ototoxicity, different concentrations of mitomycin C and application durations can be tested. Dexamethasone can also be used topically to delay healing up to 30 days, as well as hydrocortisone, which was applied for 7 days in our study but can be extended to 10 days to make TMP more persistent. Based on previous studies, mitomycin C used in conjunction with a steroid results in synergistic effects on delaying TMP healing [184].

To determine time-dependent effect of treatment on TM healing, TMs can be imaged weekly via otoendoscopy, with MS/gel drop removed to facilitate visualization and replaced with fresh gel containing aged MS. To achieve a consistent release profile, MS should be aged for days 1-21 (n=12 samples of 10mg) by suspending in PBS and rotating in a 37°C incubator. As previously described for release assays, these aliquots should be centrifuged and supernatant collected every 24h. For each imaging time point, MS can be resuspended in gel after 7 days (n=6 samples) and 14 days (n=6 samples) and used as replacement MS/gel drop after otoendoscopy.

In conjunction with otoendoscopic imaging for qualitative assessment of TM wound healing, auditory brainstem responses can be used as described previously to confirm TMP due to conductive hearing loss as a result of non-intact TM and confirm adequate wound healing determined by a renewed capacity to hear using injured ear [143,144,185]. ABRs are also used as a test of safety of ototopical treatments based on effect on hearing sensitivity [65,69,145,146]. To

more accurately determine positive effect on wound healing due to topical CM drops and CM MS treatment, ABRs can be used longitudinally in addition to imaging to track hearing sensitivity after myringotomy to induce TMP and during treatment, as well as at a time point some weeks or months after treatment to determine long term effects of treatment.

6.0 Summary and Future Directions

6.1 Overall Summary

The studies described in this dissertation address an unmet need of safe, easy-to-administer, and effective topical drug delivery systems to the tympanic membrane and middle ear. This work developed a drug delivery platform comprised of hydrolysable polymer microspheres for controlled release of various therapeutics and scaled up a previously developed gel for increased ease of application and retention of microspheres *in situ*. This drug delivery system was able to be modified during fabrication to encapsulate and release a variety of therapeutics in a variety of release profiles, indicating its potential as a delivery platform that can be modified and optimized based on therapeutic need for particular conditions.

These studies demonstrate that the PLGA MS/thermoresponsive gel system is capable of encapsulating and subsequently releasing up to 14 days of potentially therapeutically relevant levels of two different antibiotics for clearance of bacteria present in acute otitis media. *In vitro* cell viability and bacteria killing studies indicated these materials can be safe for *in vivo* and eventual clinical use while maintaining ability to clear bacteria. Histopathological evaluation suggests *in vivo* safety of the drug delivery system, with further research needed to examine material-specific toxicity response. Auditory brainstem responses indicated complete coverage of TM and ability to increase volume of material applied to increase therapeutic potential while maintaining minimal effect on quality of life due to hearing attenuation during treatment. *In vivo* studies in a chinchilla otitis media disease model demonstrated potential for the novel drug delivery system to effectively treat bacterial infection, with room for improvement and

optimization of the animal model for future efficacy studies, including accounting for variability in the disease model by testing for biofilm presence prior to treatment and determining optimal dose and treatment window after bacterial inoculation.

The PLGA MS are also capable of encapsulating and subsequently releasing MSC conditioned media, including free and extracellular vesicle-bound growth factors such as FGF-2 for up to 21 days. Further investigation is necessary to determine daily vesicle shedding from MS and total protein and FGF-2 content in these vesicles. *In vitro* cell viability testing and scratch wound proliferation assays suggest these materials can be safe for *in vivo* and clinical use and indicate wound healing ability. While there were limitations in the TMP animal model, there is evidence to suggest CM has a positive impact on wound healing and CM-loaded MS/gel placement, with some improvement and refinement of placement and removal techniques, may also have a positive effect on wound healing.

6.2 Summary of Challenges and Limitations

While promising formulations were developed for delivery of two different antibiotics and stem cell conditioned media from PLGA MS, there were a number of challenges and limitations in the studies described herein. Firstly, despite mostly acceptable levels of *in vitro* cytotoxicity, several groups resulted in slightly less than 70% cell viability at 24h in culture and several groups displayed high variability in percentage of viability. These results, along with previously reported studies on biocompatibility of both PLGA-based materials and the loaded therapeutics, suggest *in vivo* biocompatibility of this drug delivery system. However, further studies investigating time and concentration dependence may be warranted. Variable results were also noted in histological

examination of both chinchilla and guinea pig tissues. In terms of the AOM chinchilla disease model study, presence of infection leads to inherent tissue inflammation and confounds the histology results. For examination of tissue response to materials alone, materials should be applied to healthy animals and histology performed after serial sacrifice at various time points during the intended treatment duration. Further, long term *in vivo* ototoxicity was not investigated. This could be achieved using ABR at a chronic time point some weeks after end of treatment duration. In particular, ceftriaxone has not been previously used topically therefore topical safety must be investigated.

For scratch wound proliferation assays testing *in vitro* efficacy of conditioned media and CM-loaded MS releasates, a challenge was posed by presence of MS in releasates confounding imaging of scratches. This issue was addressed by filtration, however this resulted in decreased concentration of total protein in the releasates due to non-specific adsorption to the filters. Release was scaled up for total protein after filtration to match original unfiltered release. Effect of filtration on FGF concentration in releasates was not investigated. While significant differences in wound healing were observed due to CM MS 503 releasates, no significant increases were observed due to CM MS 504 releasates compared to blank MS releasates. For these studies, 24-well plates were used, which have a surface area of approximately fivefold greater than human TM surface area. Therefore, increased wound healing may be seen in smaller surface area due to greater concentration of protein localized to the scratch wound. Smaller well plates were not able to be used due to difficulty in creating the scratch. Further optimization of a more physiologically relevant *in vitro* scratch wound assay may provide more relevant and repeatable results.

While ciprofloxacin-loaded and ceftriaxone-loaded MS showed some promise in treatment of AOM *in vivo*, there were challenges with this animal model as well. First, treatment 24h after

bacterial inoculation may not have allowed enough time for infection to develop but adjustment to treatment 72h after inoculation resulted in persistent biofilm formation. Rather than randomizing animals into treatment groups, animals can be tested for presence of bacteria and biofilm formation prior to treatment, with animals exhibiting persistent biofilm treated with ceftriaxone-loaded MS while those with bacterial infection but no biofilm treated with ciprofloxacin-loaded MS. Another challenge included application of the gel/MS system directly onto the TM. An applicator using a syringe and bent 18G needle were used to improve application of precise amount of gel/MS to the TM, however a more reliable and precise system must be engineered for reliable application in animal models, as well as for humans for clinical use.

There were also challenges associated with the *in vivo* TMP model in guinea pigs. It was difficult to ensure successful TMP using an 18G needle and due to a lack of visualization, the needle occasionally injured the external auditory canal prior to perforation, with blood in the canal confounding imaging using otoendoscopy and making confirmation of successful TMP difficult. Further, dried blood and cerumen in the ear canal confounded confirmation of TMP over time as well. One solution to this limitation can be the use of a myringotomy needle attachment to otoscope to ensure better visualization during perforation. In addition to otoscopy, weekly ABR experiments were originally planned to confirm presence of TMP, as well as to track wound healing over time. However, there were time constraints associated with the number of animals that could be tested each day and complications from anesthesia resulted in one animal removed from the study. These ABR experiments are an important metric of effect of wound healing on hearing sensitivity as well as a metric of ototoxicity over time and therefore should be included in future studies with improved experimental design accounting for associated time constraints, including performing experiments on one group at a time rather than all treatment groups simultaneously.

6.3 Future Directions

Future studies will focus on further microsphere optimization and improvement of the disease models, including increased antibiotic delivery and accounting for variability in the otitis media model as well as further investigation of best practices for inducing tympanic membrane perforation and investigation of time-dependent effect of treatment on wound healing. Future work will also investigate incorporation of analgesic into the gel for local pain relief due to AOM [146,186–188] and encapsulation of other therapeutics into this drug delivery system for topical treatment of other otic conditions. In addition, there is a need for expanded testing of long-term ototoxicity due to topical ceftriaxone alone and application of all drug-loaded MS/gel, including longitudinal ABR testing to investigate chronic effect on hearing after treatment. Further, clinical translation potential can be improved by engineering design of a user-friendly applicator for the drug delivery system and investigation of best practices to remove the MS/gel at the end of the treatment duration, including use of a biodegradable gel if removal proves to be difficult.

Appendix A

Quality Control of Brimonidine Tartrate Microsphere and Gel Fabrication for Treatment of Glaucoma

Appendix A.1 Introduction

Using techniques developed for encapsulation of small molecular weight, water-soluble drugs like ciprofloxacin, a natural extension of the work described in this dissertation was to investigate encapsulation of similar drugs for other applications, such as the controlled release of brimonidine tartrate (BT) for treatment of glaucoma. Ciprofloxacin and BT have similar molecular weights of 331.346g/mol and 442.22g/mol, respectively, and are both water-soluble, therefore comparable formulation techniques can be used for encapsulation of both molecules. Further, standard topical eye drops suffer from some of the same issues as topical ear drops, including low permeability and low patient compliance due to high dosing frequency and difficult administration.

Appendix A.1.1 Glaucoma Severity and Treatment

Glaucoma, the second leading cause of blindness worldwide, is characterized by increased intraocular pressure (IOP) that damages the optic nerve which in turn causes vision impairment [38,189]. Treatment typically consists of eye drops applied topically multiple times a day for the rest of the patient's life, a high frequency dosing regimen that, in conjunction with difficulty of

administration, results in high levels of non-adherence to the proper treatment regimen. In addition, ocular drops suffer from low penetration through the cornea due to blinking, rapid lacrimal fluid turnover, and nasolacrimal drainage resulting in short retention times of drops residing on the cornea [5,38,121,189,190]. Among the commonly prescribed treatments for glaucoma are brimonidine tartrate drops. BT can reduce IOP by decreasing production of aqueous humor and also increase uveoscleral outflow. BT has also shown to have neuroprotective effects and lower pulmonary and cardiovascular side effects compared to other glaucoma treatments.

To ameliorate some of the compliance and pre-corneal residence time issues associated with standard topical drops, a variety of drug delivery systems have been investigated including nanoparticles, microspheres, hydrogels, implants, and ocular inserts [5,189,190]. An ideal topical ophthalmic drug delivery system should be easy to administer without causing irritation or adversely affecting patient's vision, decrease dosing frequency, increase pre-corneal retention to increase drug penetration and bioavailability, and decrease risk of systemic side effects. To this end, previous studies by this group investigated the development of BT-loaded PLGA microspheres that can be administered via subconjunctival injection or topically applied via a thermoresponsive gel depot [38,121].

Appendix A.1.2 Key Factors for Biomedical Translation of Biomaterials

More generally, some of the key factors for biomaterials to be used in biomedical applications include: simple fabrication and processing, biocompatibility (including easy metabolization of degradation byproducts of biodegradable materials), sufficient shelf-life for prescribed use, and ability to be sterilized without significant mechanical or functional changes [8].

Release profiles from polymer microspheres can be modulated by adjusting factors such as copolymer ratio, polymer molecular weight, microsphere size, porosity of polymer matrix, and drug concentration/dispersion in the microspheres [13–17]. In single and double emulsion fabrication methods, surfactants such as poly(vinyl alcohol) (PVA) are used as emulsifiers [20,191]. Properties of the surfactant used can affect drug encapsulation and polymer matrix porosity [13,15]. For example, altering PVA concentration in fabrication has previously shown to affect matrix porosity and in turn modulate initial burst release phase [13,192]. Additionally, surfactants have been used to increase solubility and bioavailability of hydrophobic and poorly soluble drugs as well as surface functionalization of controlled release systems such as nanoparticles to improve circulation [193–196]. For encapsulation of proteins in particular, surfactants can stabilize the oil-water interface which is known to cause protein denaturation, therefore use of an appropriate surfactant can increase encapsulation efficiency of active proteins [191,192].

For clinical use, biomedical devices and materials must be sterilized to ensure materials do not introduce any biological contaminants to patients during treatment. For ease of fabrication, final sterilization is preferable to fabrication of materials under sterile conditions [19]. Gamma irradiation is frequently used as a sterilization method for PLGA and hydrogel materials and has been shown to effectively sterilize the materials without significantly compromising their material properties or drug delivery capabilities [175–180]. Other sterilization techniques include ethylene oxide and autoclaving, however steam causes degradation of hydrolysable materials and high temperatures can adversely affect thermosensitive materials such as the pNIPAAm gel used in our studies [19]. Gamma irradiation is effective due to high penetration into the material but can cause some structural changes to the polymer and encapsulated drug, particularly proteins, including

reducing molecular weight of the polymer which can in turn reduce the duration of the lag phase of drug release [13,19]. To ensure retention of desired release profile after sterilization, it is important to perform quality control experiments on the materials in addition to endotoxin testing to confirm effect of sterilization and lack of structural changes to the materials.

In addition to quality control of sterility, it is important to investigate long term storage of biomaterials, as they should not degrade or deteriorate before their intended use [203]. In addition to time scale, storage conditions such as temperature and humidity can affect performance of polymer microspheres and gels [204,205]. PLGA microspheres are typically stored at -20°C due to lack of mobility of polymer chains and lack of moisture at temperatures below freezing. However, to account for patient noncompliance to storage requirements, it is important to investigate shelf life of materials at a variety of storage temperatures, including standard refrigeration and ambient conditions [204,205]. At high temperatures and/or high humidity, accelerated physical aging can occur which can negatively impact shelf life of polymeric materials and affect release of encapsulated therapeutics [203,205].

Appendix A.2 Materials and Methods

Materials were obtained from Sigma-Aldrich (St Louis, MO) unless otherwise noted.

Appendix A.2.1 Brimonidine and Ciprofloxacin-loaded MS Formulations

BT-loaded MS were fabricated according to previously published methods [31,114]. In brief, 200mg PLGA (MW 24-38 kDa; viscosity 0.32-0.44dL/g) were dissolved in 4mL

dichloromethane and 250µL of 50mg/mL BT (Santa Cruz Biotechnology, Santa Cruz, CA) was added. This mixture was sonicated for 10 seconds at 30% amplitude (EpiShear Probe Sonicator, Active Motif, Carlsbad, CA) and then homogenized in 60mL of 2% PVA (Appendix Table 1) for 1 minute at 7000rpm (Silverson L5M-A, East Longmeadow, MA). The resulting double emulsion was added to 80mL of 1% PVA and stirred at 600rpm for 3h. Ciprofloxacin-loaded MS were fabricated using the same methods, using 250µL of 100mg/mL ciprofloxacin. Blank MS were fabricated by substituting DI water alone for aqueous drug. All MS were washed 4 times by centrifugation, resuspended in DI water, flash frozen in liquid nitrogen, and lyophilized for 48-72 hours (Benchtop Pro, SP Scientific, Warminster, PA).

Appendix A.2.2 Surfactant Molecular Weight Determination

To investigate surfactant effect on MS release profiles, molecular weights (MW) of 4% PVA solutions were analyzed using size exclusion chromatography (SEC) via gel permeation chromatography (GPC) performed by the University of Pittsburgh Department of Chemistry. Molecular weights were determined for Polysciences brand PVA lots purchased in 2015 and 2019 (referred to as PS 2015 and PS 2019) and Alfa Aesar PVA purchased in 2019. A 4% solution of each brand of PVA was prepared by dissolving 32g of solid PVA powder in 800mL of DI H2O for 12-24h at 80°C. Absorbance spectra were determined at 280nm.

Appendix Table 1: Poly(vinyl alcohol) properties.

Brand	**Molecular weight (Da)**	**Viscosity (cP) of 4% PVA in H_2O**	**% Hydrolysis**	**Year purchased**
Polysciences (PS)	25,000	5.5-6.0	98	2015
Polysciences (PS)	25,000	5.5-6.0	98	2019
Alfa Aesar	11,000-31,000	N/A	98-99	2019
Sigma-Aldrich	31,000-50,000	5.4-6.5	98-99	2019
Acros	13,000	3.5-3.5	98-98.8	2019

Appendix A.2.3 Fluorescein Isothiocyanate-loaded MS Fabrication

MS were also fabricated with fluorescein isothiocyanate (FITC) loaded as surrogate drug. These MS were fabricated using the above methods with 50:50 lactide:glycolide PLGA with MW 24-38kDa (viscosity 0.32-0.44dL/g) and MW 38-54kDa (viscosity 0.45-0.60dL/g), 75:25 lactide:glycolide PLGA (MW 76-115kDa; viscosity 0.71-1.0dL/g), and 85:15 lactide:glycolide PLGA (MW 190-240kDa; viscosity 1.3-1.7dL/g). These will subsequently be referred to as FITC MS 503, FITC MS 504, FITC MS 756, and FITC MS 858, respectively. FITC MS 503 were fabricated using DCM or acetonitrile (ACN) as organic solvent. FITC MS 503 and FITC MS 756 were also fabricated using single emulsion with FITC dissolved in DMSO. All FITC MS formulations incorporated an appropriate amount of salt in PVA to balance osmolality of FITC solutions. A summary of these properties can be found in Appendix Table 2.

Appendix Table 2: FITC MS fabrication parameters.

Batch name	PLGA properties	Organic solvent	FITC solution
FITC MS 503	50:50 lactide:glycolide; MW 24-38kDa	DCM	20mg/mL in DI water
FITC MS 503 ACN	50:50 lactide:glycolide; MW 24-38kDa	ACN	20mg/mL in DI water
FITC MS 503 DMSO	50:50 lactide:glycolide; MW 24-38kDa	DCM	20mg/mL in DMSO
FITC MS 504	50:50 lactide:glycolide; MW 38-54kDa	DCM	20mg/mL in DI water
FITC MS 756	75:25 lactide:glycolide; MW 76-115kDa	DCM	20mg/mL in DI water
FITC MS 756 DMSO	75:25 lactide:glycolide; MW 76-115kDa	DCM	20mg/mL in DMSO
FITC MS 858	85:15 lactide:glycolide; MW 190-250kDa	DCM	20mg/mL in DI water

Appendix A.2.4 *In Vitro* Drug Release Assays

Drug release from these formulations were quantified as described previously, with 20mg BT MS, 10mg ciprofloxacin MS, or 10mg FITC MS suspended in 500mL PBS, rotated at 37°C, and supernatant collected daily by centrifugation for 5mins at 3500rpm. BT was quantified by UV/Vis absorbance at 320nm and ciprofloxacin was quantified at 246nm. FITC was quantified by fluorescence intensity at λex = 460nm and λem = 515nm (SoftMax Pro 5, Molecular Devices, Sunnyvale, CA).

Appendix A.2.5 Thermoresponsive Gel Fabrication

Gel was fabricated according to previous small-batch methods [31] via free radical polymerization of 100mg NIPAAm (Fisher Scientific, Waltham, MA) and 100µL PEG (MW ~200kDa) in the presence of 2mL of 0.5mg/mL APS and 5 µL TEMED, refrigerated for 24h, and washed in DI water at ~40ºC.

Appendix A.2.6 Material Shelf Stability and Sterilization

Microspheres and gel were stored at various storage temperatures (Appendix Table 3) for 1, 3, 6, and 12 months. These time points and temperatures were chosen based on previous studies on storage conditions and shelf stability of PLGA MS and gels [204,205]. At these time points, properties including microsphere morphology and drug release and gel LCST were tested to determine shelf-life stability. Materials were sterilized in 50mL conical Falcon tubes via gamma irradiation at $2.5x10^6$cGy at room temperature for 18h. Control and irradiated samples were

analyzed for significant differences in endotoxin concentration with Mann Whitney U testing using GraphPad Prism Software.

Appendix Table 3: Stability testing storage conditions.

Material	Storage temperatures (°C)	Storage time (months)	Properties
BT microspheres	-20, 4, 25	1, 3, 6, 12	SEM, BT release
Gel	4, 25, 30	1, 3, 6, 12	LCST

Appendix A.3 Results

Appendix A.3.1 Brimonidine and Ciprofloxacin MS Morphology and Release Profiles

Overall morphology of both BT and ciprofloxacin MS was not changed due to different PVA used during fabrication, as observed visually using SEM (Appendix Figure 1 and 2). BT concentrations in MS releasates were determined using the standard curve in Appendix Figure 3. BT MS fabricated using Sigma-Aldrich and Acros PVA degraded after 24 and 48h in PBS, respectively. The original formulation reported in Fedorchak et al 2014 [114] observed an approximately 10µg burst release followed by ~2µg/day for 28 days for an overall release magnitude of ~60µg. BT MS fabricated using Polysciences 2015 PVA exhibited greater burst release but similar release rate. BT MS fabricated using Polysciences 2019 PVA exhibited similar burst release (6.43 µg) as the original 2014 formulation but a slower release rate of 0.9µg/day for an overall release magnitude of 31.5µg, which is approximately half of the original formulation

overall magnitude. BT MS fabricated using Alfa Aesar PVA exhibited the same release rate as the PS 2019 PVA formulation but MS degraded after 14 days rather than the full 28-day release profile. These release profiles are summarized in Appendix Figure 4 and Appendix Table 4. In contrast, while there were some differences between ciprofloxacin release curves, initial burst, release rates, and overall magnitudes of release were comparable over 14 days (Appendix Figure 5).

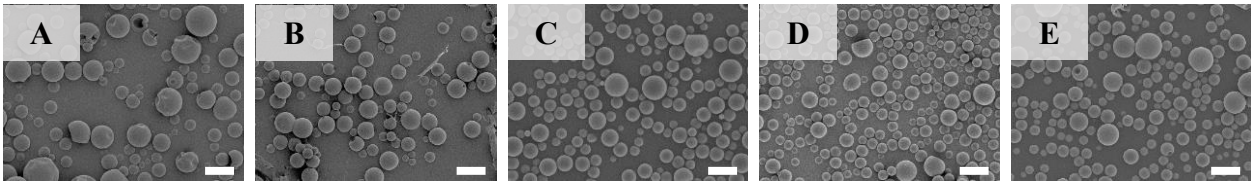

Appendix Figure 1: Scanning electron microscopy images of brimonidine tartrate microspheres. MS were fabricated using A) Polysciences 2015, B) Polysciences 2019, C) Alfa Aesar, D) Sigma-Aldrich, and E) Acros PVA. Scale bar = 10µm.

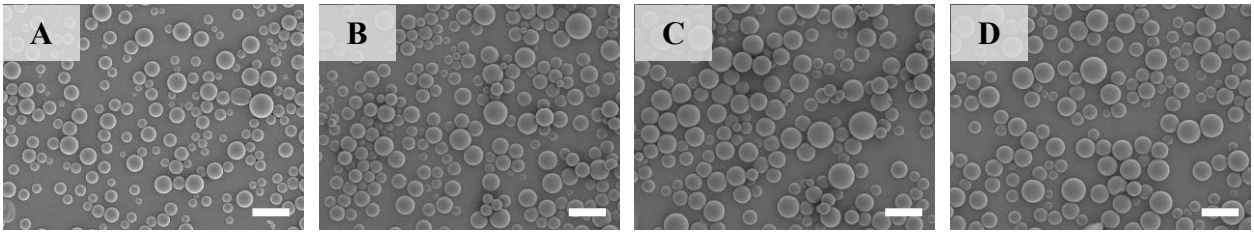

Appendix Figure 2: Scanning electron microscopy images of ciprofloxacin microspheres. MS were fabricated using A,B) Polysciences 2015, C) Polysciences 2019, and D) Alfa Aesar PVA. Scale bar = 10µm.

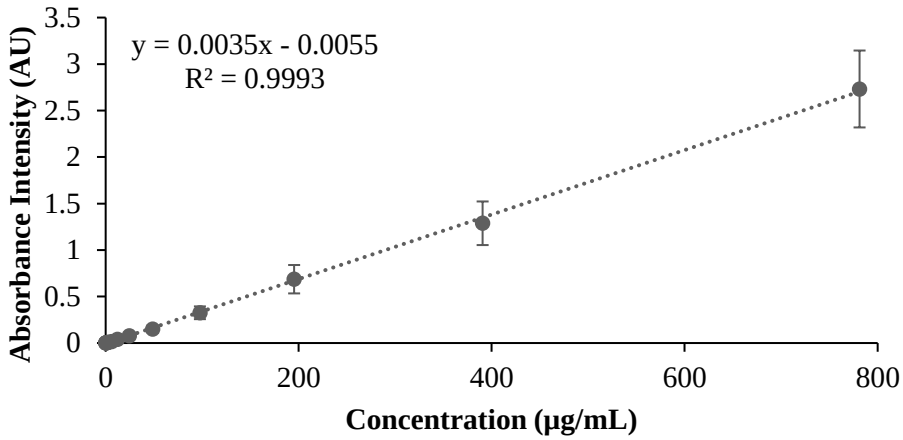

Appendix Figure 3: Brimonidine tartrate standard curve determined via spectrophotometry.

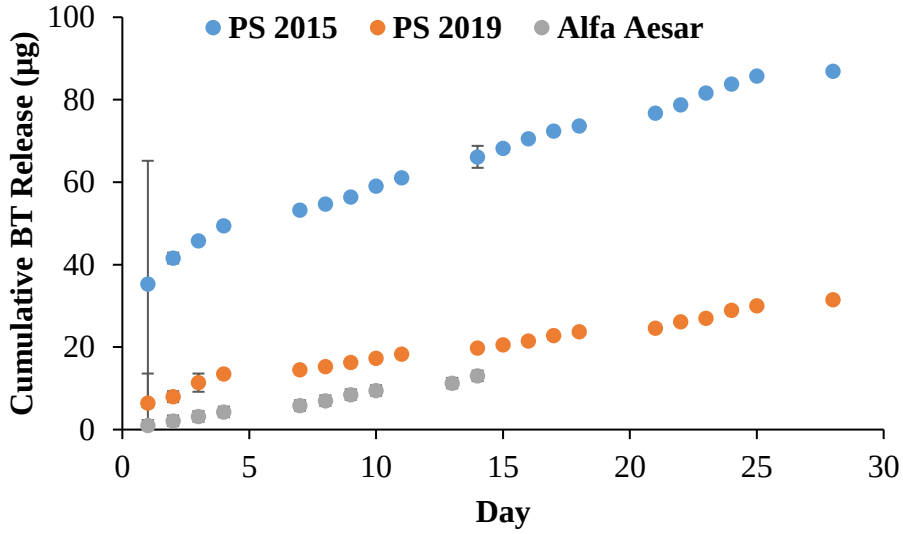

Appendix Figure 4: Brimonidine tartrate release from 10mg microspheres fabricated using different surfactants: Polysciences 2015, Polysciences 2019, and Alfa Aesar. Release assays were carried out until all microspheres were degraded: 28 days for both Polysciences lots and 14 days for Alfa Aesar. Error bars represent the mean ± standard deviation for n=3 samples.

Appendix Table 4: Brimonidine tartrate MS formulations and release parameters.

Parameter	Original 2014	PS 2015	PS 2019	Alfa Aesar
Initial burst release (µg)	~20	35.3	6.43	1.05
Overall release magnitude (µg)	~60	86.9	31.5	13.03
Release rate (µg/day)	~2	1.8	0.9	0.9

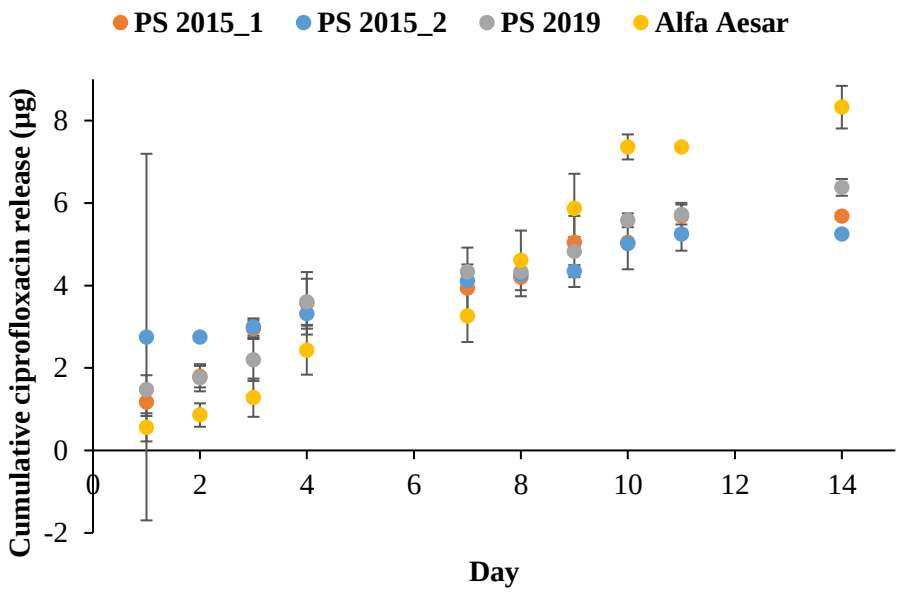

Appendix Figure 5: Ciprofloxacin release from 10mg microspheres fabricated using different surfactants: Polysciences 2015, Polysciences 2019, and Alfa Aesar. PS 2015_1 and PS 2015_2 refer to two different batches of ciprofloxacin-loaded MS fabricated with Polysciences 2015 PVA and tested on different dates. Error bars represent the mean ± standard deviation for n=3 samples.

Appendix A.3.2 Surfactant Molecular Weights

A standard curve for size exclusion chromatography was determined for a retention time range of 4.94-8.18mins corresponding to a molecular weight range of 1,350-670,000Da (Appendix Figure 6). For each lot of PVA, peaks were determined within the detection range at approximately 6-6.5mins (Appendix Figure 7). These peaks correspond to the PVA. For PS 2015, a peak at 6.29 mins corresponds to 66,000Da. For PS 2019, peaks at 6.21 and 6.74mins correspond to 76,000 and 30,000Da, respectively. For Alfa Aesar, a peak at 6.38 mins corresponds to 57,000Da. These determined molecular weights are all greater than listed molecular weights of 25,000 Da for both Polysciences lots and 11,000-31,000Da for Alfa Aesar (Appendix Table 5).

Peaks above the detection range are less than 1,350Da and may correspond to vinyl monomer, which has a molecular weight of 44.05Da. Further investigation is needed to determine the nature of the high molecular weight peaks below the detection range.

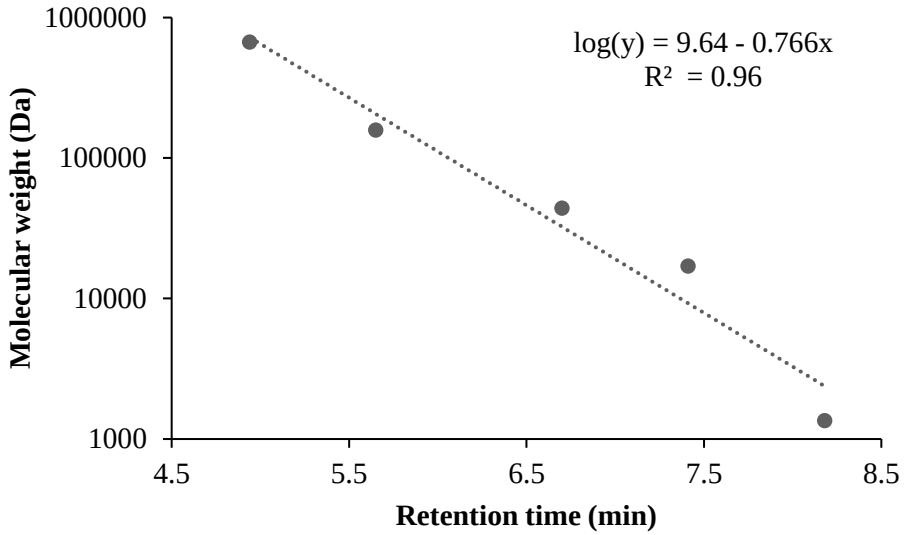

Appendix Figure 6: Standard curve for size exclusion chromatography determined at absorbance of 280nm.

Appendix Table 5: Listed and experimentally-determined molecular weights of different PVA lots.

Brand, year purchased	Listed MW (Da)	Experimental MW (Da)
Polysciences (PS), 2015	25,000	66,000
Polysciences (PS), 2019	25,000	76,000; 30,000
Alfa Aesar, 2019	11,000-31,000	57,000

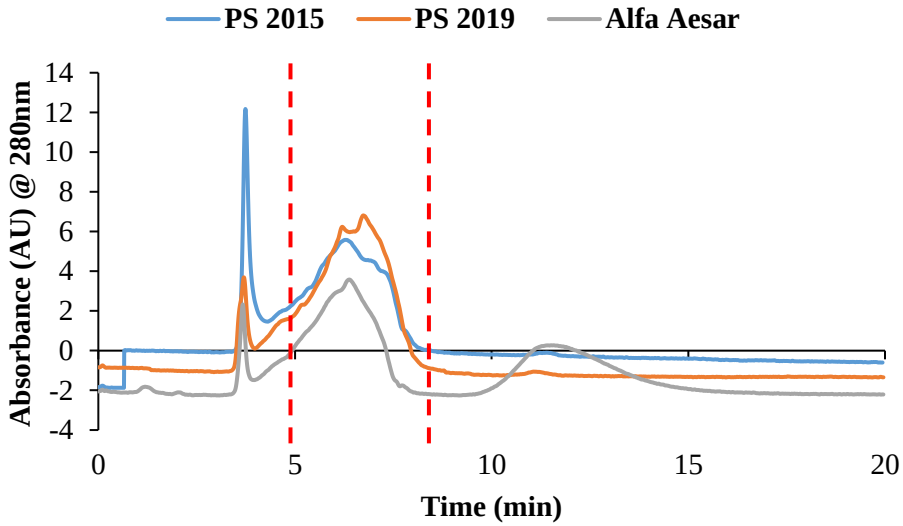

Appendix Figure 7: Size exclusion chromatography spectra for Polysciences 2015, Polysciences 2019, and Alfa Aesar PVA. Detection range of 4.94 – 8.18 minutes is indicated by red dotted lines.

Appendix A.3.3 FITC MS Morphology and Release Profiles

FITC MS morphology was overall spherical and non-porous, with the exception of MS fabricated using ACN as organic solvent, which resulted in large size distribution and distorted morphology (Appendix Figure 8). Release profiles were determining using the standard curve in Appendix Figure 9. FITC MS fabricated using different polymers, organic solvents, and double versus single emulsion resulted in differing release curves as shown in Appendix Figures 10 and 11. Standard double emulsion fabrication using 503 or 503 PLGA did not result in large differences in release profile, with MS 503 exhibiting slightly greater initial burst and overall magnitude of release. FITC 503 ACN and DMSO exhibited similar burst and release curve as well, however FITC MS 503 DMSO were degraded after 4 days rather than 7-9 days as observed in all other

release profiles. FITC MS 756 and 858, those fabricated with higher ratio of lactide to glycolide in the PLGA, exhibited lower burst and overall magnitude of release, with the lowest release correlated with the highest ratio of lactide in FITC 858 MS. FITC MS 756 DMSO exhibited a comparable release profile to FITC MS 756, with similar burst and slightly lower overall release magnitude.

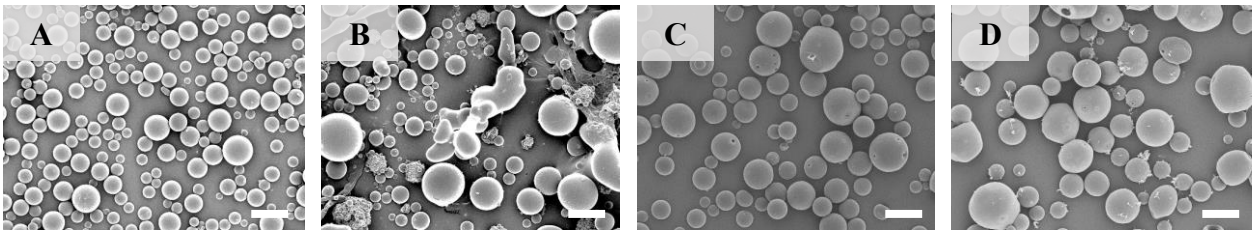

Appendix Figure 8: Scanning electron microscopy images of FITC microspheres. Representive images are shown for A) FITC MS 503, B) FITC MS 503 ACN, C) FITC MS 756, and D) FITC MS 858. Scale bar = 10µm.

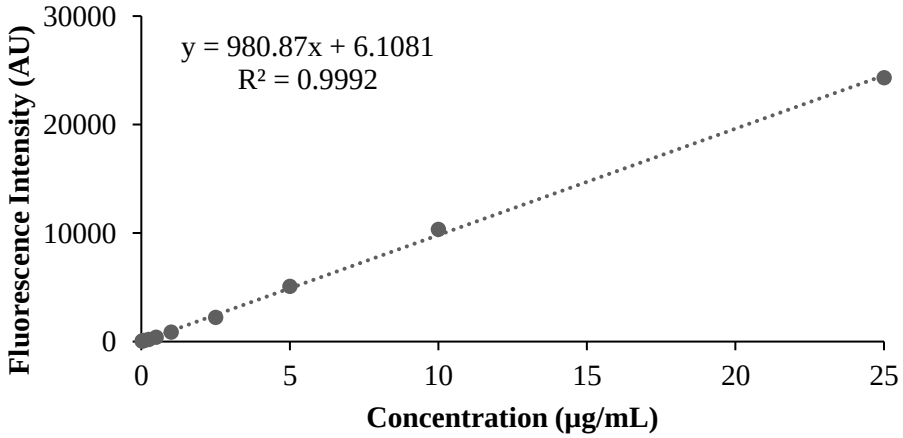

Appendix Figure 9: Fluorescein standard curve determined using spectrophotometry.

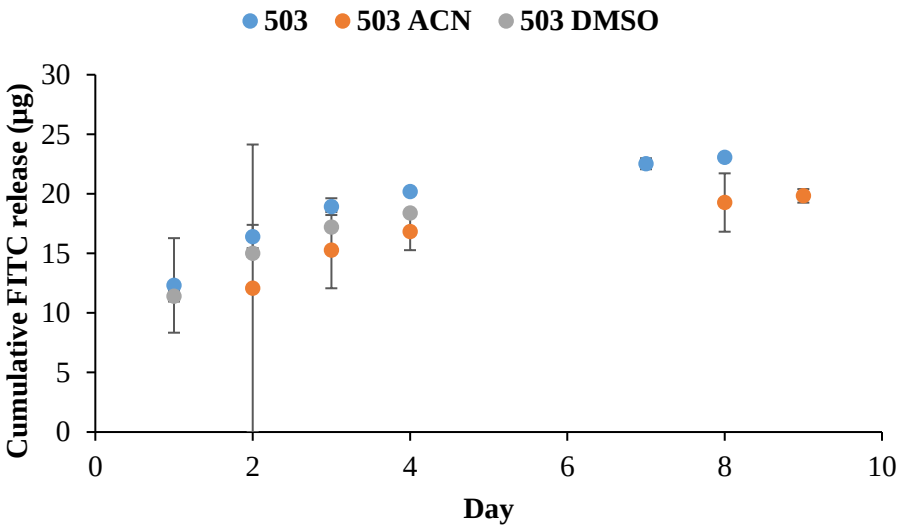

Appendix Figure 10: FITC release from 10mg of 503 microspheres with different fabrication parameters: double emulsion with dichloromethane (DCM) as organic solvent (503), double emulsion with acetonitrile (ACN) as organic solvent, and single emulsion (503 DMSO) with DCM as organic solvent. Error bars represent the mean ± standard deviation for n=3 samples.

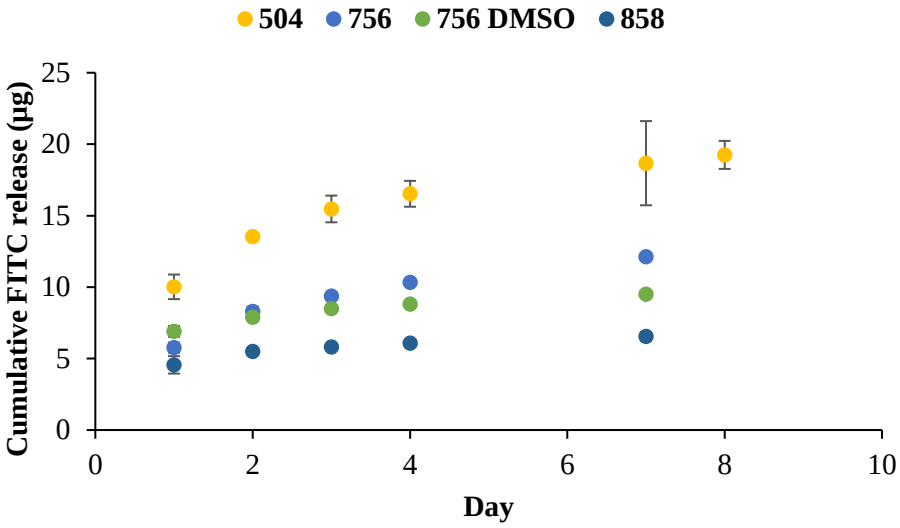

Appendix Figure 11: FITC release from 10mg of 504, 756, and 858 microspheres with different fabrication parameters: different molecular weight polymers and single emulsion fabrication for 756 DMSO. Error bars represent the mean ± standard deviation for n=3 samples.

Appendix A.3.4 Material Shelf Stability and Sterilization

Brimonidine-loaded MS morphology was maintained as spherical and generally non-porous after gamma irradiation (Appendix Figure 12) and after storage at -20°C, 4°C, and 25°C for 1, 3, 6, and 12 months (Appendix Figure 14).

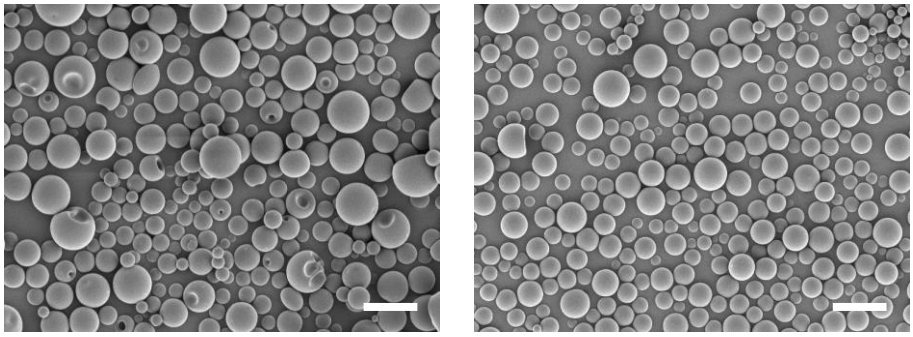

Appendix Figure 12: Scanning electron images of control BT MS (left) and gamma irradiated BT MS (right).

Scale bar = 10μm.

Gamma irradiation (Appendix Figure 13) of BT microspheres resulted in significant decrease in endotoxin concentration from 2.65 ± 1.34 EU/mL to 1.28 ± 0.09 EU/mL. No significant difference in endotoxin concentration on gel was observed, with 2.71 ± 0.45 EU/mL on control samples and 2.58 ± 0.47 EU/mL on irradiated samples. For a 100μL dose, these values are well below the recommended limit of 1 EU/dose [177,181]: 0.265 ± 0.134 EU/dose, 0.128 ± 0.009 EU/dose, 0.271 ± 0.045 EU/dose, and 0.258 ± 0.047 EU/dose for control MS, irradiated MS, control gel, and irradiated gel, respectively.

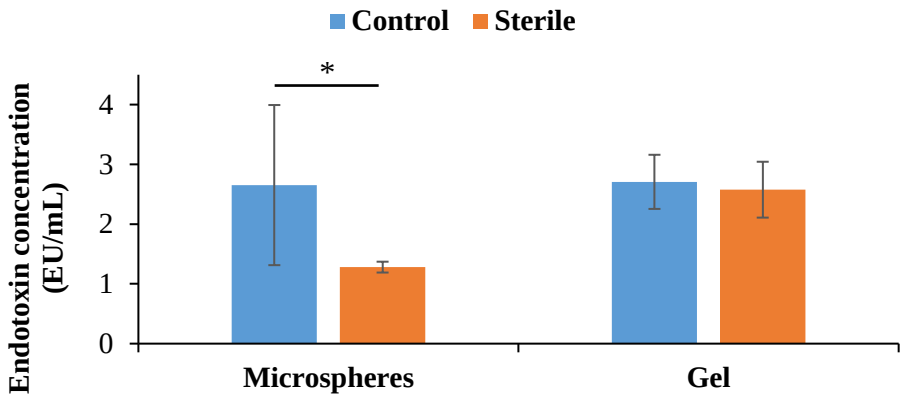

Appendix Figure 13: Endotoxin testing of control and gamma irradiated BT microspheres and PNIPAAm gel. Significance (*p<0.05) was determined using Mann Whitney U test, with significant decrease in endotoxin concentration observed after sterilization of microspheres but not gel. All endotoxin levels are below recommended limits. Error bars represent mean ± standard deviation for n=9 samples for gel, n=6 samples for control BT MS, and n=3 samples for sterilized BT MS.

No significant morphological changes were observed under SEM for BT MS stored at various storage temperatures up to 12 months (Appendix Figure 14). After 12 months of storage, there was no difference in the release curves of the MS stored at different temperatures (Appendix Figure 15). Initial burst was comparable to original formulation tested immediately after fabrication without long term storage. However, slope of the curve was flattened, resulting in slightly lower overall magnitude of release although the release magnitude remained in the same order of magnitude after long term storage.

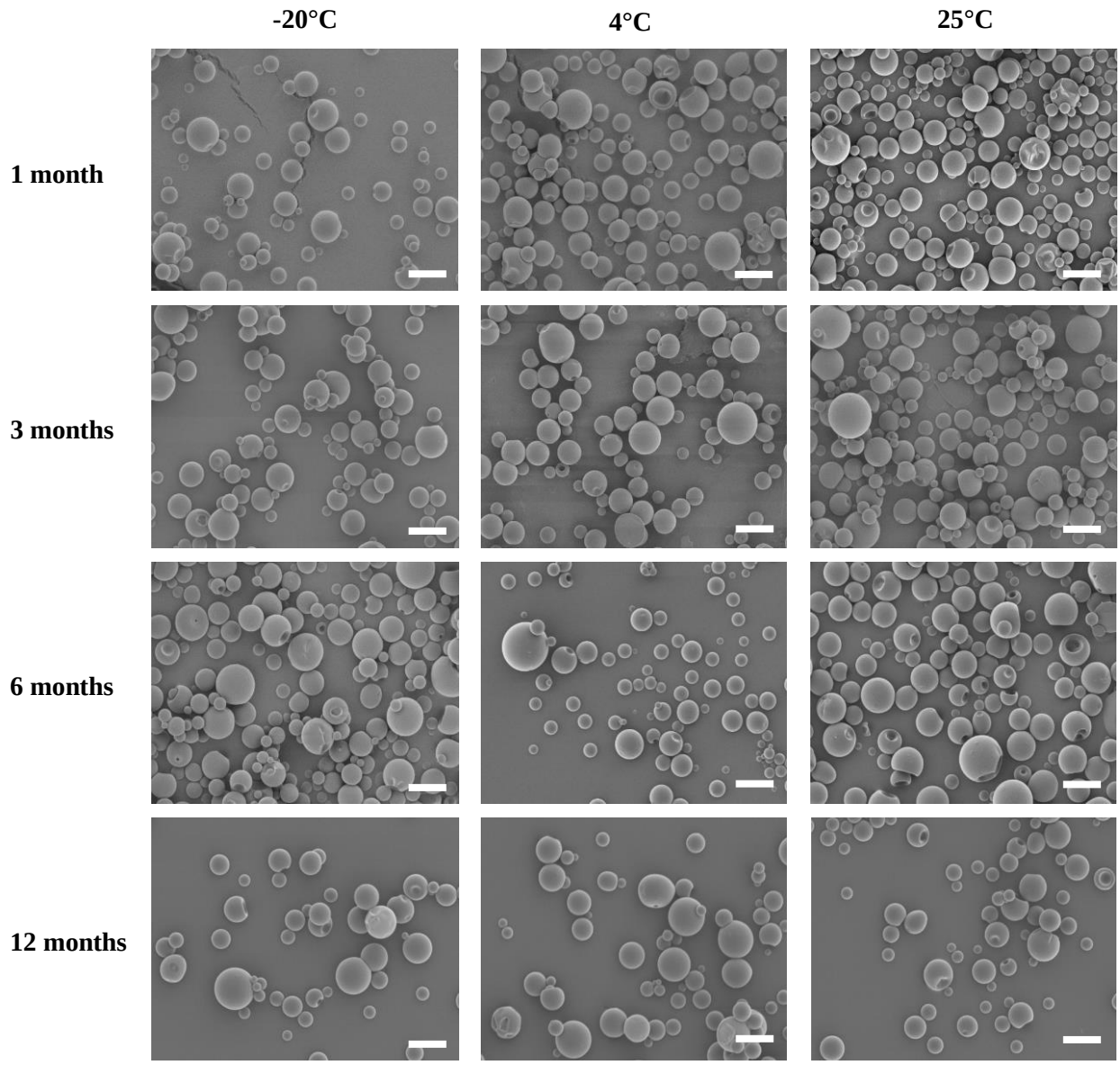

Appendix Figure 14: Scanning electron microscopy images of BT MS stored at -20°C, 4°C, and 25°C for 1, 3, 6, and 12 months. Scale bar = 10µm.

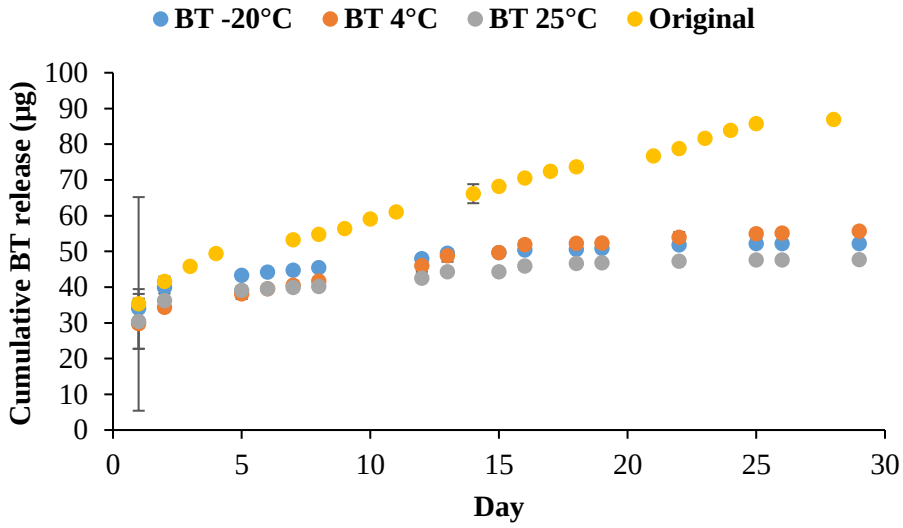

Appendix Figure 15: Release curves of BT MS stored at -20°C, 4°C, and 25°C for 12 months compared to original formulation. Error bars represent mean ± standard deviation for n=3 samples.

An increase of 1°C in LCST (35.5°C to 36.5°C) was observed for gel stored at 4°C after 6 and 12 months of storage compared to control gel. This 1°C increase in LCST was also observed for gel stored at 25°C after 3 months but not at 1 or 6 months. Gel stored at 30°C demonstrated a 1°C decrease in LCST to 34.5°C at 6 months and a 1°C increase in LCST to 36.5°C at 1, 3, and 12 months of storage. Sterilization also resulted in a 1°C increase in LCST from 35.5°C to 36.5°C. Overall, storage at various temperatures for up to 12 months (Appendix Figures 16-18) and gamma irradiation (Appendix Figure 19) did not have a major effect on LCST.

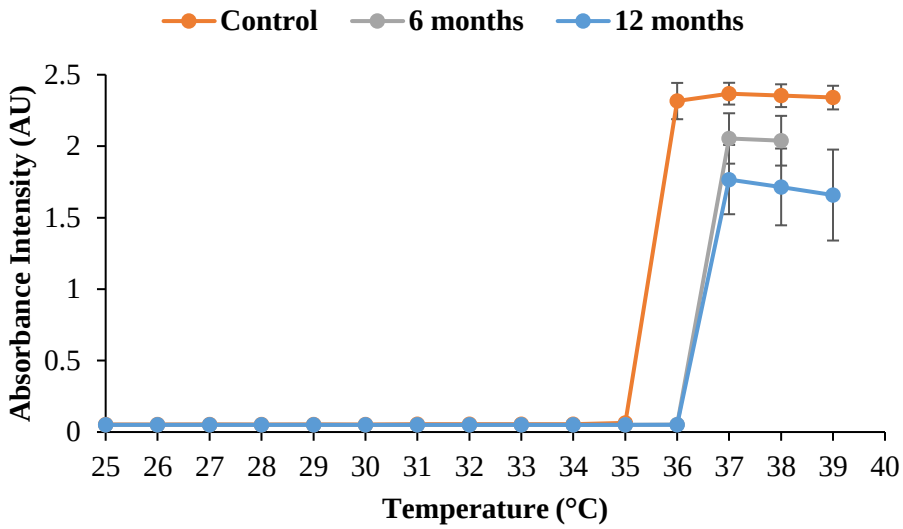

Appendix Figure 16: Lower critical solution temperature of pNIPAAm gel at t=0, 6, and 12 months of storage at 4°C. A 1°C shift in LCST is observed due to storage for 6 and 12 months compared to control**.** Error bars represent mean ± standard deviation for n=3 samples.

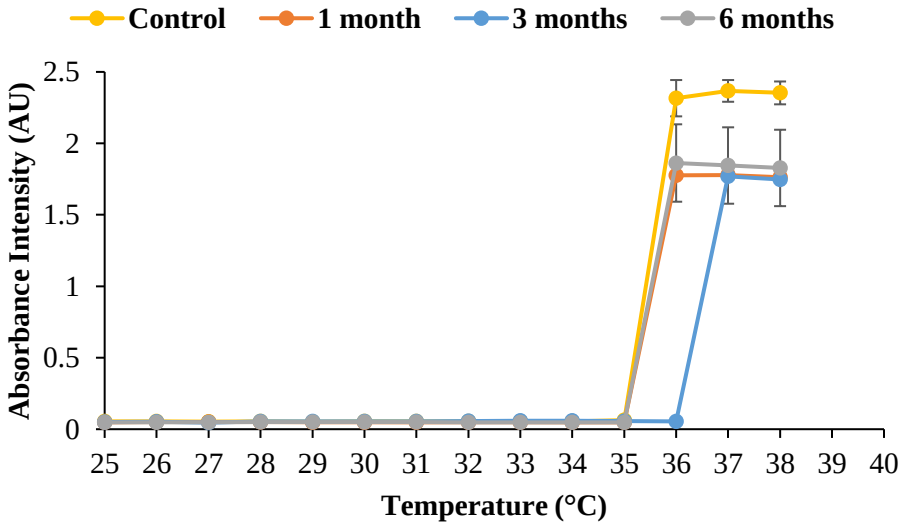

Appendix Figure 17: Lower critical solution temperature of pNIPAAm gel for control and t=1, 3, and 6 months of storage at 25°C. A 1°C shift in LCST is observed due to storage for 3 months compared to control, 1 month, and 6 months**.** Error bars represent mean ± standard deviation for n=3 samples.

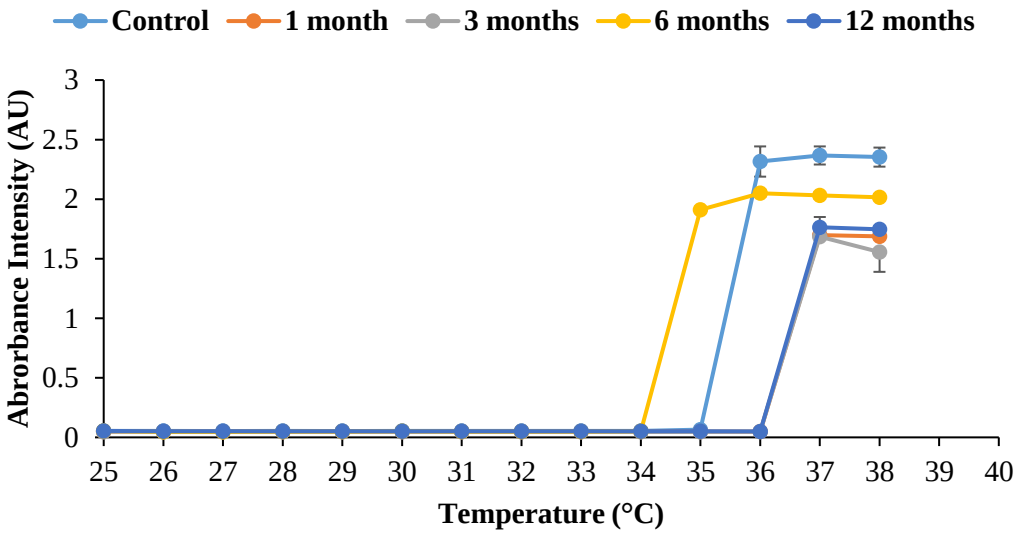

Appendix Figure 18: Lower critical solution temperature of pNIPAAm gel for control and t=1, 3, 6, and 12 months of storage at 30°C. Error bars represent mean ± standard deviation for n=3 samples.

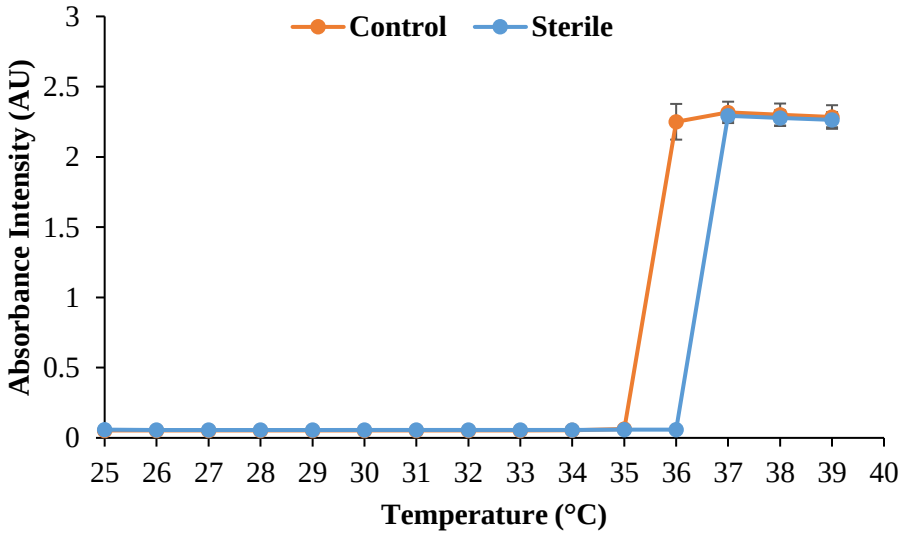

Appendix Figure 19: Lower critical solution temperature of control and sterilized pNIPAAm gel. A 1°C shift in LCST is observed in sterile gel compared to control**.** Error bars represent mean ± standard deviation for n=3 samples.

Appendix A.4 Discussion

The variety of release profiles developed with various fabrication techniques indicate that the drug delivery platform can be easily modified to produce desired release duration and magnitude. In addition, FITC-loaded MS can be fabricated to produce a variety of release profiles to use as a surrogate molecule for experiments such as permeability or distribution studies, including BT and ciprofloxacin as shown in these studies and can easily be adapted for other therapeutics. Fluorescein use allows for easy visualization with the eye, fluorescent microscopy, and/or fluorescence measurement via spectrophotometry and is a cheaper, widely commercially available alternative to using active therapeutics, which are factors than can increase ease of research into drug delivery systems.

BT MS have shown to be shelf stable at -20°C, 4C°, and 25°C for up to 12 months of storage. These results are consistent with previous studies by other groups [204,205]. In one of these studies, a dexamethasone-loaded PLGA MS/PVA gel system experienced increased initial burst release and lag phase decreased by half, shortening overall release duration [205]. Because the hydrogel and MS were stored together, water content of the hydrogel can cause hydrolysis of the PLGA MS. In addition, accelerated physical aging of the PLGA MS occurs at ambient temperatures [203,204]. BT MS were stored separately from gel, which may have contributed to better shelf stability at 25°C than if MS were stored in gel. While these stability studies indicate BT MS and gel can be stored at room temperature, it is still advisable for them to be kept at 4°C or below for optimal preservation over a 12-month shelf life. PLGA MS are typically stored at -20°C but based on both our studies and previous studies by other groups, it would be feasible to store both materials at 4°C for ease of storage in one location in patients' homes.

A decrease in overall magnitude of BT release from MS was observed when PVA used in fabrication was changed to a new lot. To investigate quality control issues associated with these different lots of PVA, several different brands and similar listed molecular weight ranges were tested and true molecular weights of PVA brands/lots that resulted in successful BT MS formulation were determined using size exclusion chromatography. It was determined that true MW was much greater than the listed MW for each of the 3 tested lots (Appendix Table 5). Because lots are packaged from a combination of high and low MW PVA and listed MW is an average, it is possible that individual packages may have higher or lower average MW than the listed average. This PS 2019 lot exhibited two peaks corresponding to 76,000Da and 30,000Da, an observation which may support this hypothesis.

To our knowledge, there have been no previous investigations of PVA molecular weight effect on MS formulations. However, a number of studies have investigated the effects on release profiles of using different surfactants as stabilizers in MS fabrication [191,192,207,208], effects of co-encapsulation of surfactants in MS [209,210], and drug-surfactant interactions [196]. It has been previously noted that investigating the underlying molecular interactions between surfactant, drug, and PLGA may be difficult but assessing PLGA MS release profiles can provide indirect insight into surfactant effect [191,192].

Two of the aforementioned studies specifically compared use of PVA to poly(vinyl pyrrolidone (PVP) [191,207]. Capan et al reported higher loading efficiency of plasmid DNA into MS fabricated using PVA (MW 30,000-70,000Da) compared to PVP (MW 40,000Da) [207]. They also observed differences in MS size and loading efficiency due to concentration of PVA used, with a 4% solution resulting in highest loading, which affirms the standard use of 4% PVA in MS fabrication methods. In contrast, Coombes et al reported lower protein loading, higher initial burst

release, and lower overall magnitude of protein release due to use of PVA (MW 13,000-23,000Da) compared to PVP (MW 10,000Da) [191]. In this particular study, it was hypothesized that PVP better stabilized the primary emulsion, shielding the protein from degradation. Additionally, studies on co-encapsulation of surfactants in MS loaded with proteins or insulin demonstrated lower encapsulation efficiency and faster overall release [209,210]. These studies hypothesized that presence of surfactant can affect the interaction of PLGA and encapsulated therapeutics.

Similar to how 4% PVA concentration yields optimal loading efficiency (compared to 1% and 7% concentrations) [207], it is possible that a narrow range of PVA MW can yield optimal release profiles for specific applications. We observed lower overall burst release and magnitude of release due to use of PS 2019 and Alfa Aesar PVA compared to the original PS 2015 lot, which had an experimentally-determined MW of 66,000Da. Alfa Aesar PVA exhibited a lower experimentally-determined MW and PS 2019 exhibited both higher and lower experimentally-determined MW. In contrast, ciprofloxacin-loaded MS fabricated using these different PVA lots did not exhibit a significant difference in release profiles. Therefore, we hypothesize that MW of PVA has an effect on MS formulation and that this effect is drug-dependent.

As previously described, use of different types and MW of surfactants can affect loading and release of therapeutics in different ways [191,207–210]. While BT interaction with surfactants has not been previously explored, one study examined the effect of drug-surfactant interactions of various drugs including timolol, which is also an anti-glaucoma drug [196]. While most surfactants tested did not have a significant effect on timolol's permeability, there was a strong inverse correlation with concentration of sodium dodecyl sulfate (SDS) on transport across a dialysis membrane. This is likely due to charge interaction of timolol and SDS which at pH 7.4 are, respectively, positively and negatively charged.

Accordingly, future quality control work can focus on determining optimal molecular weight of PVA to produce desired release profiles. Size exclusion chromatography can continue to be used to determine true MW of PVA lots and to isolate the MW of interest for use in fabrication. Due to a lack of research into molecular interactions between surfactant, drugs, and PLGA, these studies may provide more insight into surfactant effect on PLGA MS formulation and how to ensure repeatable formulation, which is important for clinical use and commercialization.

Appendix A.5 Conclusions and Future Directions

To increase commercialization potential of BT-loaded MS and gel for glaucoma treatment, quality control experimentation was performed, including investigation of surfactant effect on release curves, ability to be sterilized without significant changes to desired material properties, and confirmation of shelf-life stability up to 12 months. In addition, a variety of fabrication methods were explored for FITC-loaded MS, resulting in a variety of release profiles that can be used as a surrogate for release profiles of interest for other therapeutics. This work confirmed that a variety of release profiles can be developed by adjusting fabrication methods, which is beneficial to expanding the drug delivery platform for a variety of applications, release magnitudes, and treatment durations. Future work will be focused on further investigation of surfactant effect on MS fabrication, in particular determining optimal PVA molecular weight for reliable, repeatable BT MS fabrication and investigating any drug-dependent contribution to this effect.

Bibliography

[1] A.S. Hoffman, The origins and evolution of "controlled" drug delivery systems, J. Control. Release. 132 (2008) 153–163. https://doi.org/10.1016/j.jconrel.2008.08.012.

[2] C. Robert, C.S. Wilson, A. Venuta, M. Ferrari, C.-D. Arreto, Evolution of the scientific literature on drug delivery : A 1974–2015 bibliometric study, J. Control. Release. 260 (2017) 226–233. https://doi.org/10.1016/j.jconrel.2017.06.012.

[3] K. Park, Controlled drug delivery systems: Past forward and future back, J. Control. Release. 190 (2014) 3–8. https://doi.org/10.1016/j.jconrel.2014.03.054.

[4] J. Li, D.J. Mooney, Designing hydrogels for controlled drug delivery, Nat. Rev. Mater. 1 (2016). https://doi.org/10.1038/natrevmats.2016.71.

[5] J.E. Mealy, M.V. Fedorchak, S.R. Little, In vitro characterization of a controlled-release ocular insert for delivery of brimonidine tartrate, Acta Biomater. 10 (2014) 87–93. https://doi.org/10.1016/j.actbio.2013.09.024.

[6] S.P. Schwendeman, R.B. Shah, B.A. Bailey, A.S. Schwendeman, Injectable controlled release depots for large molecules, J. Control. Release. 190 (2014) 240–253. https://doi.org/10.1016/j.jconrel.2014.05.057.

[7] M. Biondi, F. Ungaro, F. Quaglia, P.A. Netti, Controlled drug delivery in tissue engineering, Adv. Drug Deliv. Rev. 60 (2008) 229–242. https://doi.org/10.1016/j.addr.2007.08.038.

[8] K. Sternberg, Current requirements for polymeric biomaterials in otolaryngology, GMS Curr. Top. Otorhinolaryngol. - Head Neck Surg. 8 (2009) Doc11. https://doi.org/10.3205/cto000063.

[9] A. Aksit, D.N. Arteaga, M. Arriaga, X. Wang, H. Watanabe, K.E. Kasza, A.K. Lalwani, J.W. Kysar, In-vitro Perforation of the Round Window Membrane via Direct 3-D Printed Microneedles, Biomed Microdevices. 20 (2019). https://doi.org/10.1016/j.physbeh.2017.03.040.

[10] M.E. Pichichero, Otitis Media, Pediatr. Clin. NA. 60 (2013) 391–407. https://doi.org/10.1016/j.pcl.2012.12.007.

[11] S.I. Pelton, E. Leibovitz, Recent advances in otitis media., Pediatr. Infect. Dis. J. 28 (2009) S133-7. https://doi.org/10.1097/INF.0b013e3181b6d81a.

[12] C.D. Bluestone, Epidemiology and pathogenesis of chronic suppurative otitis media: implications for prevention and treatment., Int. J. Pediatr. Otorhinolaryngol. 42 (1998) 207–223. https://doi.org/10.1016/S0165-5876(97)00147-X.

[13] S.N. Rothstein, S.R. Little, A “tool box” for rational design of degradable controlled release formulations, J. Mater. Chem. 21 (2011) 29–39. https://doi.org/10.1039/c0jm01668c.

[14] Y. Xu, C.-S. Kim, D.M. Saylor, D. Koo, Polymer degradation and drug delivery in PLGA-based drug–polymer applications: A review of experiments and theories, J. Biomed. Mater. Res. B Appl. Biomater. 105B (2017) 1692–1716. https://doi.org/10.1002/jbm.b.33648.

[15] S. Fredenberg, M. Wahlgren, M. Reslow, A. Axelsson, The mechanisms of drug release in poly(lactic-co-glycolic acid)-based drug delivery systems - A review, Int. J. Pharm. 415 (2011) 34–52. https://doi.org/10.1016/j.ijpharm.2011.05.049.

[16] H. Hamishehkar, J. Emami, A.R. Najafabadi, K. Gilani, M. Minaiyan, H. Mahdavi, A. Nokhodchi, The effect of formulation variables on the characteristics of insulin-loaded poly(lactic-co-glycolic acid) microspheres prepared by a single phase oil in oil solvent evaporation method, Colloids Surfaces B Biointerfaces. 74 (2009) 340–349. https://doi.org/10.1016/j.colsurfb.2009.08.003.

[17] S. Freiberg, X.X. Zhu, Polymer microspheres for controlled drug release, Int. J. Pharm. 282 (2004) 1–18. https://doi.org/10.1016/j.ijpharm.2004.04.013.

[18] M.N.V.R. Kumar, Nano and microparticles as controlled drug delivery devices., J. Pharm. Pharm. Sci. 3 (2000) 234–258.

[19] R. Herrero-Vanrell, I. Bravo-Osuna, V. Andrés-Guerrero, M. Vicario-de-la-Torre, I.T. Molina-Martínez, The potential of using biodegradable microspheres in retinal diseases and other intraocular pathologies, Prog. Retin. Eye Res. 42 (2014) 27–43. https://doi.org/10.1016/j.preteyeres.2014.04.002.

[20] H.K. Makadia, S.J. Siegel, Poly Lactic-co-Glycolic Acid (PLGA) as Biodegradable Controlled Drug Delivery Carrier, Polym. 3 (2012) 1377–1397. https://doi.org/10.3390/polym3031377.Poly.

[21] L. Brannon-Peppas, Recent advances on the use of biodegradable microparticles and nanoparticles in controlled drug delivery, Int. J. Pharm. 116 (1995) 1–9. https://doi.org/10.1016/0378-5173(94)00324-X.

[22] J.M. Anderson, M.S. Shive, Biodegradation and biocompatibility of PLA and PLGA microspheres, Adv. Drug Deliv. Rev. 28 (1997) 5–24. https://doi.org/10.1016/j.addr.2012.09.004.

[23] M. Mir, M.N. Ali, A. Barakullah, A. Gulzar, M. Arshad, S. Fatima, M. Asad, Synthetic polymeric biomaterials for wound healing: a review, Prog. Biomater. 7 (2018) 1–21. https://doi.org/10.1007/s40204-018-0083-4.

[24] J. Siepmann, F. Siepmann, Modeling of diffusion controlled drug delivery, J. Control. Release. 161 (2012) 351–362. https://doi.org/10.1016/j.jconrel.2011.10.006.

[25] A.K. Bajpai, S.K. Shukla, S. Bhanu, S. Kankane, Responsive polymers in controlled drug delivery, Prog. Polym. Sci. 33 (2008) 1088–1118. https://doi.org/10.1016/j.progpolymsci.2008.07.005.

[26] A. Alexander, Ajazuddin, J. Khan, S. Saraf, S. Saraf, Polyethylene glycol (PEG)-Poly(N-isopropylacrylamide) (PNIPAAm) based thermosensitive injectable hydrogels for biomedical applications, Eur. J. Pharm. Biopharm. 88 (2014) 575–585. https://doi.org/10.1016/j.ejpb.2014.07.005.

[27] P. Gupta, K. Vermani, S. Garg, Hydrogels: From controlled release to pH-responsive drug delivery, Drug Discov. Today. 7 (2002) 569–579. https://doi.org/10.1016/S1359-6446(02)02255-9.

[28] L. Klouda, A.G. Mikos, Thermoresponsive hydrogels in biomedical applications, Eur. J. Pharm. Biopharm. 68 (2008) 34–45. https://doi.org/10.1016/j.ejpb.2007.02.025.

[29] T.R. Hoare, D.S. Kohane, Hydrogels in drug delivery: Progress and challenges, Polymer (Guildf). 49 (2008) 1993–2007. https://doi.org/10.1016/j.polymer.2008.01.027.

[30] M. Patenaude, T. Hoare, Injectable, Degradable Thermoresponsive Poly(N-isopropylacrylamide) Hydrogels, ACS Macro Lett. 1 (2012) 409–413. https://doi.org/10.1021/mz200121k.

[31] P.W. Drapala, E.M. Brey, W.F. Mieler, D.C. Venerus, J.J.K. Derwent, V.H. Perez-Luna, Role of Thermo-responsiveness and Poly(ethylene glycol) Diacrylate Cross-link Density on Protein Release from Poly(N-isopropylacrylamide) Hydrogels, J. Biomater. Sci. 22 (2011) 59–75. https://doi.org/10.1163/092050609x12578498952315.

[32] B. Jeong, S.W. Kim, Y.H. Bae, Thermosensitive sol – gel reversible hydrogels, Adv. Drug Deliv. Rev. 64 (2012) 154–162. https://doi.org/10.1016/j.addr.2012.09.012.

[33] X.-Z. Zhang, Y.-Y. Yang, T.-S. Chung, K.-X. Ma, Preparation and Characterization of Fast Response Macroporous Poly (N-isopropylacrylamide) Hydrogels, Langmuir. 17 (2001) 6094–6099. https://doi.org/10.1021/la010105v.

[34] J.F. Pollock, K.E. Healy, Mechanical and swelling characterization of poly(N-isopropyl acrylamide-co-methoxy poly(ethylene glycol) methacrylate) sol-gels, Acta Biomater. 6 (2010) 1307–1318. https://doi.org/10.1016/j.actbio.2009.11.027.

[35] X.Z. Zhang, D.Q. Wu, C.C. Chu, Synthesis, characterization and controlled drug release of thermosensitive IPN-PNIPAAm hydrogels, Biomaterials. 25 (2004) 3793–3805. https://doi.org/10.1016/j.biomaterials.2003.10.065.

[36] X.-Z. Zhang, P.J. Lewis, C.-C. Chu, Fabrication and characterization of a smart drug delivery system: microsphere in hydrogel, Biomaterials. 26 (2005) 3299–3309. https://doi.org/10.1016/j.biomaterials.2004.08.024.

[37] P. Menter, Acrylamide Polymerization—A Practical Approach, n.d. http://scholar.google.com/scholar?hl=en&btnG=Search&q=intitle:Acrylamide+Polymerization+?+A+Practical+Approach#0.

[38] M. V Fedorchak, I.P. Conner, J.S. Schuman, A. Cugini, S.R. Little, Long Term Glaucoma Drug Delivery Using a Topically Retained Gel/Microsphere Eye Drop, Sci. Rep. 7 (2017) 1–11. https://doi.org/10.1038/s41598-017-09379-8.

[39] A.S. Lieberthal, A.E. Carroll, T. Chonmaitree, T.G. Ganiats, A. Hoberman, M.A. Jackson, M.D. Joffe, D.T. Miller, R.M. Rosenfeld, X.D. Sevilla, R.H. Schwartz, P.A. Thomas, D.E. Runkel, The Diagnosis and Management of Acute Otitis Media, Am. Acad. Pediatr. 131 (2013) 964–999.

[40] D. Teele, J. Klein, B. Rosner, Epidemiology of Otitis Media During the First Seven Years of Life in Children in Greater Boston: A Prospective, Cohort Study, J. Infect. Dis. 160 (1989) 83–94. https://doi.org/10.1093/infdis/160.1.83.

[41] A. Vergison, R. Dagan, A. Arguedas, J. Bonhoeffer, R. Cohen, I. DHooge, A. Hoberman, J. Liese, P. Marchisio, A.A. Palmu, G.T. Ray, E.A. Sanders, E.A. Simões, M. Uhari, J. van Eldere, S.I. Pelton, Otitis media and its consequences: beyond the earache, Lancet Infect. Dis. 10 (2010) 195–203. https://doi.org/10.1016/S1473-3099(10)70012-8.

[42] R.M. Siegel, Acute Otitis Media Guidelines, Antibiotic Use, and Shared Medical Decision-Making, Pediatrics. 125 (2010) 384–386. https://doi.org/10.1542/peds.2009-3208.

[43] A. Minovi, S. Dazert, Diseases of the middle ear in childhood, Curr. Top. Otorhinolaryngol. Head Neck Surg. 13 (2014). https://doi.org/10.1016/B978-1-4831-6795-4.50016-6.

[44] A.M. Al-Mahallawi, O.M. Khowessah, R.A. Shoukri, Nano-transfersomal ciprofloxacin loaded vesicles for non-invasive trans-tympanic ototopical delivery: In-vitro optimization, ex-vivo permeation studies, and in-vivo assessment, Int. J. Pharm. 472 (2014) 304–314. https://doi.org/10.1016/j.ijpharm.2014.06.041.

[45] C.W. Gan, W.H. Chooi, H.C.A. Ng, Y.S. Wong, S.S. Venkatraman, L.H.Y. Lim, Development of a novel biodegradable drug-eluting Ventilation tube for chronic otitis media with effusion, Laryngoscope. 123 (2013) 1770–1777. https://doi.org/10.1002/lary.23895.

[46] A. Kurabi, K.K. Pak, M. Bernhardt, A. Baird, A.F. Ryan, Discovery of a Biological Mechanism of Active Transport through the Tympanic Membrane to the Middle Ear, Sci. Rep. 6 (2016). https://doi.org/10.1038/srep22663.

[47] N. Nwokoye, L. Egwari, O. Olubi, Occurrence of otitis media in children and assessment of treatment options, J. Laryngol. Otol. 129 (2015) 779–783. https://doi.org/10.1017/S0022215115001127.

[48] A. Amali, N. Hosseinzadeh, S. Samadi, S. Nasiri, J. Zebardast, Sensorineural hearing loss in patients with chronic supparative otitis media: Is there a significant correlation?, Electron. Physician. 9 (2017) 3823–3827. https://doi.org/http://dx.doi.org/10.19082/3823.

[49] S.S. da Costa, L.S.R. Petersen, C. Dornelles, Sensorineural hearing loss in patients with chronic otitis media, Eur Arch Otorhinolaryngol. 266 (2009) 221–224. https://doi.org/10.1007/s00405-008-0739-0.

[50] R.G. Jensen, A. Koch, P. Homøe, The risk of hearing loss in a population with a high prevalence of chronic suppurative otitis media, Int. J. Pediatr. Otorhinolaryngol. 77 (2013) 1530–1535. https://doi.org/10.1016/j.ijporl.2013.06.025.

[51] G. Gates, Cost-effectiveness considerations in otitis media treatment, Otolaryngol Head Neck Surg. 114 (1996) 525–530.

[52] L. Monasta, L. Ronfani, F. Marchetti, M. Montico, L.V. Brumatti, A. Bavcar, D. Grasso, C. Barbiero, G. Tamburlini, Burden of Disease Caused by Otitis Media: Systematic Review and Global Estimates, PLoS One. 7 (2012). https://doi.org/10.1371/journal.pone.0036226.

[53] M. Fradis, A. Brodksy, J. Ben-David, I. Srugo, J. Larboni, L. Podoshin, Chronic Otitis Media Treated Topically With Ciprofloxacin or Tobramycin, Arch. Otolaryngol. Head Neck Surg. 123 (1997).

[54] L.O. Bakaletz, Bacterial Biofilms in Otitis Media: Evidence and Relevance, Pediatr. Infect. Dis. J. 26 (2007) S17-19.

[55] K. Belfield, R. Bayston, J. Birchall, D. Matija, Do orally administered antibiotics reach concentrations in the middle ear sufficient to eradicate planktonic and biofilm bacteria? A review, Int. J. Pediatr. Otorhinolaryngol. 79 (2015) 296–300. https://doi.org/10.1016/j.ijporl.2015.01.003.

[56] M. Daniel, R. Chessman, S. Al-Zahid, B. Richards, C. Rahman, W. Ashraf, J. McLaren, H. Cox, O. Qutachi, H. Fortnum, N. Fergie, K. Shakesheff, J.P. Birchall, R.R. Bayston, Biofilm Eradication With Biodegradable Modified-Release Antibiotic Pellets, Arch. Otolaryngol. Neck Surg. 138 (2012) 942. https://doi.org/10.1001/archotol.2013.238.

[57] X. Khoo, E.J. Simons, H.H. Chiang, J.M. Hickey, V. Sabharwal, S.I. Pelton, J.J. Rosowski, R. Langer, D.S. Kohane, Formulations for trans-tympanic antibiotic delivery, Biomaterials. 34 (2013) 1281–1288. https://doi.org/10.1016/j.biomaterials.2012.10.025.

[58] Cetraxal, US Food Drug Adm. (1987).

[59] M.R. Jacobs, S. Bajaksouzian, A. Zilles, G. Lin, G.A. Pankuch, P.C. Appelbaum, Susceptibilities of Streptococcus pneumoniae and Haemophilus influenzae to 10 Oral Antimicrobial Agents Based on Pharmacodynamic Parameters : 1997 U . S . Surveillance Study Susceptibilities of Streptococcus pneumoniae and Haemophilus influenzae to 10 Ora, Antimicrob. Agents Chemother. 43 (1999) 1901–1908.

[60] C. Thornsberry, P. Ogilvie, H. Holley, D. Sahm, Survey of Susceptibilities of Streptococcus pneumoniae, Haemophilus influenzae, and Moraxella catarrhalis Isolates to 26 Antimicrobial Agents: a Prospective U.S. Study, Antimicrob. Agents Chemother. 43 (1999) 2612–2623.

[61] C.H. Jang, S.Y. Park, Emergence of ciprofloxacin-resistant pseudomonas in pediatric otitis media, Int. J. Pediatr. Otorhinolaryngol. 67 (2003) 313–316. https://doi.org/10.1016/S0165-5876(03)00033-8.

[62] A. Agius, A. Reid, C. Hamilton, Patient compliance with short-term topical aural antibiotic therapy, Clin. Otolaryngol. 19 (1994) 138–141.

[63] R. England, J. Homer, P. Jasser, A.D. Wilde, Accuracy of patient self-medication with topical eardrops, J. Laryngol. Otol. 114 (2000) 24–25.

[64] M. Furue, D. Onozuka, S. Takeuchi, H. Murota, M. Sugaya, K. Masuda, S. Kaneko, S. H, Y. Shintani, Y. Tsunemi, S. Abe, M. Kobayahi, Y. Kitami, M. Tanioka, S. Imafuku, M. Abe, N. Inomata, D. Morisky, N. Katoh, Poor adherence to oral and topical medication in 3096 dermatological patients as assessed by the Morisky-Medication Adherence Scale-8, Br. J. Dermatol. 172 (2015) 272–275. https://doi.org/10.1111/bjd.13377.

[65] F. Piu, X. Wang, R. Fernandez, L. Dellamary, A. Harrop, Q. Ye, J. Sweet, R. Tapp, D.F. Dolan, R. a Altschuler, J. Lichter, C. LeBel, OTO-104: a sustained-release dexamethasone hydrogel for the treatment of otic disorders., Otol. Neurotol. 32 (2011) 171–179. https://doi.org/10.1097/MAO.0b013e3182009d29.

[66] X. Wang, R. Fernandez, N. Tsivkovskaia, A. Harrop-Jones, H.J. Hou, L. Dellamary, D.F. Dolan, R. a Altschuler, C. LeBel, F. Piu, OTO-201: nonclinical assessment of a sustained-release ciprofloxacin hydrogel for the treatment of otitis media., Otol. Neurotol. 35 (2014) 459–69. https://doi.org/10.1097/MAO.0000000000000261.

[67] E.A. Mair, J.R. Moss, J.E. Dohar, P.J. Antonelli, M. Bear, C. LeBel, Randomized Clinical Trial of a Sustained-Exposure Ciprofloxacin for Intratympanic Injection During Tympanostomy Tube Surgery, Ann. Otol. Rhinol. Laryngol. (2015). https://doi.org/10.1177/0003489415599001.

[68] R. Yang, V. Sabharwal, O.S. Okonkwo, N. Shlykova, R. Tong, L.Y. Lin, W. Wang, S. Guo, J.J. Rosowski, S.I. Pelton, D.S. Kohane, Treatment of otitis media by transtympanic delivery of antibiotics, Sci. Transl. Med. 8 (2016).

[69] R. Yang, V. Sabharwal, N. Shlykova, O.S. Okonkwo, S.I. Pelton, D.S. Kohane, Treatment of Streptococcus pneumoniae otitis media in a chinchilla model by transtympanic delivery of antibiotics, JCI Insight. 3 (2018). https://doi.org/doi.org/10.1172/jci. insight.123415.

[70] P. Karande, A. Jain, K. Ergun, V. Kispersky, S. Mitragotri, Design principles of chemical penetration enhancers for transdermal drug delivery, 2005 (2005).

[71] A. Hoberman, J.L. Paradise, H.E. Rocketter, D.H. Kearney, S. Bhatnager, T.R. Shope, J.M. Martin, M. Kurs-Lasky, S.J. Copelli, D.K. Colborn, S.L. Block, J.J. Labella, T.G. Lynch, N.L. Cohen, M. Haralam, M.A. Pope, J.P. Nagg, M.D. Green, N. Shaikh, Shortened Antimicrobial Treatment for Acute Otitis Media in Young Children, N. Engl. J. Med. 375 (2016) 2446–2456. https://doi.org/10.1056/NEJMoa1606043.

[72] D.W. Laidlaw, P.D. Costantino, S. Govindaraj, D.H. Hiltzik, P.J. Catalano, Tympanic Membrane Repair With a Dermal Allograft, Laryngoscope. 111 (2001) 702–707.

[73] Z. Lou, J. Yang, Y. Tang, J. Xiao, Risk factors affecting human traumatic tympanic membrane perforation regeneration therapy using fibroblast growth factor-2, Growth Factors. 33 (2015) 410–418. https://doi.org/10.3109/08977194.2015.1122003.

[74] Q. Zhang, Z. Lou, Impact of basic fibroblast growth factor on healing of tympanic membrane perforations due to direct penetrating trauma: a prospective non-blinded/controlled study, Clin. Otolaryngol. 37 (2012) 446–451.

[75] H. Kaftan, M. Noack, N. Friedrich, H. Volzke, W. Hosemann, Prevelance of chronic tympanic membrane perforation in the adult population, HNO. 56 (2008) 145–50. https://doi.org/0.1007/s00106-007-1574-0.

[76] J. Pulec, C. Deguine, Traumatic perforation: blast injury, Ear Nose Throat J. 82 (2003) 665.

[77] F. Orji, C. Agu, Determinants of spontaneous healing in traumatic perforations of the tympanic membrane, Clin. Otolaryngol. 33 (2008) 420–426. https://doi.org/10.1111/j.1749-4486.2008.01764.

[78] Z. Lou, Y. Wang, K. Su, Comparison of the healing mechanisms of human dry and endogenous wet traumatic eardrum perforations, Eur Arch Otorhinolaryngol. 271 (2014) 2153–2157. https://doi.org/10.1007/s00405-013-2689-4.

[79] N. Hakuba, M. Iwanaga, S. Tanaka, Y. Hiratsuka, Y. Kumabe, M. Konishi, Y. Okanoue, N. Hiwatashi, T. Wada, Basic Fibroblast Growth Factor Combined With Atelocollagen for Closing Chronic Tympanic Membrane Perforations in 87 Patients, Otol. Neurotol. 31 (2010) 118–121.

[80] Z.C. Lou, J.G. He, A randomised controlled trial comparing spontaneous healing, gelfoam patching and edge-approximation plus gelfoam patching in traumatic tympanic membrane perforation with inverted or everted edges, Clin. Otolaryngol. 36 (2011) 221–226. https://doi.org/10.1111/j.1749-4486.2011.02319.x.

[81] Z.C. Lou, Z.H. Lou, A moist edge environment aids the regeneration of traumatic tympanic membrane perforations, J. Laryngol. Otol. 131 (2017) 564–571. https://doi.org/10.1017/S0022215117001001.

[82] J. Dornhoffer, Cartilage Tympanoplasty: Indications, Techniques, And Outcomes in a 1,000 Patient Series, Laryngoscope. 113 (2003) 1844–1856.

[83] P. Agrawal, S. Soni, G. Mittal, A. Bhatnagar, Role of Polymeric Biomaterials as Wound Healing Agents, Int. J. Low. Extrem. Wounds. 13 (2014) 180–190. https://doi.org/10.1177/1534734614544523.

[84] P.S. Camnitz, W.S. Bost, Traumatic perforations of the tympanic membrane: Early closure with paper tape patching, Otolaryngol. Neck Surg. 93 (1985) 220–223.

[85] M.K. Park, K.H. Kim, J.D. Lee, B.D. Lee, Repair of Large Traumatic Tympanic Membrane Perforation with a Steri-Strips Patch, Otolaryngol. Neck Surg. 145 (2011) 581–585. https://doi.org/10.1177/0194599811409836.

[86] E.D. Kozin, N.L. Black, J.T. Cheng, M.J. Cotler, M.J. Mckenna, D.J. Lee, J.A. Lewis, J.J. Rosowski, A.K. Remenschneider, Design, fabrication, and in vitro testing of novel three-dimensionally printed tympanic membrane grafts, Hear. Res. 340 (2016) 191–203. https://doi.org/10.1016/j.heares.2016.03.005.

[87] S.H. Kim, J.Y. Jeong, H.J. Park, B.M. Moon, Y.R. Park, O.J. Lee, M.T. Sultan, D.K. Kim, H.S. Park, J.H. Lee, C.H. Park, Application of a Collagen Patch Derived from Duck Feet in Acute Tympanic Membrane Perforation, Tissue Eng. Regen. Med. 14 (2017) 233–241. https://doi.org/10.1007/s13770-017-0039-0.

[88] Y. Shen, S. Redmond, B.M. Teh, S. Yan, Y. Wang, M.D. Atlas, R.J. Dilley, M. Zeng, R.J. Marano, Tympanic membrane repair using silk fibroin and acellular collagen scaffolds, Laryngoscope. 123 (2013) 1976–1982. https://doi.org/10.1002/lary.23940.

[89] Y. Shen, S.L. Redmond, B.M. Teh, S. Yan, Y. Wang, L. Zhou, C.A. Budgeon, R.H. Eikelboom, M.D. Atlas, R.J. Dilley, M. Zheng, R.J. Marano, Scaffolds for Tympanic Membrane Regeneration in Rats, Tissue Eng. Part A. 19 (2013) 657. https://doi.org/10.1089/ten.tea.2012.0053.

[90] J.H. Lee, J.S. Lee, D. Kim, C.H. Park, H.R. Lee, Clinical Outcomes of Silk Patch in Acute Tympanic Membrane Perforation, Clin. Exp. Otorhinolaryngol. 8 (2015) 117–122.

[91] R. Ghassemifar, S. Redmond, Zainuddin, T. V. Chirila, Advancing towards a tissue-engineered tympanic membrane: Silk fibroin as a substratum for growing human eardrum keratinocytes, J. Biomater. Appl. 24 (2010) 591–606. https://doi.org/10.1177/0885328209104289.

[92] W.J. McFeely, D.I. Bojrab, J.M. Kartush, Tympanic membrane perforation repair using AlloDerm, Otolaryngol Head Neck Surg. 123 (2000) 17–21. https://doi.org/10.1067/mhn.2000.105920.

[93] J. Kim, S.W. Kim, S. Park, K.T. Lim, H. Seonwoo, Y. Kim, Bacterial Cellulose Nanofibrillar Patch as a Wound Healing Platform of Tympanic Membrane Perforation, Adv. Healthc. Mater. (2013) 1525–1531. https://doi.org/10.1002/adhm.201200368.

[94] J.H. Kim, J. Bae, K.T. Lim, P.-H. Choung, J.-S. Park, S.J. Choi, A.L. Im, E.T. Lee, Y.-H. Choung, J.H. Chung, Development of water-insoluble chitosan patch scaffold to repair

traumatic tympanic membrane perforations, J. Biomed. Mater. Res. Part A. 90A (2008) 446–455. https://doi.org/10.1002/jbm.a.32119.

[95] A. Parekh, B. Mantle, J. Banks, J.D. Swarts, S.F. Badylak, J.E. Dohar, P.A. Hebda, Repair of the Tympanic Membrane with Urinary Bladder Matrix, Laryngoscope. 119 (2009) 1206–1213. https://doi.org/10.1002/lary.20233.Repair.

[96] D.E. Weber, M.T. Semaan, J.K. Wasman, R. Beane, L.J. Bonassar, C.A. Megerian, Tissue-Engineered Calcium Alginate Patches in the Repair of Chronic Chinchilla Tympanic Membrane Perforations, Laryngoscope. 116 (2006) 700–704. https://doi.org/10.1097/01.mlg.0000208549.44462.fa.

[97] H. Seonwoo, S.W. Kim, J. Kim, T. Chunjie, K.T. Lim, Y.J. Kim, S. Pandey, P.-H. Choung, Y.-H. Choung, J.H. Chung, Regeneration of Chronic Tympanic Membrane Perforation Using an EGF-Release Chitosan Patch, Tissue Eng. Part A. 19 (2013). https://doi.org/10.1089/ten.tea.2012.0617.

[98] Jian-Yang, Zi-Han-Lou, Yahui-Fu, Zheng-cai-Lou, A retrospective study of EGF and ofloxacin drops in the healing of human large traumatic eardrum perforation, Am. J. Otolaryngol. - Head Neck Med. Surg. 37 (2016) 294–298. https://doi.org/10.1016/j.amjoto.2016.03.005.

[99] Z. Lou, Z. Lou, A comparative study to evaluate the efficacy of EGF, FGF-2, and 0.3% (w/v) ofloxacin drops on eardrum regeneration, Medicine (Baltimore). 96 (2017) e7654.

[100] Z.C. Lou, J. Yang, Y. Tang, Y.H. Fu, Topical application of epidermal growth factor with no scaffold material on the healing of human traumatic tympanic membrane perforations, Clin. Otolaryngol. 41 (2016) 744–749. https://doi.org/10.1111/coa.12627.

[101] C.Y. Kuo, E. Wilson, A. Fuson, N. Gandhi, R. Monfaredi, A. Jenkins, M. Romero, M. Santoro, J.P. Fisher, K. Cleary, B. Reilly, Repair of Tympanic Membrane Perforations with Customized Bioprinted Ear Grafts Using Chinchilla Models, Tissue Eng. Part A. 24 (2018) 527–535. https://doi.org/10.1089/ten.tea.2017.0246.

[102] C. Jang, Y. Cho, M. Yeo, H. Lee, E. Min, B. Lee, G. Kim, Regeneration of chronic tympanic membrane perforation using 3D collagen with topical umbilical cord serum, Int. J. Biol. Macromol. 62 (2013) 232–240. https://doi.org/10.1016/j.ijbiomac.2013.08.049.

[103] N. Hakuba, M. Taniguchi, Y. Shimizu, A. Sugimoto, Y. Shinomuri, K. Gyo, A New Method for Closing Tympanic Membrane Perforations Using Basic Fibroblast Growth Factor, Laryngoscope. 113 (2003) 1352–1355.

[104] Y. Ozkaptan, M. Gerek, S. Simsek, S. Deveci, Effects of fibroblast growth factor on the healing process of tympanic membrane perforations in an animal model, Eur Arch Otorhinolaryngol. 254 (1994) S2-5.

[105] M. Fina, S. Bresnick, A. Bairp, A. Ryan, Improved Healing of Tympanic Membrane Perforations with Basic Fibroblast Growth Factor, Growth Factors. 5 (1991) 265–272. https://doi.org/10.3109/08977199109000290.

[106] A. Rahman, M. Von Unge, P. Olivius, J. Dirckx, Healing time, long-term result and effects of stem cell treatment in acute tympanic membrane perforation, Int. J. Pediatr. Otorhinolaryngol. 71 (2007) 1129–1137. https://doi.org/10.1016/j.ijporl.2007.04.005.

[107] Z. Lou, Y. Wang, Evaluation of the optimum time for direct application of fibroblast growth factor to human traumatic tympanic membrane perforations, Growth Factors. 33 (2015) 65–70. https://doi.org/10.3109/08977194.2014.980905.

[108] A. Beenken, M. Mohammadi, The FGF family: biology, pathophysiology and therapy, Nat Rev Drug Discov. 8 (2009) 235–253. https://doi.org/10.1038/nrd2792.

[109] C.H. Jang, S.H. Ahn, J.W. Lee, B.H. Lee, H. Lee, G.H. Kim, Mesenchymal stem cell-laden hybrid scaffold for regenerating subacute tympanic membrane perforation, Mater. Sci. Eng. C. 72 (2017) 456–463. https://doi.org/10.1016/j.msec.2016.11.094.

[110] D. Tartarini, E. Mele, Adult Stem Cell Therapies for Wound Healing: Biomaterials and Computational Modles, Front. Bioeng. Biotechnol. 3 (2016).

[111] M. von Unge, J.J. Dirckx, N.P. Olivius, Embryonic stem cells enhance the healing of tympanic membrane perforations, Int. J. Pediatr. Otorhinolaryngol. 67 (2003) 215–219.

[112] S. Goncalves, E. Bas, B.J. Goldstein, S. Angeli, Effects of Cell-Based Therapy for Treating Tympanic Membrane Perforations in Mice, Otolaryngol Head Neck Surg. 154 (2016) 1106–1114. https://doi.org/10.1177/0194599816636845.

[113] S. Goncalves, E. Bas, M. Langston, A. Grobman, B.J. Goldstein, S. Angeli, Histologic changes of mesenchymal stem cell repair of tympanic membrane perforation, Acta Otolaryngol. 137 (2017) 411–416. https://doi.org/10.1080/00016489.2016.1261411.

[114] A. Rahman, P. Olivius, J. Dirckx, M. Von Unge, Stem cells and enhanced healing of chronic tympanic membrane perforation, Acta Otolaryngol. 128 (2008) 352–359. https://doi.org/10.1080/00016480701762508.

[115] S. Taverna, G. Ghersi, A. Ginestra, S. Rigogliuso, S. Pecorella, G. Alaimo, F. Saladino, V. Dolo, P.D. Era, A. Pavan, G. Pizzolanti, P. Mignatti, M. Presta, M.L. Vittorelli, Shedding of Membrane Vesicles Mediates Fibroblast Growth Factor-2 Release from Cells, J. Biol. Chem. 278 (2003) 51911–51919. https://doi.org/10.1074/jbc.M304192200.

[116] E. Tassi, A. Al-Attar, A. Aigner, M.R. Swift, K. McDonnell, A. Karavanov, A. Wellstein, Enhancement of Fibroblast Growth Factor (FGF) Activity by an FGF-binding Protein, J. Biol. Chem. 276 (2001) 40247–40253. https://doi.org/10.1074/jbc.M104933200.

[117] P.W. Kriebel, V.A. Barr, E.C. Rericha, G. Zhang, C.A. Parent, Collective cell migration requires vesicular trafficking for chemoattractant delivery at the trailing edge, J. Cell Biol. 183 (2004) 949–961. https://doi.org/10.1083/jcb.200808105.

[118] M. V. Fedorchak, I.P. Conner, C.A. Medina, J.B. Wingard, J.S. Schuman, S.R. Little, 28-Day Intraocular Pressure Reduction With a Single Dose of Brimonidine Tartrate-Loaded Microspheres, Exp. Eye Res. 125 (2014) 210–216. https://doi.org/10.1016/j.exer.2014.06.013.

[119] M. V Fedorchak, I.P. Conner, J.S. Schuman, A. Cugini, S.R. Little, Long Term Glaucoma Drug Delivery Using a Topically Retained Gel / Microsphere Eye Drop, Sci. Rep. (2017) 1–11. https://doi.org/10.1038/s41598-017-09379-8.

[120] X. Wang, R. Fernandez, N. Tsivkovskaia, A. Harrop-Jones, H.J. Hou, L. Dellamary, D.F. Dolan, R. a Altschuler, C. LeBel, F. Piu, OTO-201: nonclinical assessment of a sustained-release ciprofloxacin hydrogel for the treatment of otitis media., Otol. Neurotol. 35 (2014) 459–69. https://doi.org/10.1097/MAO.0000000000000261.

[121] M. V Fedorchak, I.P. Conner, C.A. Medina, J.B. Wingard, J.S. Schuman, S.R. Little, 28-day intraocular pressure reduction with a single dose of brimonidine tartrate-loaded microspheres, Exp. Eye Res. 125 (2014) 210–216. https://doi.org/10.1016/j.exer.2014.06.013.

[122] A. Mammen, E.G. Romanowski, M. V. Fedorchak, D.K. Dhaliwal, R.M. Shanks, R.P. Kowalski, Endophthalmitis Prophylaxis Using a Single Drop of Thermoresponsive Controlled-Release Microspheres Loaded with Moxifloxacin in a Rabbit Model, Transl. Vis. Sci. Technol. 5 (2016) 12. https://doi.org/10.1167/tvst.5.6.12.

[123] G. Gates, Safety of ofloxacin otic and other ototopical treatments in animal models and in humans, Pediatr. Infect. Dis. J. 20 (2001) 104–7. https://doi.org/10.1097/00006454-200101000-00038.

[124] R. Samarei, Comparison of Local and Systemic Ciprofloxacin Ototoxicity in the Treatment of Chronic Media Otitis, Glob. J. Health Sci. 6 (2014) 144–149. https://doi.org/10.5539/gjhs.v6n7p144.

[125] S.M. Green, S.G. Rothrock, Single-Dose Intramuscular Ceftriaxone for Acute Otitis Media in Children, Pediatrics. 91 (1993) 23–30.

[126] E. Leibovitz, L. Piglanksy, S. Raiz, D. Greenberg, P. Yagupsky, J. Press, D.M. Fliss, A. Leiberman, R. Dagan, Bacteriologic efficacy of a three-day intramuscular ceftriaxone regimen in nonresponsive acute otitis media, Pediatr. Infect. Dis. J. 17 (1998) 1126–1131.

[127] E. Leibovitz, L. Piglansky, S. Raiz, J. Press, A. Leiberman, R. Dagan, Bacteriological and clinical efficacy of one day vs. three day intramuscular ceftriaxone for treatment of nonresponsive acute otitis media in children, Pediatr. Infect. Dis. J. 19 (2000) 1040–1045.

[128] R. Cohen, M. Navel, J. Grunberg, M. Boucherat, P. Geslin, M. Derriennic, F. Pichon, J.-M. Goehrs, One dose ceftriaxone vs ten days of amoxicillin/clavalanate therapy for acute otitis media: clinical efficacy and change in nasopharyngeal flora, Pediatr. Infect. Dis. J. 18 (1999) 403–409.

[129] P. Gehanno, L. Nguyen, B. Barry, M. Derriennic, F. Pichon, J.M. Goehrs, P. Berche, Eradication by Ceftriaxone of Streptococcus pneumoniae Isolates with Increased Resistance to Penicillin in Cases of Acute Otitis Media, Antimicrob. Agents Chemother. 43 (1999) 16–20.

[130] T. Kanwal, M. Kawish, R. Maharjan, I. Ghaffar, H.S. Ali, M. Imran, S. Perveen, S. Saifullah, S.U. Simjee, M.R. Shah, Design and development of permeation enhancer containing self-nanoemulsifying drug delivery system (SNEDDS) for ceftriaxone sodium improved oral pharmacokinetics, J. Mol. Liq. 289 (2019). https://doi.org/10.1016/j.molliq.2019.111098.

[131] G.M. Pacifici, G. Marchini, Clinical Pharmacology of Ceftriaxone in Neonates and Infants: Effects and Pharmacokinetics, Int. J. Pediatr. 5 (2017) 6383–6411. https://doi.org/10.22038/ijp.2017.26942.2320.

[132] A. Mammen, E.G. Romanowski, M. V Fedorchak, D.K. Dhaliwal, R.M. Shanks, R.P. Kowalski, Endophthalmitis Prophylaxis Using a Single Drop of Thermoresponsive Controlled-Release Microspheres Loaded with Moxifloxacin in a Rabbit Model, Transl. Vis. Sci. Technol. 5 (2016). https://doi.org/10.1167/tvst.5.6.12.

[133] B. Kundu, C. Soundrapandian, S.K. Nandi, P. Mukherjee, N. Dandapat, S. Roy, Development of New Localized Drug Delivery System Based on Ceftriaxone-Sulbactam Composite Drug Impregnated Porous Hydroxyapatite : A Systematic Approach for In Vitro and In Vivo Animal Trial, Pharm. 27 (2010) 1659–1676. https://doi.org/10.1007/s11095-010-0166-y.

[134] D. Lim, Structure and function of the tympanic membrane: a review, Acta Otorhinolaryngol Belg. 49 (1995) 101–115.

[135] E. Bellotti, M. V Fedorchak, S. Velanker, S.R. Little, Tuning of thermoresponsive pNIPAAm hydrogels for the topical retention of controlled release ocular therapeutics, J. Mater. Chem. B. 7 (2019) 1276–1283. https://doi.org/10.1039/c8tb02976h.

[136] S.L. Wilson, M. Ahearne, A. Hopkinson, An overview of current techniques for ocular toxicity testing, Toxicology. (2015). https://doi.org/10.1016/j.tox.2014.11.003.

[137] A. Natsch, C. Bauch, L. Foertsch, F. Gerberick, K. Norman, A. Hilberer, H. Inglis, R. Landsiedel, S. Onken, H. Reuter, A. Schepky, R. Emter, The intra- and inter-laboratory reproducibility and predictivity of the KeratinoSens assay to predict skin sensitizers in vitro: Results of a ring-study in five laboratories, Toxicol. Vitr. 25 (2011) 733–744. https://doi.org/10.1016/j.tiv.2010.12.014.

[138] Key event based test guideline 442D: In vitro skin sensitisation assays addressing the AOP key event on keratinocyte activation, OECD Guidel. Test. Chem. Sect. 4. (2018).

[139] W. Li, J. Zhou, Y. Xu, Study of the in vitro cytotoxicity testing of medical devices (Review), Biomed. Reports. 3 (2015) 617–620. https://doi.org/10.3892/br.2015.481.

[140] G. Fotakis, J.A. Timbrell, In vitro cytotoxicity assays: Comparison of LDH, neutral red, MTT and protein assay in hepatoma cell lines following exposure to cadmium chloride, Toxicol. Lett. 160 (2006) 171–177. https://doi.org/10.1016/j.toxlet.2005.07.001.

[141] R.F. Gray, A. Sharma, S.L. Vowler, Relative humidity of the external auditory canal in normal and abnormal ears, and its pathogenic effect, Clin. Otolaryngol. 30 (2005) 105–111. https://doi.org/10.1111/j.1365-2273.2004.00950.x.

[142] M. Gimeno, P. Pinczowski, M. Pérez, A. Giorello, M.Á. Martínez, J. Santamaría, M. Arruebo, L. Luján, A controlled antibiotic release system to prevent orthopedic-implant associated infections: An in vitro study, Eur. J. Pharm. Biopharm. 96 (2015) 264–271. https://doi.org/10.1016/j.ejpb.2015.08.007.

[143] X. Guan, R.Z. Gan, Mechanisms of tympanic membrane and incus mobility loss in acute otitis media model of guinea pig, JARO - J. Assoc. Res. Otolaryngol. 14 (2013) 295–307. https://doi.org/10.1007/s10162-013-0379-y.

[144] Z. Yokell, X. Wang, R.Z. Gan, Dynamic Properties of Tympanic Membrane in a Chinchilla Otitis Media Model Measured With Acoustic Loading, J. Biomech. Eng. 137 (2015). https://doi.org/10.1115/1.4030410.

[145] L. Feng, J.A. Ward, S.K. Li, G. Tolia, J. Hao, D.I. Choo, Assessment of PLGA-PEG-PLGA Copolymer Hydrogel for Sustained Drug Delivery in the Ear, Curr Drug Deliv. 11 (2014) 279–286.

[146] R.T. Horie, T. Sakamoto, T. Nakagawa, Y. Tabata, N. Okamura, N. Tomiyama, M. Tachibana, J. Ito, Sustained Delivery of Lidocaine into the Cochlea using Poly Lactic/Glycolic Acid Microparticles, Laryngoscope. 120 (2010) 377–383. https://doi.org/10.1002/lary.20713.

[147] T. Caon, C.M.O. Simões, Effect of freezing and type of mucosa on ex vivo drug permeability parameters., AAPS PharmSciTech. 12 (2011) 587–592. https://doi.org/10.1208/s12249-011-9621-2.

[148] B. Godin, E. Touitou, Transdermal skin delivery: Predictions for humans from in vivo, ex vivo and animal models, Adv. Drug Deliv. Rev. 59 (2007) 1152–1161. https://doi.org/10.1016/j.addr.2007.07.004.

[149] R. Yang, T. Wei, H. Goldberg, W. Wang, K. Cullion, D.S. Kohane, Getting Drugs Across Biological Barriers, Adv. Mater. 29 (2017) 1–25. https://doi.org/10.1002/adma.201606596.

[150] M.R. Prausnitz, Microneedles for transdermal drug delivery, Adv. Drug Deliv. Rev. 56 (2004) 581–587. https://doi.org/10.1016/j.addr.2003.10.023.

[151] A.K. Lalwani, J.W. Kysar, System and method to locally delivery therapeutic agent to inner ear, 14/667,322, 2015. https://patents.google.com/patent/US20150265824A1/en.

[152] A. Kurabi, D. Schaerer, V. Noack, M. Bernhardt, K. Pak, T. Alexander, J. Husseman, Q. Nguyen, J.P. Harris, A.F. Ryan, Active Transport of Peptides Across the Intact Human Tympanic Membrane, Sci. Rep. 8 (2018). https://doi.org/10.1038/s41598-018-30031-6.

[153] W. Hong, P. Khampang, A.R. Kerschner, A.C. Mackinnon, K. Yan, P.M. Simpson, J.E. Kerschner, Antibiotic modulation of mucins in otitis media; should this change our approach to watchful waiting?, Int. J. Pediatr. Otorhinolaryngol. 125 (2019) 134–140. https://doi.org/10.1016/j.ijporl.2019.07.002.

[154] W. Hong, R.A. Juneau, B. Pang, W.E. Swords, Survival of Bacterial Biofilms within Neutrophil Extracellular Traps Promotes Nontypeable Haemophilus influenzae Persistence in the Chinchilla Model for Otitis Media, J. Innate Immun. 1 (2009) 215–224. https://doi.org/10.1159/000205937.

[155] W. Hong, K. Mason, J. Jurcisek, L. Novotny, L.O. Bakaletz, W.E. Swords, Phosporylcholine Decreases Early Inflammation and Promotes the Establishment of Stable Biofilm Communities of Nontypeable Haemophilus influenzae Strain 86-028NP in a Chinchilla Model of Otitis Media, Infect. Immun. 75 (2007) 958–965. https://doi.org/10.1128/IAI.01691-06.

[156] A.A.S. Albuquerque, M. Rossato, J.A.A. De Oliveira, M.A. Hyppolito, Understanding the anatomy of ears from guinea pigs and rats and its use in basic otologic research., Braz. J. Otorhinolaryngol. 75 (2009) 43–49. https://doi.org/S0034-72992009000100007 [pii].

[157] J. Shanks, D. Lilly, An Evaluation of Tympanometric Estimates of Ear Canal Volume, J Speech Hear Res. 24 (1981) 557–566. https://doi.org/10.1044/jshr.2404.557.

[158] E. Onusko, Tympanometry, Arch. Otolaryngol. 70 (2004) 1713–20. https://doi.org/10.1001/archotol.1970.04310030038009.

[159] Y.-S. Jeong, H.-B. Kwak, H.J. Park, G.-H. Park, J.-Y. Ahn, Y.-J. Lee, J.-E. Shin, W.-J. Moon, Tympanometry and CT Measurement of Middle Ear Volumes in Patients with Unilateral Chronic Otitis Media, Clin. Exp. Otorhinolaryngol. 1 (2008) 139. https://doi.org/10.3342/ceo.2008.1.3.139.

[160] R. Mittal, J. Kodiyan, R. Gerring, K. Mathee, J.D. Li, M. Grati, X.Z. Liu, Role of innate immunity in the pathogenesis of otitis media, Int. J. Infect. Dis. 29 (2014) 259–267. https://doi.org/10.1016/j.ijid.2014.10.015.

[161] S.-F. Ng, J.J. Rouse, F.D. Sanderson, V. Meidan, G.M. Eccleston, Validation of a static Franz diffusion cell system for in vitro permeation studies, AAPS PharmSciTech. 11 (2010) 1432–1441. https://doi.org/10.1208/s12249-010-9522-9.

[162] M.A. Mujica-Mota, A. Bezdjian, P. Salehi, J. Schermbrucker, S.J. Daniel, Assessment of ototoxicity of intratympanic administration of Auralgan in a chinchilla animal model, Laryngoscope. 125 (2015) 1444–1448. https://doi.org/10.1002/lary.25080.

[163] C. Nie, D. Yang, S.F. Morris, Local delivery of adipose-derived stem cells via acellular dermal matrix as a scaffold : A new promising strategy to accelerate wound healing, Med. Hypotheses. 72 (2009) 679–682. https://doi.org/10.1016/j.mehy.2008.10.033.

[164] B.P. Dodson, A.D. Levine, Challenges in the translation and commercialization of cell therapies, BMC Biotechnol. 15 (2015) 1–15. https://doi.org/10.1186/s12896-015-0190-4.

[165] P. Hourd, A. Chandra, N. Medcalf, D.J. Williams, Regulatory challenges for the manufacture and scale-out of autologous cell therapies | StemBook, StemBook. (2012) 438–447. https://doi.org/10.3824/stembook.1.96.1.1.

[166] S. Kim, H. Kim, Engineering of extracellular vesicles as drug delivery vehicles, Stem Cell Investig. 4 (2017). https://doi.org/10.21037/sci.2017.08.07.

[167] D. Angoulvant, F. Ivanes, R. Ferrera, P.G. Matthews, S. Nataf, M. Ovize, Mesenchymal stem cell conditioned media attenuates in vitro and ex vivo myocardial reperfusion injury, J. Hear. Lung Transplant. 30 (2011) 95–102. https://doi.org/10.1016/j.healun.2010.08.023.

[168] C.-Y. Wang, H.-B. Yang, H.-S. Hsu, L.-L. Chen, C.-C. Tsai, K.-S. Tsai, T.-L. Yek, Y.-H. Kao, S.-C. Hung, Mesenchymal stem cell-conditioned medium facilitates angiogenesis and fracture healing and diabetic rats, J. Tissue Eng. Regen. Med. 6 (2012) 559–569. https://doi.org/10.1002/term.461.

[169] X. Wang, E. Wank, X. Cang, L. Meinel, G. Vunjak-Novakovic, D.L. Kaplan, Growth Factor Gradients via Microsphere Delivery in Biopolymer Scaffolds for Osteochondral Tissue Engineering, J. Control. Release. 134 (2009) 81–90. https://doi.org/10.1016/j.jconrel.2008.10.021.

[170] M.L. Ratay, A.J. Glowacki, S.C. Balmert, A.P. Acharya, J. Polat, L.P. Andrews, M. V. Fedorchak, J.S. Schuman, D.A.A. Vignali, S.R. Little, Treg-recruiting microspheres prevent inflammation in a murine model of dry eye disease, J. Control. Release. 258 (2017) 208–217. https://doi.org/10.1016/j.jconrel.2017.05.007.

[171] S. Jhunjhunwala, S.C. Balmert, G. Raimondi, E. Dons, E. Nichols, A.W. Thomson, S.R. Little, Controlled Release Formulations of IL-2, TGF-β1 and Rapamycin for the Induction of Regulatory T Cells, J Control Release. 159 (2012) 78–84. https://doi.org/10.1016/j.jconrel.2012.01.013.Controlled.

[172] S. Jhunjhunwala, G. Raimondi, A.J. Glowacki, S.J. Hall, D. Maskarinec, S.H. Thorne, A.W. Thomson, S.R. Little, Bioinspired Controlled Release of CCL22 Recruits Regulatory T Cells In Vivo, Adv. Mater. 24 (2012) 4735–4738. https://doi.org/10.1002/adma.201202513.

[173] R. Madonna, F. V Renna, C. Cellini, R. Cotellese, N. Picardi, F. Francomano, P. Innocenti, R. De Caterina, Age-dependent impairment of number and angiogenic potential of adipose

tissue-derived progenitor cells, Eur J Clin Invest. 41 (2011) 126–133. https://doi.org/10.1111/j.1365-2362.2010.02384.x.

[174] M. Zhu, E. Kohan, J. Bradley, M. Hedrick, P. Benhaim, P. Zuk, The effect of age on osteogenic, adipogenic and proliferative potential of female adipose-derived stem cells, J. Tissue Eng. Regen. Med. 3 (2009) 290–301. https://doi.org/10.1002/term.

[175] B.M. Schipper, K.G. Marra, W. Zhang, A.D. Donnenberg, J.P. Rubin, Regional Anatomic and Age Effects on Cell Functions of Human Adipose-Derived Stem Cells, Ann Plast Surg. 60 (2008) 538–544. https://doi.org/10.1097/SAP.0b013e3181723bbe.Regional.

[176] M. van de Weert, W.E. Hennink, W. Jiskoot, Protein instability in Poly(Lactic-co-Glycolic Acid) Microparticles, Pharm. Res. 17 (2000) 1159–1167. https://doi.org/10.1023/A:1026498209874.

[177] M. Walter, K. Wright, H. Fuller, S. Macneil, W. Johnson, Mesenchymal stem cell-conditioned medium accelerates skin wound healing: An in vitro study of fibroblast and keratinocyte scratch assays, Exp. Cell Res. 316 (2010) 1271–1281. https://doi.org/10.1016/j.yexcr.2010.02.026.

[178] H. Sah, Microencapsulation techniques using ethyl acetate as a dispersed solvent: effects of its extraction rate on the characteristics of PLGA microspheres, J. Control. Release. 47 (1997) 233–245. https://doi.org/10.1016/S0168-3659(97)01647-7.

[179] L.M. Doyle, M.Z. Wang, Overview of Extracellular Vesicles, Their Origin, Composition, Purpose, and Methods for Exosome Isolation and Analysis, Cells. 8 (2019) 727. https://doi.org/10.1016/b978-0-12-386050-7.50008-3.

[180] E.D. Miller, G.W. Fisher, L.E. Weiss, L.M. Walker, P.G. Campbell, Dose-dependent cell growth in response to concentration modulated patterns of FGF-2 printed on fibrin, Biomaterials. 27 (2006) 2213–2221. https://doi.org/10.1016/j.biomaterials.2005.10.021.

[181] M. Lee, B.M. Wu, M. Stelzner, H.M. Reichardt, J.C.Y. Dunn, Intestinal Smooth Muscle Cell Maintenance by Basic Fibroblas Growth Factor, Tissue Eng. Part A. 14 (2008) 1395–1402. https://doi.org/10.1089/ten.tea.2007.0232.

[182] Z. Lou, Y. Wang, G. Yu, Effects of basic fibroblast growth factor dose on traumatic tympanic membrane perforation, Growth Factors. 32 (2014) 150–154. https://doi.org/10.3109/08977194.2014.952411.

[183] A.Y. Wang, Y. Shen, L.J. Liew, J.T. Wang, M. von Unge, M.D. Atlas, R.J. Dilley, Rat model of chronic tympanic membrane perforation: Ventilation tube with mitomycin C and dexamethasone, Int. J. Pediatr. Otorhinolaryngol. 80 (2016) 61–68. https://doi.org/10.1016/j.ijporl.2015.11.010.

[184] A.Y. Wang, Y. Shen, J.T. Wang, P.L. Friedland, M.D. Atlas, R.J. Dilley, Animal models of chronic tympanic membrane perforation : A ‘ time-out ’ to review evidence and standardize design, Int. J. Pediatr. Otorhinolaryngol. 78 (2014) 2048–2055. https://doi.org/10.1016/j.ijporl.2014.10.007.

[185] S.C. Babu, J.M. Kartush, A. Patni, Otologic effects of topical mitomycin C: Phase I - Evaluation of ototoxicity, Otol. Neurotol. (2005). https://doi.org/10.1097/00129492-200503000-00002.

[186] R. Yang, R. Saarinen, O.S. Okonkwo, Y. Hao, M. Mehta, D.S. Kohane, Transtympanic Delivery of Local Anesthetics for Pain in Acute Otitis Media, Mol. Pharm. 16 (2019) 1555–1562. https://doi.org/10.1021/acs.molpharmaceut.8b01235.

[187] P. Bolt, P. Barnett, F.E. Babl, L.N. Sharwood, Topical lignocaine for pain relief in acute otitis media: results of a double-blind placebo-controlled randomised trial, Arch. Dis. Child. 93 (2008) 40–44. https://doi.org/10.1136/adc.2006.110429.

[188] S. Prasad, B. Ewigman, Use anesthetic drops to relieve acute otitis media pain., J. Fam. Pract. 57 (2008) 370–373.

[189] J. Sun, Y. Lei, Z. Dai, X. Liu, T. Huang, J. Wu, Z.P. Xu, X. Sun, Sustained Release of Brimonidine from a New Composite Drug Delivery System for Treatment of Glaucoma, ACS Appl. Mater. Interfaces. 9 (2017) 7990–7999. https://doi.org/10.1021/acsami.6b16509.

[190] M.H. Aburahma, A.A. Mahmoud, Biodegradable Ocular Inserts for Sustained Delivery of Brimonidine Rartarate: Preparation and In vitro/In vivo Evaluation, AAPS PharmSciTech. 12 (2011) 1335–1347. https://doi.org/10.1208/s12249-011-9701-3.

[191] A.G.A. Coombes, M.-K. Yeh, E.C. Lavelle, S.S. Davis, The control of protein release from poly(DL-lactide co-glycolide) microparticles by variation of the external aqueous phase surfactant in the water-in oil-in water method, J. Control. Release. 52 (1998) 311–320. https://doi.org/10.1016/S0168-3659(98)00006-6.

[192] C. Bouissou, J.J. Rouse, R. Price, C.F. Van Der Walle, The influence of Surfactant on PLGA Microsphere Glass Transition and Water Sorption: Remodeling the Surface Morphology to Attenuate the Burst Release, Pharm. Res. 23 (2006) 1295–1305. https://doi.org/10.1007/s11095-006-0180-2.

[193] P.A. Bhat, G.M. Rather, A.A. Dar, Effect of Surfactant Mixing on Partitioning of Model Hydrophobic drug, Naproxen, between Aqueous and Micellar Phases, J. Phys. Chem. B. 113 (2009) 997–1006. https://doi.org/10.1021/jp807229c.

[194] C. Peetla, V. Labhasetwar, Effect of Molecular Structure of Cationic Surfactants on Biophysical Interactions of Surfactant-Modified Nanoparticles with a Model Membrane and Cellular Uptake, Langmuir. 25 (2009) 2369–2377. https://doi.org/10.1021/la803361y.

[195] M.J. Lawrence, Surfactant Systems: Their Use in Drug Delivery, Chem. Soc. Rev. 23 (1994) 417–424. https://doi.org/10.1039/CS9942300417.

[196] D. Khossravi, Drug-surfactant interactions: Effect on transport properties, Int. J. Pharm. 155 (1997) 179–190. https://doi.org/10.1016/S0378-5173(97)00162-2.

[197] Y. Yang, Y. Gao, X. Mei, Effects of gamma-irradiation on PLGA microspheres loaded with thienorphine, Pharmazie. 66 (2011) 694–697. https://doi.org/10.1691/ph.2011.1007.

[198] J.Y. Lai, P.L. Lu, K.H. Chen, Y. Tabata, G.H. Hsiue, Effect of charge and molecular weight on the functionality of gelatin carriers for corneal endothelial cell therapy, Biomacromolecules. 7 (2006) 1836–1844. https://doi.org/10.1021/bm0601575.

[199] S. Jain, P. Malyala, M. Pallaoro, M. Guiliani, H. Peterson, D.T. O'Hagan, M. Singh, A Two-Stage Strategy for Sterilization of Poly(lactide-co-glyolide) Particles by γ-irradiation Does Not Impair Their Potency for Vaccine Delivery, J. Pharm. Sci. 100 (2011) 646–654. https://doi.org/10.1002/jps.

[200] C.E. Holy, C. Cheng, J.E. Davies, M.S. Shoichet, Optimizing the sterilization of PLGA scaffolds for use in tissue engineering, Biomaterials. 22 (2001) 25–31.

[201] K.-G.H. Desai, S. Kadous, S.P. Schwendeman, Gamma Irradiation of Active Self-healing PLGA Microspheres for Efficient Aqueous Encapsulation of Vaccine Antigens, Pharm. Res. 30 (2013) 1768–1778. https://doi.org/10.1007/s11095-013-1019-2.

[202] D.I. Braghirolli, D. Steffens, K. Quintiliano, G.A.X. Acasigua, D. Gamba, R.A. Fleck, C.L. Petzhold, P. Pranke, The effect of sterilization methods on electronspun poly(lactide-co-glycolide) and subsequent adhesion efficiency of mesenchymal stem cells, J. Biomed. Mater. Res. - Part B. 102B (2014) 700–708. https://doi.org/10.1002/jbm.b.33049.

[203] D.W.L. Hukins, A. Mahomed, S.N. Kukureka, Accelerated aging for testing polymeric biomaterials and medical devices, Med. Eng. Phys. 30 (2008) 1270–1274. https://doi.org/10.1016/j.medengphy.2008.06.001.

[204] A. Rawat, D.J. Burgess, Effect of physical ageing on the performance of dexamethasone loaded PLGA microspheres, Int. J. Pharm. 415 (2011) 164–168. https://doi.org/10.1016/j.ijpharm.2011.05.067.

[205] Y. Wang, D.J. Burgess, Influence of storage temperature and moisture on the performance of microsphere/hydrogel composites, Int. J. Pharm. 454 (2013) 310–315. https://doi.org/10.1016/j.ijpharm.2013.06.012.

[206] P. Malyala, M. Singh, Endotoxin Limits in Formulations for Preclinical Research, J. Pharm. Sci. 97 (2008) 2041–2044. https://doi.org/10.1002/jps.

[207] Y. Capan, B.H. Woo, S. Gebrekidan, S. Ahmed, P.P. DeLuca, Influence of formulation parameters on the characteristics of poly(D,L-lactide-co-glycolide) microspheres containing poly(L-lysine) complexed plasmid DNA, J. Control. Release. 60 (1999) 279–286. https://doi.org/10.1016/S0168-3659(99)00076-0.

[208] R.V. Diaz, I. Soriano, A. Delgado, M. Llabrés, C. Evora, Effect of surfactant agents on the release of 125I-bovine calcitonin from PLGA microspheres: In vitro - in vivo study, J. Control. Release. 43 (1997) 59–64. https://doi.org/10.1016/S0168-3659(96)01470-8.

[209] D. Blanco, M.J. Alonso, Protein encapsulation and release from poly(lactide-co-glycolide) microspheres: Effect of the protein and polymer properties and of the co-encapsulation of surfactants, Eur. J. Pharm. Biopharm. 45 (1998) 285–294. https://doi.org/10.1016/S0939-6411(98)00011-3.

[210] G. De Rosa, R. Iommelli, M.I. La Rotonda, A. Miro, F. Quaglia, Influence of the co-encapsulation of different non-ionic surfactants on the properties of PLGA insulin-loaded microspheres, J. Control. Release. 69 (2000) 283–295. https://doi.org/10.1016/S0168-3659(00)00315-1.